

RICE UNIVERSITY

Nonlinear Stochastic Analysis of Motorcycle Dynamics

by

Luis Alejandro Robledo Ricardo

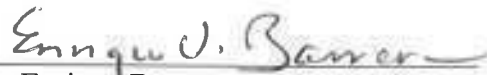
A THESIS SUBMITTED
IN PARTIAL FULFILLMENT OF THE
REQUIREMENTS FOR THE DEGREE

Doctor of Philosophy

APPROVED, THESIS COMMITTEE:



Dr. Pol D. Spanos, Chair
L. B. Ryon Professor of Mechanical
Engineering and Materials Science



Dr. Enrique Barrera
Professor of Mechanical Engineering
and Materials Science



Dr. Andrew Dick
Assistant Professor of Mechanical
Engineering and Materials Science



Dr. Leonardo Dueñas Osorio
Assistant Professor of Civil
and Environmental Engineering

HOUSTON, TEXAS
FEBRUARY, 2013

Abstract

Nonlinear Stochastic Analysis of Motorcycle Dynamics

by

Luis Alejandro Robledo Ricardo

Off-road and racing motorcycles require a particular setup of the suspension to improve the comfort and the safety of the rider. Further, due to ground unevenness, off-road motorcycle suspensions usually experience extreme and erratic excursions in performing their function. In this regard, the adoption of nonlinear devices, such as progressive springs and hydro pneumatic shock absorbers, can help limiting both the acceleration experienced by the sprung mass and the excursions of the suspensions. For dynamic analysis purposes, this option involves the solution of the nonlinear differential equations that govern the motion of the motorcycle, which is excited by the stochastic road ground profile. In this study a 4-degree-of-freedom (4-DOF) nonlinear motorcycle model is considered. The model involves suspension elements with asymmetric behaviour. Further, it is assumed that the motorcycle is exposed to loading of a stochastic nature as it moves with a specified speed over a road profile defined by a particular power spectrum. It is shown that a meaningful analysis of the motorcycle response can be conducted by using the technique of statistical linearization. The validity of the proposed approach is established by comparison with results from pertinent Monte Carlo studies. In this context the applicability of auto-regressive (AR) filters for efficient implementation of the Monte Carlo simulation is pointed out. The advantages of these methods for the synthesis of excitation signals from a given power spectrum, are shown by comparison with other methods. It is

shown that the statistical linearization method allows the analysis of multi-degree-of-freedom (M-DOF) systems that present strong nonlinearities, exceeding other nonlinear analysis methods in both accuracy and applicability. It is expected that the proposed approaches can be used for a variety of parameter/ride quality studies and as preliminary design tool by the motorcycle industry.

Acknowledgements

I would like to express my gratitude to my mentor Dr. Pol Spanos, for giving me the opportunity to work under his guidance and for being to me a great source of inspiration. I really appreciate his patience and kind support, especially during the hard times I had to face over the course of my time as a graduate student, which could potentially prevent me from finishing the program. His advice and continuous encouragement set me up in the right direction to achieve the goals of this research.

I wish to also thank Dr. Enrique Barrera, Dr. Andrew Dick, and Dr. Leonardo Dueñas Osorio for serving on my thesis committee. To all of them, I express my most sincere gratitude for devoting their time to carefully review my work and discuss with me those aspects which needed clarification.

I wish to extend a special word of thanks to Francesco Marino whose help and patience eased my understanding of stochastic mechanics. The time we spent together discussing the details in the implementation of the statistical linearization method and the possible ways of approaching the problem is invaluable.

I am deeply indebted to the following people: María Maldonado, Ellen Burns (†), David Hernández, Milton Esteva, Atakan Tamer, and Joseph Chakkungal for their sincere friendship and valuable support along this process. I am certain that without their help and encouragement I would not be able to stay in Houston to conclude my doctoral program. In particular, I would like to express my deepest gratitude and admiration to Ms. María Maldonado and Miss Ellen Burns (†) for their unconditional help and love rendered to me. Thank you Mrs. María, and Miss Ellen for teaching me by your personal example the value of helping others.

I also greatly appreciate all the support and advice I received from Tiffany Okoye and Sherry Vanderslice; they are wonderful persons!

I wish to express my gratitude to my family for their lovely support and for enlightening my life. I have no words to express my gratitude and admiration to my father Luis and my mother Clara (†) who have shaped the person I am. I have been blessed to be their son. My siblings Guadalupe, Karen, Gabriela and Román have always encouraged me to pursue my goals, thank you for your love. My deepest gratitude goes towards my wife Gaby, my daughter Alma, and my son Andrés, who have also added incredible joy and meaning to my life.

Last but not least, I wish to express my most deeply gratitude to God for His providence which, through the intercession of Jesus Christ and his holy mother the Virgin Mary, has made all this possible.

In memory of Clara Ricardo and Ellen Burns.

Table of Contents

Abstract	ii
Acknowledgements	iv
List of Figures	xi
List of Tables	xvi
Chapter 1 Literature Review	1
1.1 Introduction	1
1.2 Bibliographical Review on Motorcycle Dynamics	4
1.3 Motivation and Objectives	7
1.4 Thesis Outline	9
Chapter 2 An Overview of Stochastic Processes and Linear Systems	12
2.1 Introduction	12
2.2 General Concepts of Stochastic Processes	13
2.3 Broad Band Processes	22
2.4 General Concepts on Linear Systems and Digital Signal Processing	24
2.5 Mathematical Modeling	25
2.5.1 Lagrange's Equations	25
2.5.2 Other Modeling Approaches	26
2.6 General Excitation-Response Relations	27
2.7 Complex Frequency Response	29
2.8 Mean Square Response	31
2.9 Generalization of the Excitation-Response Relations to M-DOF Systems	31

2.10	State-Space Models	33
2.11	General Concepts on Digital Signal Processing	34
2.11.1	Classification of Signals	34
2.12	Estimation of the Power Spectrum of Stationary Random Signals	35
Chapter 3	Methods of Nonlinear Analysis	37
3.1	Introduction	37
3.2	The Monte Carlo Method	38
3.3	Perturbation Methods	41
3.4	Closure Techniques	42
3.5	Markov Methods	43
3.6	Probability Density Evolution Method	44
3.7	Statistical Linearization Method	46
Chapter 4	Statistical Linearization Method Applied to M-DOF Systems	47
4.1	Introduction	47
4.2	General Formulation of Statistical Linearization Method	48
4.3	Spectral Approach Solution Procedure	51
Chapter 5	Road Profile Modeling and Synthetic Road Realization	53
5.1	Introduction	53
5.2	Characterization of Road Roughness	53
5.2.1	General Considerations on the Characterization of Roughness	57
5.3	Road Roughness Model	58
5.4	Synthesis of Road Realizations	65
5.5	The Autoregressive Approximation	66

5.6	AR Fitting of a combined Dodds-Narayanan Road Power Spectrum	68
5.7	Analysis of Results. Target Power Spectrum Fitting	71
5.8	Analysis of Results. Generation of Time Histories	73
5.8.1	Fitting of an Acceleration Power Spectrum	75
Chapter 6	Modeling of Motorcycle Dynamics	79
6.1	Introduction	79
6.2	General Description of a Motorcycle	80
6.2.1	Kinematic Description of a Motorcycle	81
6.2.2	Geometric Parameters of a Motorcycle	82
6.3	Simplifying Criteria for Obtaining a 4-DOF In-Plane Model	85
6.3.1	In-plane Vibration Modes of a Motorcycle	85
6.3.2	Simplified Model of Motorcycle Suspension	86
6.3.2.1	Suspension Modeling	86
6.3.2.2	Reduced Stiffness of the Suspension	87
6.3.2.3	Reduced Damping of the Suspension	88
6.4	Motorcycle Tires	89
6.4.1	Tire Modeling	89
6.4.2	Vibration modes of the Tires	90
6.5	The Linear 4-DOF In-Plane Model	92
6.5.1	General Assumptions and Nomenclature	92
6.5.2	Motorcycle Data	92
6.5.3	Derivation of the Linear Model of Motion in Absolute Coordinates ...	93
6.5.4	Equations of Motion in Relative Coordinates	95

6.5.5	Free Vibration	97
6.6	Motorcycle Response to Road Profile. Frequency Domain Approach	98
6.6.1	Frequency Response Function Matrix	98
6.6.1.1	Frequency Response Function Matrix in Absolute Coordinates	99
6.6.1.2	Frequency Response Function Matrix in Relative Coordinates	100
6.6.2	Computation of the Frequency Response Function Matrix	101
6.7	Dynamical Analysis by Monte Carlo Simulation	105
6.7.1	Validating Solution (Frequency-Domain Method)	105
6.7.2	Response Power Spectrum Fitting by Monte Carlo Simulation	109
Chapter 7	Statistical Linearization of the Nonlinear 4-DOF Motorcycle Model	112
7.1	Introduction	112
7.2	The Nonlinear 4-DOF Motorcycle Model	112
7.3	The Statistical Linearization Solution	116
7.3.1	Motorcycle Offset	116
7.3.2	The Equivalent Linear System	118
7.3.3	The Frequency-Domain Representation	122
7.4	Implementation of the Statistical Linearization Method	124
Chapter 8	Numerical Results	126
8.1	Introduction	126
8.2	Case 1. Front Suspension with Nonlinear Springs and Nonlinear Dashpots	126
8.2.1	Monte Carlo Simulation	128
8.2.1.1	Normality Test	136
8.3	Case 2. Front Suspension with Linear Springs and Nonlinear Dashpots	144

Chapter 9 Concluding Remarks	140
9.1 Conclusions	140
9.2 Future Work	142
References	143

List of Figures

Figure 1.1. Harley Davidson XL1200R Roadster.	2
Figure 1.2. Suzuki GSXR1000 2010.	2
Figure 1.3. Yamaha YZ250 2006.	2
Figure 1.4. Elements of motorcycle dynamics analysis.	3
Figure 2.1. Ensemble from a stochastic process and averaging.	16
Figure 2.2. Typical graph of $R_x(\tau)$ and its properties for a stationary random process.	19
Figure 2.3. The area enclosed by the power spectrum graph equals the mean square value of $x(t)$	20
Figure 2.4. PSD of the elevation of a typical road.	22
Figure 2.5. Broad band process. Power spectrum and time history.	23
Figure 2.6. Power spectrum of ideal white noise.	23
Figure 2.7. Power spectrum of clipped white noise.	24
Figure 2.8. General schematic representation of a system.	25
Figure 2.9. Single-degree of freedom linear model.	28
Figure 3.1. Schematic representation of Monte Carlo method.	42
Figure 5.1. Terrain profiles measured in off-road locomotion studies.	57
Figure 5.2. Power spectral density of terrain 1.	59
Figure 5.3. Power spectral density of terrain 2.	59
Figure 5.4. Typical power spectrum of road profile and two approximations.	63
Figure 5.5. Power spectra for an average quality road.	64
Figure 5.6. Sections of power spectrum fitted by two different roughness models.	66

Figure 5.7. Power spectrum of road roughness and fitting.	66
Figure 5.8. Combined PSD obtained with two different models.	67
Figure 5.9. Acceleration power spectrum.	68
Figure 5.10. Linear-linear plot of PSD of average road profile.	72
Figure 5.11. Log-log plot of PSD of average road profile.	73
Figure 5.12. PSD of road profile obtained from AR(45) filter and target PSD.	74
Figure 5.13. Log-log of road profile obtained from AR(45) filter and target spectrum.	75
Figure 5.14. Sample time history of the excitation.	77
Figure 5.15. Autocorrelation of time history.	77
Figure 5.16. PSD of induced acceleration and AR(45) power spectrum.	78
Figure 5.17. Log-log graph of PSD of induced acceleration and AR(45) power spectrum.	79
Figure 5.18. Sample time history of acceleration.	80
Figure 5.19. Autocorrelation of acceleration.	81
Figure 6.1. Kinematic description of a motorcycle.	85
Figure 6.2. Geometry of a motorcycle.	86
Figure 6.3. Typical modes of vibration of an in-plane motorcycle model.	88
Figure 6.4. Reduced suspension model.	90
Figure 6.5. In-plane tire's mode of vibration.	93
Figure 6.6. 4-DOF In Plane Model.	94
Figure 6.7. 4-DOF In Plane Model in relative coordinates.	100
Figure 6.8a. FRF's of rear sprung mass of 4-DOF linear model for several speeds.	106

Figure 6.8b. FRF's of front sprung mass of 4-DOF linear model for several speeds.	107
Figure 6.8c. FRF's of rear unsprung mass of 4-DOF linear model for several speeds.	107
Figure 6.8d. FRF's of front unsprung mass of 4-DOF linear model for several speeds.	108
Figure 6.9a. Power spectrum of road profile.	109
Figure 6.9b. Power spectrum of accelerations.	109
Figure 6.10a. FRF of the z_r coordinate.	110
Figure 6.10b. FRF of the z_f coordinate.	110
Figure 6.10c. FRF of the z_{pr} coordinate.	110
Figure 6.10d. FRF of the z_{pf} coordinate.	110
Figure 6.11a. PSD of Response for z_r coordinate.	111
Figure 6.11b. PSD of Response for z_f coordinate.	111
Figure 6.11c. PSD of Response for z_{pr} coordinate.	111
Figure 6.11d. PSD of Response for z_{pf} coordinate.	111
Figure 6.12a. PSD of Response for \ddot{z}_r coordinate.	112
Figure 6.12b. PSD of Response for \ddot{z}_f coordinate.	112
Figure 6.12c. PSD of Response for \ddot{z}_{pr} coordinate.	112
Figure 6.12d. PSD of Response for \ddot{z}_{pf} coordinate.	112
Figure 6.13a. Approximation of PSD of Response for z_r coordinate using 800 time histories.	113

Figure 6.13b. Approximation of PSD of Response for z_f coordinate using 800 time histories.	113
Figure 6.13c. Approximation of PSD of Response for z_{pr} coordinate using 800 time histories.	113
Figure 6.13d. Approximation of PSD of Response for z_{pf} coordinate using 800 time histories.	113
Figure 6.14a. Approximation of PSD of response for \dot{z}_r coordinate using 800 time histories.	114
Figure 6.14b. Approximation of PSD of response for \dot{z}_f coordinate using 800 time histories.	114
Figure 6.14c. Approximation of PSD of response for \dot{z}_{pr} coordinate using 800 time histories.	114
Figure 6.14d. Approximation of PSD of response for \dot{z}_{pf} coordinate using 800 time histories.	114
Figure 7.1. Schematic representation of a generalized nonlinear motorcycle system. All the possible nonlinear elements are indicated, but different configurations can be defined from this model.	117
Figure 8.1. Comparison of the linear and nonlinear behavior of a common motorcycle suspension. Elastic force.	131
Figure 8.2. Comparison of the linear and nonlinear behavior of a common motorcycle suspension. Viscous force.	132
Figure 8.3. Displacement PSD fitting by AR filter and function PWELCH.	133

Figure 8.4. Sample time history obtained from the displacement PSD fitting by AR filter.	134
Figure 8.5. Autocorrelation of AR filter time histories (displacement).	135
Figure 8.6. Velocity PSD fitting by AR filter and function PWELCH.	135
Figure 8.7. Sample time history obtained from the velocity PSD fitting by AR filter.	136
Figure 8.8. Ensemble of response time histories.	137
Figure 8.9. Averaged response time history for $q(t)$	138
Figure 8.10. Averaged response time histories for $z_f(t)$	139
Figure 8.11. Variance of response time history for $z_f(t)$	139
Figure 8.12. Averaged response time history for $\ddot{q}(t)$	140
Figure 8.13. Variance of response time history for $\ddot{q}(t)$	140
Figure 8.14. Normality test.	141
Figure 8.15. Offset of motorcycle z_f at different speeds.	143
Figure 8.16. Standard deviation of z_f at different speeds.	143
Figure 8.17. Offset of motorcycle at different speeds z_f	144

List of Tables

Table 5.1 Road quality constants.	59
Table 5.2 Parameters and equations for average quality roughness PSD with V=15m/s, and $\omega_{co}=250$ rad/s.	69
Table 5.3 Areas under PSD's of Figures 5.12 and 5.13.	73
Table 5.4 Areas under PSD's of Figures 5.16 and 5.17.	76
Table 6.1 Motorcycle data sheet.	96
Table 6.2 rms values of responses (accelerations) for the analytical and MC simulation.	111
Table 7.1 Six kinds (j=1, ..., 6) of nonlinear sources.	115

Chapter 1

Literature Review

1.1 Introduction

Since the first two-wheeled motorized vehicle was created in 1867 [1], the motorcycle has evolved to become a quite complex machine not only devoted to the task of transportation, but also to leisure and sports. Many kinds, makers, and models are available in the world market nowadays. As an example of this diversity in motorcycle applications, it is noted that cruiser motorcycles, see for instance Figure 1.1, are designed to provide comfort to the rider and stability while driving on a straight path, and their design is intended to allow the rider to travel long distances by limiting fatigue and carrying heavy loads while keeping a stable straight motion. On the contrary, racing motorcycles, see for instance Figure 1.2, are designed to sustain high speeds and to allow the rider to make quick changes in direction in spite of sacrificing stability [43]. Further, off-road motorcycles, see for instance Figure 1.3, require to be light weight and easy to handle, and to have a stronger chassis as well [5]. In all these cases adherence to the road (wheel grip) is an important safety factor, which varies from type to type. Thus, wheel grip and comfort are two features a motorcycle must provide to more or less a degree depending on its potential use. These two requirements are achieved by means of a suspension system, which in general, must provide the following features [26, 93]:

- I. To isolate the main body of the motorcycle along with the driver from excessive and dangerous destabilizing vibrations produced by the interaction of the wheels and the road roughness;



Figure 1.1. Harley Davidson XL1200R Roadster (From [207]).



Figure 1.2. Suzuki GSXR1000 2010 (From [208]).

- II. To ensure road adherence, by allowing the wheel to follow the road profile;
- III. To allow proper dynamical interaction between the tire and the road that ensures transmission of the necessary driving and braking forces.

Thus, the motorcycle suspension characteristics play a crucial role in ride quality, handling, and the generation of dynamic tire forces.

Basically, three elements are involved in a motorcycle dynamics analysis [93]:

- I. A *model*, which involves the dynamic characteristics of the mechanical system. It is specified by a set of ordinary differential equations (ODE's) that can be either linear or nonlinear.



Figure 1.3 Yamaha YZ250 2006 (From [209]).

- II. An *excitation source*, in this case the road roughness which is specified by its power spectrum.
- III. The *system response*, which corresponds to the solution of the ODE's and may be specified by time histories or a power spectrum.

A more detailed explanation of each of these elements (Figure 1.4) is provided in chapters 2, 5, and 6.

Besides comfort and ride, a dynamic analysis can provide useful information related to the motorcycle's response properties that can be used to explore other areas such as [164]:

- I. Speed limitation due to road roughness and/or vehicle configuration
- II. Optimization of suspension characteristics
- III. Fatigue stresses and strains of vehicle structure due to vibration
- IV. Estimation of power losses due to vehicle vibration

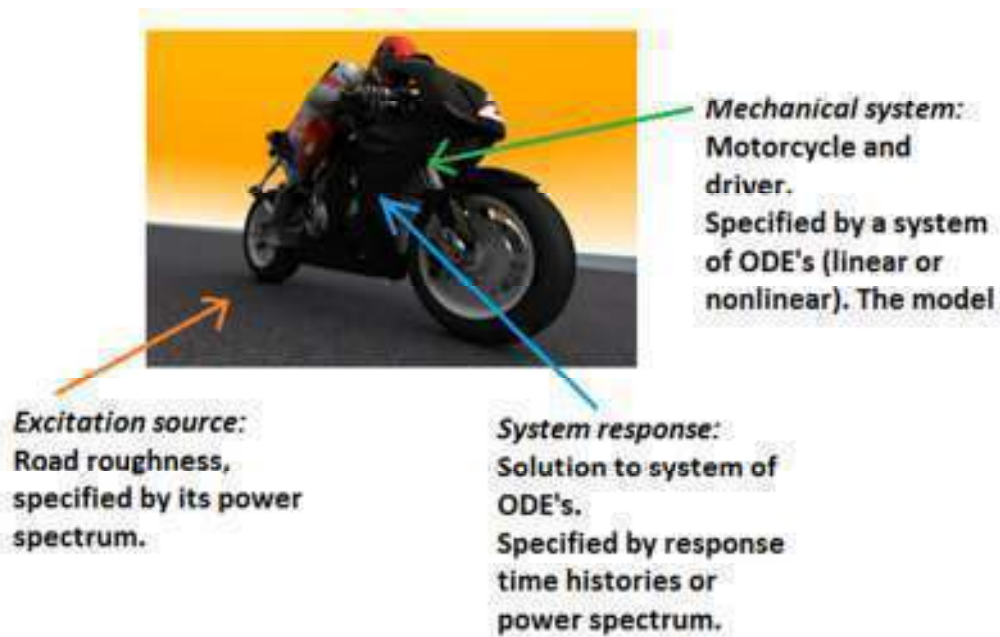


Figure 1.4 Elements of motorcycle dynamics analysis (adapted from [210]).

1.2 Bibliographical Review on Motorcycle Dynamics

A substantial body of literature has been devoted to study several aspects of single-track vehicles in which different concepts of motorcycle mathematical models are used with varying complexity which depends on the purpose of the study. Some of the areas of motorcycle research that involve the use of motorcycle models are [1, 43]: quantification of ride quality, analysis of modal behavior, motorcycle control, rider's safety, motorcycle simulators, and experimental characterization of dynamic properties. Due to such multiplicity of applications, this review does not aim to be exhaustive; rather the goal is to present a general perspective of important contributions to the motorcycle dynamics field that help to set up the emphasis of this dissertation and to identify themes of opportunity for further contribution in this field.

The first attempts to mathematically describe a two-wheeled vehicle, seem to be the works that appeared in the 1890's due to Klein and Sommerfeld [10], who set up the equations of motion of a bicycle; and the study of the stability of the motion of a bicycle by Whipple [11]. The pneumatic tire was invented in 1888, thus the effect of tire on the bicycle dynamics was not considered in those analyses [1]. Döhning and Braunschweig [12], based on the analysis of Klein and Sommerfeld, set up the linearized equations of motion for a motorcycle, and, by carrying out measurements on three vehicles, obtained machine constants to solve the equations of motion. Other researchers, like Collins [13] and Singh [14], conducted a more detailed analysis investigating the effects of several motorcycle parameters on its stability, and validated their results with experimental. One of the seminal contributions to motorcycle modeling was made by Sharp in 1971 [2]. This work contributed, through the use of a linearized model, to understanding the dynamic

behavior of a motorcycle in straight-running, moving forward at constant speed with freedom to sideslip, to yaw, and to roll (under small perturbations). The model comprises two rigid frames joined at an inclined steering axis, the rider being rigidly attached to the rear frame. This configuration is described by four degrees of freedom, namely lateral motion, yaw, roll, and steer. The equations are obtained using a Lagrangian approach, and they are linearized by assuming small perturbations during straight running at constant speed. From this study Sharp predicted the existence of three important modes which he called “*weave*“, “*wobble*“ and “*capsize*“. The term *weave* denotes an oscillation of the whole vehicle that involves yaw, roll, and steer motions. It is a low frequency (2-3 Hz) oscillation, highly damped at low speeds and less damped at higher speeds, which may become unstable. *Wobble* becomes present in the range of 7-9 Hz, it is highly damped, thus stable at low speeds, but turning lightly damped at high speeds. *Wobble* is a motion that involves primarily the rotation of the front steering system relative to the rear frame. Finally, *capsize* is a slow speed divergent instability of the whole vehicle falling onto its side. In a second contribution, Sharp [3] improves his previous model by taking into account the torsional flexibility of the rear wheel. The new results showed that, while the wobble and capsize modes were not noticeably affected, the weave mode damping was lower at medium and high speeds. Sharp’s model has been used, in some cases with certain modifications, by himself and other researchers to investigate the acceleration and breaking in motorcycles [18, 19], and the effects of frame compliance on the straight running vibrational modes [21-24]. Black and Taylor [5] made an in-plane dynamic analysis of a 4-degree-of-freedom (4-DOF) nonlinear model of an off-road motorcycle. The modes involved in the analysis are bounce, pitch, and movement of each wheel. The motorcycle moves at constant speed and the ground excitation is modeled as a sinusoidal ground

profile. The study follows a time domain approach. The results show that the response is highly nonlinear. The authors also concluded that the maximum acceleration experienced by the driver occurs when the vehicle is forced in a pitching motion. However, they were not able to obtain experimental data to validate the results. De Molina [6] applied the finite element method (FEM) to the simulation of the driving behavior of motorcycles. His results showed discrepancies with experimental data. Nevertheless, it was perhaps the first dynamic analysis of a motorcycle in which the finite element method was used. Yokomori et al. [32] investigated the effect of rider leaning on controlling the in-plane motion of a motorcycle moving at low speed.

The need to improve the stability aspects of motorcycles at high speeds has also attracted the attention of researchers who have used in-plane models to analyze wobble and weave modes and their relation to stability [24, 25, 27, and 28]. To achieve a better description of the dynamical behavior of a motorcycle in cornering –where both, in-plane and out-of-plane modes of vibration are coupled– more complex models have been proposed. Cossalter and Lot [29] developed a 3D multi-body model that involves eleven degrees of freedom and takes into account the non-linear properties of tires and suspensions. The natural coordinates approach was applied in the derivation of the equations of motion. Constant cornering and a flat road (no roughness) were considered. This model has been used to study the vibrational modes of a motorcycle in straight running and on a curve [33]. The complexity required in the description of a 3D model has led other researchers to opt for a computer assisted multi-body modeling approach [28, 29, and 31]. The availability of 3D models and multi-body codes has allowed the development of several motorcycle simulators [34, 35, and 37].

1.3 Motivation and Objectives

Even though the amount of publications related to motorcycle dynamics is large, most of them present almost identical approaches for solving the governing nonlinear differential equations. Efforts for presenting new methods of simulating road excitations, which are stochastic in nature, are scarce. It is the stochastic nature of the road roughness, as it influences the motorcycle dynamics, which will be the focal point of this thesis. Naturally, this will lead to the formulation of a nonlinear stochastic dynamics problem.

Note there are several numerical techniques that are in use to solve nonlinear systems stochastic dynamic problems. However, with the exception of the Monte Carlo (MC) method, most methods present serious limitations when the nonlinear problems involve strong nonlinearities. A detailed discussion of these nonlinear methods is presented in Chapter 3. Clearly, if the model used is linear, besides the time domain approach, a frequency domain approach can be used [36]. However, when nonlinearities are present the traditional frequency domain approach does not apply [136]. Thus, if both nonlinear behavior and road randomness are to be considered in the dynamic analysis of motorcycles, the number of techniques available to deal with the problem is limited.

With regards to roughness modeling for time domain deterministic analysis, most of the studies in which the response of the motorcycle to ground excitation is studied, involve a sinusoidal type roughness. For stochastic approach studies, white noise is considered as the excitation in most of the cases. In other studies a sinusoidal excitation with either random amplitude or random angular phase is used. If the excitation is obtained from certain road power spectrum the harmonic superposition simulation method is the common choice among researchers.

The previous discussion leads to consider the necessity of investigating alternate methods that can be included in motorcycle dynamics research, which may be implemented in a practical and reliable way, and to allow a significant reduction in the computing time.

To the author's best knowledge, at the present time there are no reported studies that treat the case of the interaction between a motorcycle and the road by using a time domain approach in which the excitation complies with certain road roughness power spectrum and is generated by autoregressive (AR) filters. Further, neither use of the statistical linearization method (SLM) in both, the time domain approach and the frequency domain approach, is made in motorcycle dynamics studies.

In context with the preceding comments, the primary objective of this work is to propose the SLM as an alternate and reliable technique to tackle nonlinear problems that appear in the motorcycle dynamics field and involve strong nonlinearities. The SLM is chosen due to its computational simplicity and fast convergence to an accurate solution. The reason for choosing this particular method becomes clearer when investigating the problem presented in Chapter 7, concerning the estimation of the spectral characteristics of the response of a motorcycle model that includes nonlinear elements in its front and rear suspension systems, and is subjected to stationary road excitation. The thesis will show that, when the SLM is used to obtain the nonlinear system response from a linear approach, the results obtained are reliable in a wide range of velocities and for different kinds and degrees of nonlinearities included in the motorcycle model. To achieve this purpose, the results obtained from applying the SLM are validated by pertinent MC simulations, since no access to experimental data has been possible.

As previously mentioned, motorcycle dynamics analysis requires the generation of accurate excitation signals which comply with a prescribed road power spectrum. Thus, the

secondary objective of this dissertation is to advocate the use of AR filters for generating the input signals for the time domain analysis of the nonlinear system. Several features make these filters an effective tool in fitting a power spectrum and synthesizing signals that comply with it. They are computationally robust, and efficient, and allow reaching the desirable accuracy by simply increasing the order of the filter [64].

1.4 Thesis Outline

Chapter 2 introduces the topic of random processes and provides a discussion of the necessary concepts to understand the response of the motorcycle to road excitation as a stochastic process. The statistical parameters required to characterize a stochastic process are also reviewed. The justifications of certain assumptions used in the analyses presented are discussed here, in the case of the assumed normality of both the excitation and the system's response. A brief discussion of concepts useful in signal processing is given, since it is required to work with signals in both the time and the frequency domains. The mathematical relationships employed in the spectral analyses of the motorcycle's response are also included in this chapter. Certain elements of linear systems theory are also reviewed. Finally, the concepts presented with respect to a single-DOF system are extended to the case of multi-DOF (M-DOF) systems.

Chapter 3 presents a discussion of the methods of analysis of nonlinear systems commonly used in the automotive field. Advantages and drawbacks of each method are contrasted versus the SLM, which is proposed in the thesis as a method for the analysis of nonlinear M-DOF models of motorcycles.

Chapter 4 presents a discussion of the general formulation of the SLM applied to M-DOF systems. A brief discussion of the state of the art of the method is provided, and a link

with the spectral theory is established. This chapter serves as the general background required to implement the technique in any field, while the particular details of implementation for the analysis of motorcycle dynamics are left for a subsequent chapter.

Chapter 5 is devoted to the description of road roughness and the generation of time series compatible with a given road power spectrum. An account of the state of the art in this subject is presented, and the concepts on random processes discussed in Chapter 2 are used to explain how roads are characterized. The main body of Chapter 5 is devoted to the synthesis of excitation time histories by means of auto-regressive-moving-average (AR) filters. The theory of this algorithm is briefly discussed and it is shown, by an example, how the technique can be applied.

Chapter 6 reviews certain elements of motorcycle dynamics. The classification of the motorcycle motion in two general modes is established, but the discussion is focused primarily on in-plane motion. Nevertheless, a general description of the motorcycle in geometric terms is given. Also, the main components of a motorcycle that are essential to obtain a simplified model are discussed along with the required simplifying assumptions. A 4-DOF motorcycle model is presented. The derivation of the governing equations is discussed along with the derivation of the relationships between the absolute coordinate system and the relative coordinate system in which the motorcycle model may be expressed. This chapter also presents a dynamic analysis of the 4-DOF model to road roughness. It highlights the effect of the wheelbase filtering effect on the dynamic response of the motorcycle, and the importance of analyzing the frequency response function of the motorcycle for various velocities as a way to ensure the appropriate implementation of the SLM and for assessing the range of velocities in which the results obtained by this method are reliable. As a way of validating the correct implementation of the MC technique, which

in turn is used to validate the results obtained with the SLM, a linear 4-DOF model is analyzed in the frequency domain and its solution is compared with that obtained via MC simulation. A discussion of results is provided.

Chapter 7 contains the implementation details of the statistical linearization method. The specific assumptions required to adapt the method to the analysis of motorcycle dynamics are explained, along with the kind of nonlinearities considered. A step-by-step implementation outline is described at the end of the chapter.

Chapter 8 presents two cases where the statistical linearization technique is applied. Along with the results obtained with the statistical linearization method, MC simulations are reported. Comparisons between the two set of results are presented along with a discussion of the results.

Chapter 9 provides an overview of the needs detected, the methods of solution proposed, and the implementation methodologies employed. The results obtained are assessed, and further research is proposed.

Chapter 2

An Overview of Stochastic Processes and Linear Systems

2.1 Introduction

This chapter provides a discussion of the main concepts involved in the analysis of linear systems subjected to random vibrations. This material is part of the background knowledge required to understand how the excitation of the road and the motorcycle's response are treated as signals in a stochastic manner, and to understand how the SLM is implemented.

A brief description of concepts in random processes is presented. For a more thorough treatment of concepts on random processes the reader may consult references [55-57, and 87].

Several concepts of mechanical vibrations are involved in this thesis, and those considered relevant for the present work are explained. The theory of mechanical vibrations is quite broad and many books are available; some examples are references [45, 46, 48, 53, and 54].

To set up the appropriate theoretical background for studying random vibrations, a S-DOF system is used to show how these elements can be combined with the concepts of stochastic processes presented. Further, the results discussed are extended to the case of M-DOF systems. References [26, 39-42, 54, 55, and 61] are suggested for an in depth explanation of random vibrations.

Finally, since it is necessary to obtain the power spectrum of the time histories synthesized by the auto-regressive filter and of those obtained as the motorcycle's response, an introduction to spectrum estimation is also provided.

2.2 General Concepts of Stochastic Processes

If the description and analysis of the response of mechanical systems can be done by an explicit mathematical relationship between the input variables of a system and its response, a deterministic approach can be used. However, if randomness plays a key role the problem must be treated from a different perspective. By *randomness* it is meant that, under the same conditions, a series of experiments, all of them performed in the same fashion, will lead to different responses, even though on the ‘average’, they have the same overall behavior. It turns out that, in general, one record or time history is not enough to describe the response of the system, but rather a collection, or an *ensemble* of possible time histories, also called *realizations*. Later in this chapter it will be shown that under certain conditions, a single record of sufficient length can often be used to obtain the statistical characteristics of the process.

A random process must be specified in terms of statistical parameters, such as its *mean* and *variance*, and functions such as the *power spectrum*. These concepts will be defined and discussed in the chapter. The description of a random process is given in terms of a *random variable* (rv). The rv can be characterized in a probabilistic manner by means of its *probability density function* or pdf, which is expressed as $f_x(x)$.

The pdf of the rv x is a statistical measure that defines a probability distribution for a random variable. If the pdf of a random variable x is available, certain statistical measures can be calculated, namely the mean, mean square, standard deviation, and variance. The *mean value* or *expected value* computes a statistical average of the rv x by using its pdf as a weighing function, and is defined as

$$E\{x\} \triangleq \mu_x = \int_{-\infty}^{\infty} x f_x(x) dx. \quad (2.1)$$

The mean can be interpreted as the ‘center of gravity’ of the pdf associated to x .

Based on the expected value operation a description of certain useful aspects of the pdf can be made. The *moments* of x are defined as

$$E\{x^m\} = \int_{-\infty}^{\infty} x^m f_x(x) dx. \quad (2.2)$$

According to this definition, the first moment ($m=1$) corresponds to the mean value μ_x .

The second moment or *mean-square value* of x is then defined as

$$E\{x^2\} = \int_{-\infty}^{\infty} x^2 f_x(x) dx. \quad (2.3)$$

The square root of Equation (2.3) is called the *root mean square value* (rms).

The variance of x , denoted by σ_x^2 , is also called the *second central moment* of x and is defined as the average value of the square of the deviation of x from its mean value μ_x [41].

That is,

$$\sigma_x^2 \triangleq E\{(x - E\{x\})^2\} = E\{x^2\} - (E\{x\})^2. \quad (2.4)$$

The square root of σ_x^2 , also called the *standard deviation* of x , is a measure of the dispersion of the x values around its mean μ_x .

It is a well known fact that in nature many phenomena follow a symmetric bell-shaped pdf centered at μ_x . This pdf is called the *Gaussian* or *normal distribution*, and is given by the equation

$$f_x(x) = \frac{1}{\sqrt{2\pi}\sigma} e^{-\frac{(x-\mu)^2}{2\sigma^2}}. \quad (2.5)$$

Due to this fact, in many practical engineering applications it is assumed that the random process is Gaussian. The mathematical justification for this assumption is based on the *Central Limit Theorem*, which states that the sum of infinitely many independent random variables, having individual arbitrary distributions, will tend to have a Gaussian probability distribution [57].

It is worth noting that the Gaussian distribution is completely determined by its first two moments, the mean μ_x , and the variance σ_x^2 . One property of a Gaussian random variable that is of great importance in random vibrations is that any linear combination of Gaussian random variables is Gaussian, as well. Hence, when analyzing stochastic linear systems one can expect that given a Gaussian input, the system output is Gaussian, as well [39].

In engineering, the experiments carried out involve time and some others space as well. The general idea of a random variable as the numerical value related to an experiment's outcome is now extended to the concept of *stochastic* or random process, which can be conceived as an infinite set, or 'ensemble' of all possible time histories, or 'realizations' $x_1(t), x_2(t), x_3(t), \dots, etc.$ Together, these realizations make up the stochastic process. Each realization is the outcome of one experiment carried out under the same conditions as the others. The whole random process is denoted by $\{x(t)\}$. Even though in practice it is not possible to obtain an infinite set of realizations, it is feasible to obtain a large number of them, which allows a good approximation for the infinite ensemble of a random process. An ensemble from a stochastic process is shown in Figure 2.1.

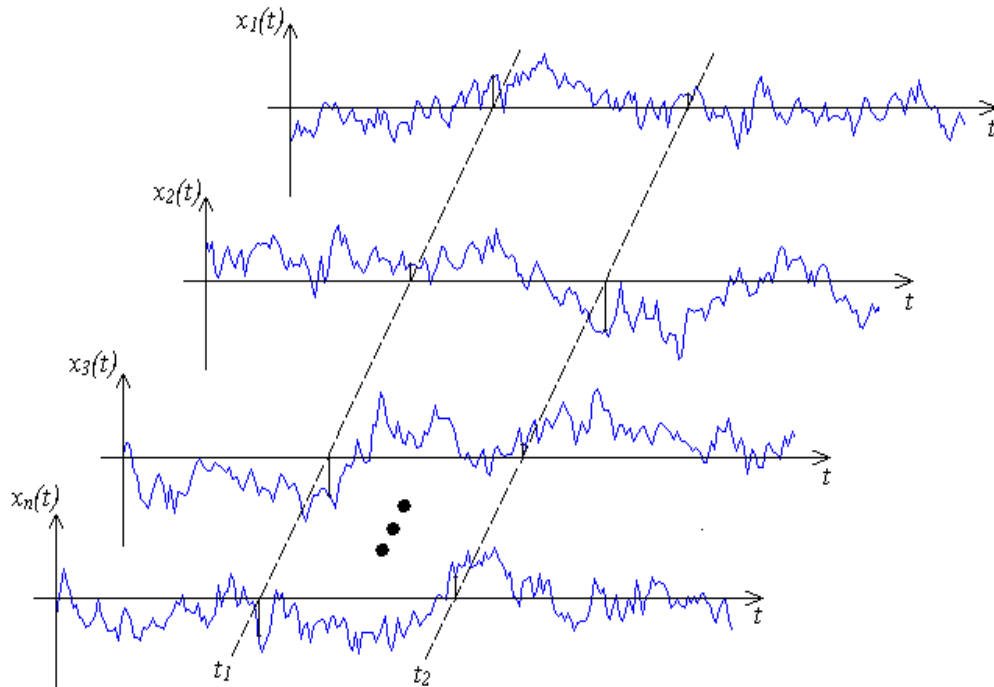


Figure 2.1 Ensemble from a stochastic process and averaging.

Ensemble averaging is an alternate way of calculating averages, and involves measuring the averages across the ensemble, refer again to Figure 2.1. If enough sample functions are available, the first-order probability distribution for $\{x(t)\}$ at t_1 can be calculated by determining the value of each sample at time t_1 . Moreover, the second-order probability distribution for $\{x(t)\}$ at t_1 and $\{x(t)\}$ at t_2 can be found by obtaining a second series of measurements at time t_2 .

A stochastic process is called *stationary* if its statistical properties do not change with time. In practical terms, this means that all the experiments are carried out under the same conditions, so that the probability distributions obtained for the ensemble of time histories $\{x(t)\}$, are dependent only on the time difference $t_2 - t_1$, i.e. they are independent of absolute time t [42]. As a consequence, the mean value μ_x , and the standard deviation σ_x are constants [39]. If, in addition the experimental conditions remain

steady during each experiment the stochastic process is called *ergodic*, which, statistically speaking, means that at any one time, the quantities $x_1(t_1), x_2(t_1), \dots$, have a distribution equal to the distribution with respect to time of any single member function of the random process [42].

An important consequence of regarding a stochastic process as ergodic is that once the statistical properties of a single time history $x(t)$ are determined, the statistical properties of the ensemble $\{x(t)\}$ can be defined. This allows the use of a single long enough time history to determine the statistical characteristics of the ensemble [39]. The characterization of the statistical properties of a given road or its roughness is an example of this conclusion. A section of adequate length of a road that possesses certain random properties is used to characterize that type of road instead of using several sections of a road. This approach simplifies greatly the characterization process and gives accurate statistical results from the data obtained [67-69, and 164]. Chapter 5, dedicated to road roughness, explains in more detail this procedure.

In the characterization of a stochastic process $\{x(t)\}$ the *autocorrelation function* R_x of $x(t)$ plays an important role. Denoting by τ the time lag between two x values on the same time history, that is $\tau = t_2 - t_1$, R_x is defined as the expected value of the product $x(t)x(t + \tau)$, or $E\{x(t)x(t + \tau)\}$. With reference to Fig. 2.1, the computation of the autocorrelation function is made by sampling the process at instants t and $t + \tau$, and the expected value of the product $x(t)x(t + \tau)$ computed for the ensemble. For a stationary process, R_x will be independent of absolute time t and will depend only on the time lag τ , hence it can be written

$$R_x(\tau) = E\{x(t)x(t + \tau)\}. \quad (2.6)$$

Some useful properties of $R_x(\tau)$ that are quite helpful in the stochastic analysis of the dynamic response of linear and nonlinear systems subjected to random excitation can be mentioned. Specifically, based on the fact that for a stationary random process, the mean value μ_x , and the standard deviation σ_x are constants, it can be proved that the value of the autocorrelation function is bounded as follows [41]

$$-\sigma_x^2 + \mu_x^2 \leq R_x(\tau) \leq \sigma_x^2 + \mu_x^2 = E\{x^2\}. \quad (2.7)$$

If the time lag τ is zero, the autocorrelation function equals the mean square value of the process

$$R_x(\tau = 0) = E\{x^2\}. \quad (2.8)$$

As the time lag between the values $x(t)$ and $x(t + \tau)$ increases, the coherent relationship between these two values decreases, and as a result as $t \rightarrow \infty$, the value of R_x becomes the mean value of $\{x(t)\}^2$,

$$R_x(\tau \rightarrow \infty) \rightarrow \mu_x^2. \quad (2.9)$$

The last property of the autocorrelation function discussed in this section considers the fact that for a stationary process, $R_x(\tau)$ depends only on the time lag τ . This leads to the conclusion that $R_x(\tau)$ is an even function. That is

$$R_x(\tau) = E\{x(t)x(t + \tau)\} = E\{x(t)x(t - \tau)\} = R_x(-\tau). \quad (2.10)$$

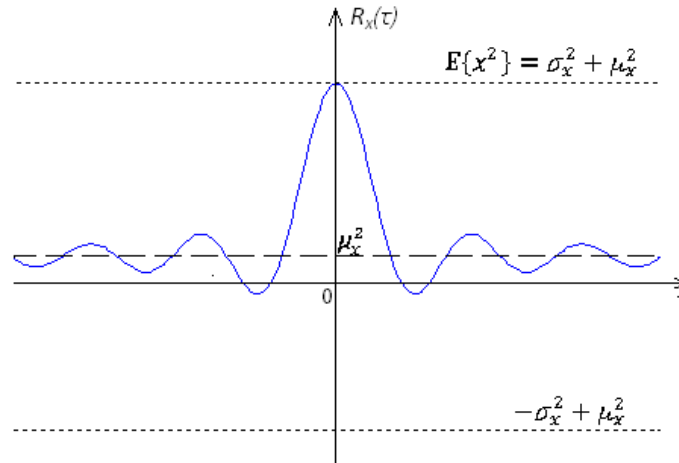


Figure 2.2 Typical graph of $R_x(\tau)$ and its properties for a stationary random process.

The properties of the autocorrelation function discussed above are graphically captured in Figure 2.2.

The autocorrelation function is useful in describing the manner of the fluctuation of a quantity, but this description is better achieved if, along with the concept of autocorrelation function, a harmonic analysis approach is adopted. Section 2.7 presents a brief discussion of the main concepts needed in the description of random processes in terms of frequency content, and it will be shown how they are applied in the study of the mechanical behavior of a linear system operating in a random environment.

To obtain information about the frequency composition of a stationary stochastic process $\{x(t)\}$, its autocorrelation function $R_x(\tau)$ is analyzed by means of a Fourier transform approach. The *spectral density* $S_x(\omega)$, also known as the *power spectrum*, is defined as the Fourier transform of the autocorrelation function, $R_x(\tau)$ and describes the distribution of variance in frequency of the random process.

$$S_x(\omega) = \frac{1}{2\pi} \int_{-\infty}^{\infty} R_x(\tau) e^{i\omega\tau} d\tau. \quad (2.11)$$

Its inverse is defined by

$$R_x(\tau) = \int_{-\infty}^{\infty} S_x(\omega) e^{-i\omega\tau} d\omega. \quad (2.12)$$

Equations (2.11) and (2.12) are also known as the Wiener-Khinchine relations.

By considering the limiting case of Equation (2.12) in which $\tau=0$

$$R_x(0) = E\{x^2(t)\} = \int_{-\infty}^{\infty} S_x(\omega) d\omega. \quad (2.13)$$

Therefore, the mean square value of a stationary random process equals the area under the power spectral density curve, as shown in Figure 2.3.

Both $R_x(\tau)$ and $S_x(\omega)$ are even functions, hence they can be written as

$$S_x(\omega) = \frac{1}{2\pi} \int_{-\infty}^{\infty} R_x(\tau) \cos(\omega\tau) d\tau, \quad (2.14)$$

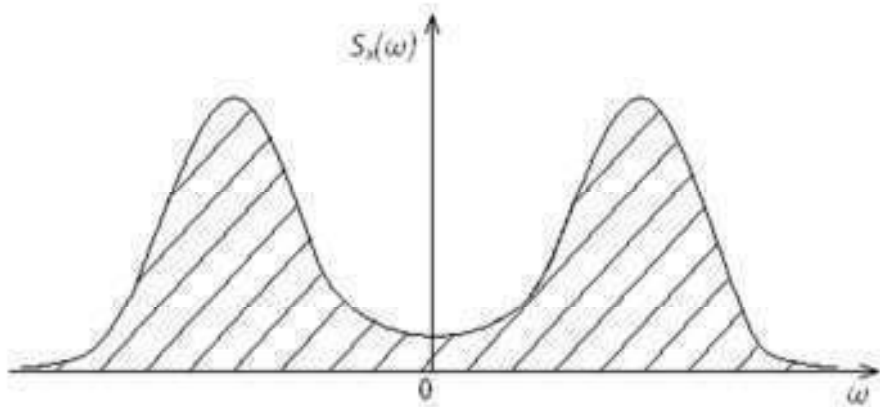


Figure 2.3 The area enclosed by the power spectrum graph equals the mean square value of $x(t)$.

and

$$R_x(\tau) = \int_{-\infty}^{\infty} S_x(\omega) \cos(\omega\tau) d\omega. \quad (2.15)$$

The dimensions of $S_x(\omega)$ are mean square per unit of circular frequency.

The preceding definition of the power spectrum $S_x(\omega)$ is convenient for analytical investigations. However, for some practical purposes, as in the case of automotive studies, the *experimental spectral density* is used, and is denoted by $W(f)$, where f is the frequency in cycles per unit time or Hertz (Hz). The relation between $S_x(\omega)$ and $W(f)$ is simply [41]

$$W(f) = 4\pi S_x(\omega). \quad (2.16)$$

An example of the experimental spectral density is given in Figure 2.4 where the PSD of the roughness of certain road for a vehicle traveling at 50 mph is shown. Some characteristics of typical road roughness PSDs can be observed from Figure 2.4. The data are represented in a log-log plane and the real road data is shown along with the average data. As it will be seen later the log-log graphs present some advantages over linear-linear graphs when analyzing random data.

In place of Equation (2.13) one has

$$R_x(0) = E\{x^2(t)\} = \int_0^{\infty} W(f) df. \quad (2.17)$$

It can be proved that the spectral density $S_{\dot{x}}(\omega)$ of the derivative process $\{\dot{x}(t)\}$, can be obtained from the spectral density $S_x(\omega)$ of $\{x(t)\}$ by means of the relation

$$S_{\dot{x}}(\omega) = \omega^2 S_x(\omega). \quad (2.18)$$

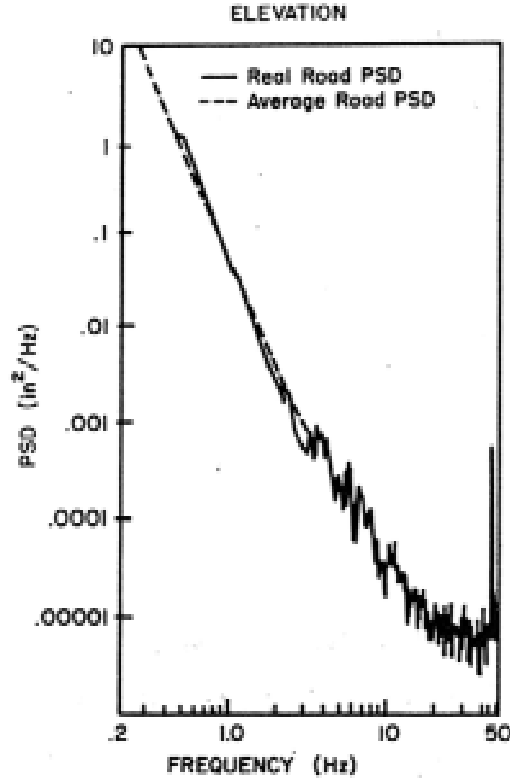


Figure 2.4 PSD of the elevation of a typical road (from [93]).

Similarly, for the second derivative,

$$S_{\ddot{x}}(\omega) = \omega^4 S_x(\omega) = \omega^2 S_{\dot{x}}(\omega). \quad (2.19)$$

Equations (2.18) and (2.19) ease the dynamic analysis by providing simple relationships between the PSDs of displacement (ground elevation), velocity and acceleration.

2.3 Broad Band Processes

The classification of stationary stochastic processes into broad and narrow processes does not correspond to precisely defined frequency intervals. A *broad* or *wide process* is characterized by a power spectrum whose frequency values lie within a band of frequencies, which is about the same order of magnitude as the center frequency of the

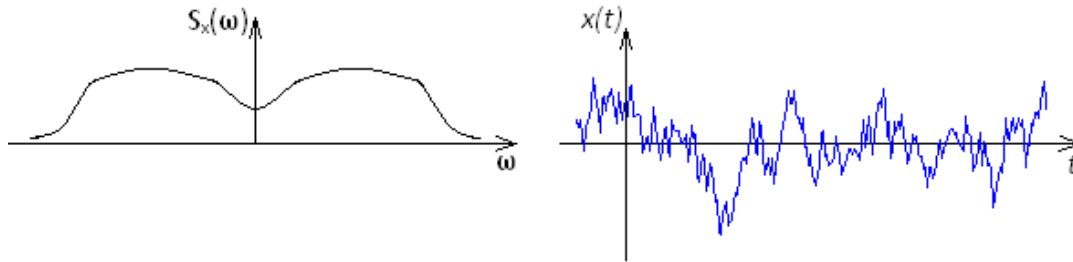


Figure 2.5 Broad band process. Power spectrum and time history.

band. The time history of a broad band process is a combination of the whole band of frequencies involved. Figure 2.5 depicts a typical broad band process and its associated time history. Road roughness PSDs and response PSDs of vehicles traveling over rough roads are examples of broad band processes.

A quite common and useful idealization of a broad band process is the one called *white noise*. This process is the result of assuming a uniform power spectrum S_0 which spans over the frequency interval $(-\infty, \infty)$, Figure 2.6. This definition of white noise implies that the mean square value of the process would be infinite making it not physically possible to obtain. However, in analyzing a process, the frequency bandwidth can be extended enough to include all the frequencies of interest.

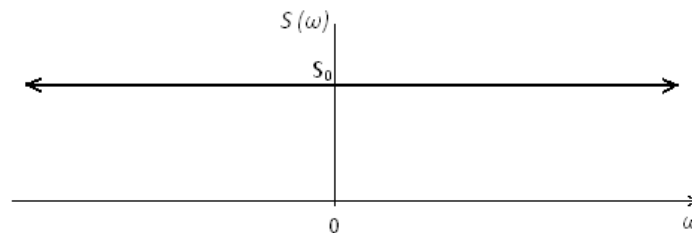


Figure 2.6 Power spectrum of ideal white noise.

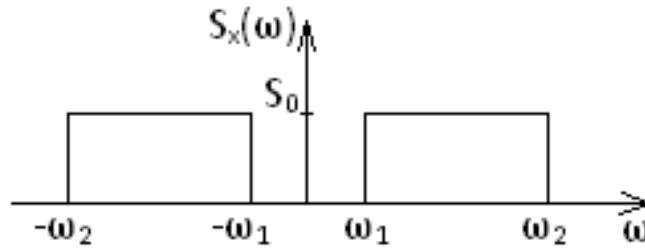


Figure 2.7 Power spectrum of clipped white noise.

This *band-limited* or *clipped white noise* can be used to obtain reliable results that represent a close approximation to the actual process, provided that the system being analyzed is not sensitive to the frequencies that lie beyond the chosen bandwidth limits. The power spectrum of band-limited white noise is shown in Figure 2.7.

2.4 General Concepts on Linear Systems and Digital Signal Processing

A system is often represented in a *black box* fashion, as shown in Figure 2.8. The system may have several inputs and outputs, all of them vary with time.

The description of the system can be made in mathematical terms through the use of an equation or a set of equations depending on how the system is deemed. This is called *modeling the system* and the equation or set of equations correspond to the *model*. Depending on the type of equations used, models are classified in several ways [49]. If the criterion for classification employed is the spatial characteristics of the system, or in other words, if the system is considered as a continuum or as a set of interconnected discrete parts, then the model could be called a distributed mass model in the first case or as a lumped model in the second case. The classification of the mathematical model could be done based on the continuity of the time variable in which case the model is considered continuous-time or discrete-time.

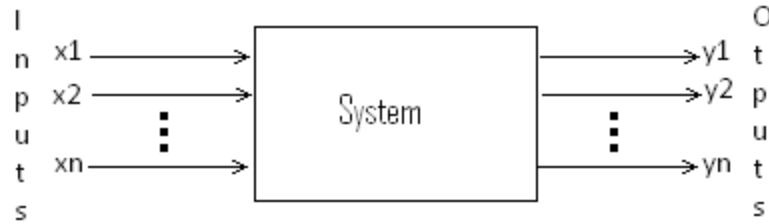


Figure 2.8 General schematic representation of a system.

Other criteria for classifying a model can involve parameters variation, linear or nonlinear behavior, etc. Of course, a combination of the previous criteria and others not mentioned here is possible.

2.5 Mathematical Modeling

2.5.1 Lagrange's Equations

In order to derive the equations of motion of a M-DOF system, vector quantities such as force and acceleration, are required while applying Newton's laws. This procedure can become very tedious. The use of Lagrange's equations eases this task [39]. Instead of vector quantities, scalar quantities, like work and kinetic energy, are required. Lagrange's equations can be derived from the principle of virtual displacements [47] or from Hamilton's principle. Here, they are briefly presented.

Every point within an n-DOF system is specified by a set of n independent quantities q_i ($i=1, 2, \dots, n$) called *generalized coordinates*. For the n-DOF system the kinetic energy T , and the potential energy V , can be expressed in terms of the generalized coordinates and their first time derivatives. The virtual work of nonconservative forces δW_{nc} , is expressed in terms of arbitrary variations in the generalized coordinates δq_i .

Thus,

$$\begin{aligned}
T &= T(q_1, q_2, \dots, q_n, \dot{q}_1, \dots, \dot{q}_n), \\
V &= V(q_1, q_2, \dots, q_n, t), \\
\delta W_{nc} &= Q_1 \delta q_1 + Q_2 \delta q_2 + \dots + Q_n \delta q_n,
\end{aligned}$$

where Q_1, Q_2, \dots, Q_n are called the *generalized forces*

Lagrange's equations have the form

$$\frac{d}{dt} \left(\frac{\partial T}{\partial \dot{q}_i} \right) - \frac{\partial T}{\partial q_i} + \frac{\partial V}{\partial q_i} = Q_i, \quad i = 1, 2, \dots, n \quad (2.20)$$

Lagrange's equations are applicable in the derivation of the equations of either linear or nonlinear systems.

2.5.2 Other Modeling Approaches

Although Lagrange's approach represent an easier way of deriving the equations of motion of n-DOF systems than Newton's approach, the derivation process will become cumbersome as the number of degrees of freedom increases [29]. Thus, alternative approaches have been considered for motorcycle modeling. Cossalter and Lot [29] used the natural coordinate's approach [62] to develop an 11-DOF model which included two sub-models: a 6-DOF motorcycle model with the rider considered firmly attached to the rear assembly, and a 5-DOF tire model that allows the correct description of tire dynamics at large camber angles. Bos [147] analyzed the steering behavior of a motorcycle by using a model derived by applying bond graphs, an approach developed by Karnopp and Rosenberg [146].

During recent years the use of multibody dynamics software for dynamics analysis has also become popular among the research community. Goncalves and Ambrosio [7]

modeled a car suspension employing a FEM software to represent the interaction among the multiple flexible components of the system. Lot, Cossalter and Massaro [170] described a motorcycle model obtained by automatic derivation of the symbolic linearized equation of motions.

Although automated multibody analysis software simplifies the derivation of equations process, at some point it may present certain limitations regarding the description of the features of the model into consideration. As a consequence, to obtain a model that includes all the aspects required in the analysis becomes problematic. In such a case, the researcher has to resort in the techniques of mathematical modeling and dispense with the modeling software. Furthermore, regarding computational efficiency, mathematical modeling leads to faster simulations [29].

2.6 General Excitation-Response Relations

Figure 2.9 shows a typical representation of a single-degree of freedom (S-DOF) linear model characterized by its mass m , damping c , and stiffness k . These parameters are assumed to be constant, i.e., they are not changing with time. Thus this type of system is also called *linear time-invariant*, or *LTI*.

If the system of Figure 2.9 is subjected to a time varying force $F(t)$ then, according to Newton's second law, its equation of motion is expressed as

$$m\ddot{x} + c\dot{x} + kx = F(t). \quad (2.21)$$

Equation (2.21) exemplifies a mathematical characteristic of an LTI system; its equation of motion has the form of a linear differential equation with constant coefficients.

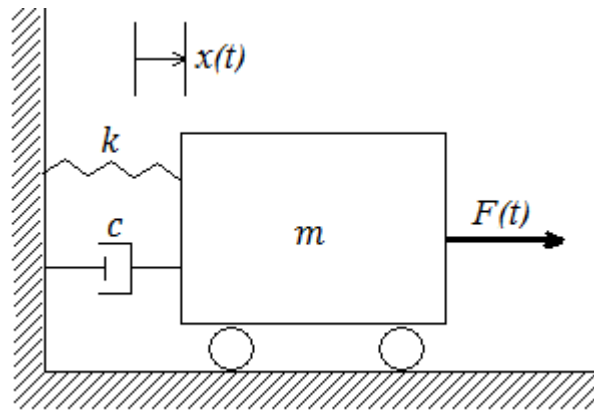


Figure 2.9 Single-degree of freedom linear model.

The system discussed can also be represented using a black-box diagram, similar to the one depicted in Figure 2.8. In this case, there is only one prescribed input, the excitation force $F(t)$; and, under given initial conditions, one output corresponding to the displacement $x(t)$. The introduction of this pictorial representation is useful in describing the dynamic characteristics of a linear system based on the determination of the response to a sine wave input.

A property of a linear system is that for a deterministic excitation a deterministic response can be found by integrating the differential equations of motion, provided the initial conditions are specified. For this purpose among the established methods available [45-48] a time domain approach and a frequency domain approach are considered.

If the system is subject to a random excitation, the response is also random. In this situation the system's response is characterized by various statistical parameters that are determined from the statistical parameters of the excitation, and the system's equations of motion. An important characteristic of a linear system under random excitation is that if this excitation is Gaussian, then the system's response is also Gaussian [39]. For most physical linear systems this is a reasonable assumption based on the Central Limit Theorem

(section 2.2), which allows a criterion for characterizing the probability distribution of the response, especially in the absence of knowledge of the true probability distribution.

2.7 Complex Frequency Response

For a steady state simple harmonic excitation $F(t)$ acting on a LTI system, the corresponding response $x(t)$ is also a steady state simple harmonic motion, whose amplitude and phase will be functions of the driving frequency ω . Mathematically this can be expressed as

$$F(t) = e^{i\omega t}, \quad (2.22a)$$

and

$$x(t) = H(\omega) e^{i\omega t}. \quad (2.22b)$$

The *complex frequency response* $H(\omega)$ describes this dependence; for an arbitrary excitation the response can be obtained, provided $H(\omega)$ is known. It can be obtained by substituting $F(t)$ and $x(t)$ as given by Equation (2.22a) and (2.22b) into Equation (2.21), and solving for $H(\omega)$.

For a linear system, the *principle of superposition* holds. This principle allows to treat a periodic excitation $F(t)$ as built up of sinusoids (a Fourier series). The same reasoning applies for the periodic response $x(t)$. In a similar fashion, if $F(t)$ is not periodic but has a Fourier transform, the output $x(t)$ can be expressed in the frequency domain as [40]

$$X(\omega) = H(\omega)F(\omega), \quad (2.23)$$

where

$$F(\omega) = \int_{-\infty}^{\infty} F(t)e^{i\omega t} dt; \quad X(\omega) = \int_{-\infty}^{\infty} x(t)e^{i\omega t} dt. \quad (2.24)$$

In motorcycle dynamics, and in general, in vehicle dynamics, the input-output relationship Equation (2.23) is a potent way of characterizing the dynamic behavior of the vehicle, this is due to the fact that a linear relationship between the input (driving force) and the output (response) is established, in which the dynamic properties of the system are contained in $H(\omega)$. This equation also allows identifying $H(\omega)$ as the ratio of the output to the input. One clear advantage of using this approach is that the input of the system considered may be any of the excitations discussed, or a combination thereof. Typically, interest is focused on the vibrations on the body as the system's output. The "gain" for the dynamic system is defined as the ratio of output to input amplitudes. A common way to denote the gain is by the term "transmissibility", which, for a system subjected to steady-state forced vibration, is the dimensionless ratio of response amplitude to excitation amplitude. Displacements, velocities, accelerations or even forces can be used in this ratio [93].

If both $F(t)$ and $x(t)$ are stationary stochastic processes, a quite important connection, in the frequency domain, between the power spectra (Equation (2.11)) of the input and the output exists. Specifically,

$$S_x(\omega) = H(-\omega)H(\omega)S_F(\omega), \quad (2.25)$$

or, since $H(\omega)$ is a complex quantity

$$S_x(\omega) = |H(\omega)|^2 S_F(\omega). \quad (2.26)$$

Equation (2.26) plays a key role in random vibration theory. It shows the response changes according to the change in the random driving force.

2.8 Mean Square Response

Based on the result of Equation (2.26) and (2.13), the mean square value of the response can be expressed as

$$E\{x^2(t)\} = \int_{-\infty}^{\infty} S_x(\omega) d\omega = \int_{-\infty}^{\infty} |H(\omega)|^2 S_F(\omega) d\omega. \quad (2.27)$$

When dealing with stationary driving inputs, Equation (2.26) and (2.27) are the main tools used in random vibration analysis. This approach is applied in this work for the analysis of a motorcycle traveling at a constant forward velocity over a random road surface.

2.9 Generalization of the Excitation-Response Relations to M-DOF Systems

In many applications the description of the vibratory motion of a mechanical system can be done with a good degree of approximation by means of a single (independent) coordinate and a single second-order differential equation, which are associated to one single body. However, many mechanical devices and structures cannot be modeled as a S-DOF system. Single-track vehicles, such as motorcycles, and machines with many moving parts have many degrees of freedom. These systems can be treated as *lumped-parameter-models*, in which the mass is ‘lumped’ into a finite number of rigid bodies [39]. This approach allows obtaining a *M-DOF model*. For mechanical systems these models consist of dampers and springs, which serve as connectors, and permit the interaction between masses; or between masses and the system’s surroundings. It is important to note that the

number of degrees of freedom associated to a lumped-parameter model is equal to or greater than the number of lumped masses.

For a linear lumped-parameter n degree of freedom system the general form for the equations of motion associated to it can be expressed in matrix notation as

$$\mathbf{M}\ddot{\mathbf{q}} + \mathbf{C}\dot{\mathbf{q}} + \mathbf{K}\mathbf{q} = \mathbf{Q}, \quad (2.28)$$

where the $n \times n$ symmetric matrices \mathbf{M} , \mathbf{C} , and \mathbf{K} stand for inertia, damping, and stiffness respectively. The $n \times 1$ vector \mathbf{q} contains the n generalized displacements of the system and the $n \times 1$ vector \mathbf{Q} contains the n generalized forces, corresponding to \mathbf{q} .

Similarly, the input-output relations associated with this M-DOF system in the frequency domain are

$$\mathbf{Y}(\omega) = \mathbf{H}(\omega)\mathbf{X}(\omega), \quad (2.29)$$

where the *frequency response function matrix* $\mathbf{H}(\omega)$ can be computed as follows

$$\mathbf{H}(\omega) = [-\omega^2\mathbf{M} + i\omega\mathbf{C} + \mathbf{K}]^{-1}, \quad (2.30)$$

this matrix can be used to compute the spectral density matrix of the response $\mathbf{S}_x(\omega)$ in terms of the power spectral matrix of the excitation $\mathbf{S}_F(\omega)$, specifically,

$$\mathbf{S}_x(\omega) = \mathbf{H}(\omega)\mathbf{S}_F(\omega)\mathbf{H}(\omega)^{T*}, \quad (2.31)$$

where the symbols T and * denote transposition and conjugation, respectively.

Upon determining $\mathbf{S}_x(\omega)$, the covariance matrix of the response process can be obtained as

$$\sigma_{\hat{\mathbf{x}}}^2 = \int_{-\infty}^{\infty} \mathbf{S}_x(\omega) d\omega, \quad (2.32)$$

and

$$\sigma_{\dot{x}}^2 = \int_{-\infty}^{\infty} \omega^2 \mathbf{S}_x(\omega) d\omega. \quad (2.33)$$

Once the mathematical model has been set up, it must be placed within a theoretical framework required to analyze and describe the behavior of the system under the action of the prescribed inputs. Within the context of the present work, namely a motorcycle subjected to road excitation, the theory of vibrations provides such a theoretical framework.

2.10 State-Space Models

If one is interested only in the input-output relationships of a linear n-DOF system, a mathematical model, as the one represented in matrix form by Equation (2.28), can be constructed. However, in many cases some important aspects of the system's behavior can be analyzed by taking into account the other variables that are internal to the system. This can be accomplished by means of a *state-space* model, which can be obtained by defining a set of independent variables, commonly known as *state variables*. In general, these state variables differ from the output variables, but may include one or more of them. The state variables must be chosen so that knowledge of their values at any reference time t_0 and knowledge of the inputs for all $t \geq t_0$ is sufficient to determine the outputs and state variables for all $t \geq t_0$. This approach has found applications in diverse disciplines such as filter design, automatic control, robotics, and aerospace. The reader can find more details about the theory of state-space models in references [39, 46, 49, 51, 58-60].

The set of n coupled differential equations in Equation (2.28) can be expressed in state-space form by defining the $2n$ *state-vector* $\mathbf{z}(t)$

$$\mathbf{z}(t) = \begin{bmatrix} \mathbf{q} \\ \dot{\mathbf{q}} \end{bmatrix}, \quad (2.34)$$

which allows to obtain a first order matrix equation of the form

$$\dot{\mathbf{z}} = \mathbf{A}\mathbf{z} + \mathbf{f}, \quad (2.35)$$

where \mathbf{A} is a $2n \times 2n$ matrix so that

$$\mathbf{A} = \begin{bmatrix} \mathbf{0} & \mathbf{I} \\ -\mathbf{M}^{-1}\mathbf{K} & -\mathbf{M}^{-1}\mathbf{C} \end{bmatrix}, \quad (2.36)$$

and \mathbf{f} is the $2n \times 1$ excitation vector

$$\mathbf{f} = \begin{bmatrix} \mathbf{0} \\ -\mathbf{M}^{-1}\mathbf{Q} \end{bmatrix}. \quad (2.37)$$

2.11 General Concepts on Digital Signal Processing

2.11.1 Classification of Signals

A signal corresponds to a time-amplitude representation of the attributes or behavior of a physical phenomenon.

Usually a signal is not pure in the sense that along with the information that is of interest for the researcher, it carries undesirable random disturbances or unwanted signals that conflict with the desired signal. These disturbances are known as *noise*.

There is no unique way of classifying signals. According to continuity in time a common distinction is between *discrete-time signals*, also known as time series; and *continuous-time signals* or simply continuous signals.

In terms of its predictability signals are classified in two main groups: deterministic, and stochastic or random. *Deterministic signals* can be described by means of a definite

mathematical relationship, although in reality, there is always some noise added. However, in many applications it is advantageous to approximate or model a signal by means of a deterministic function. Deterministic signals are subdivided into two groups: periodic and aperiodic signals. *Periodic signals* follow a repetitive pattern every certain amount of time called the period of the signal. A single period is sufficient to describe a periodic signal. This repetitive behavior can be expressed mathematically as

$$x(t) = x(t + nT),$$

where T is the period (usually in seconds) and n is an integer.

Aperiodic signals are divided in two groups: almost periodic and transient signals. Almost periodic signals have a discrete description in the frequency domain although they are not periodic in the mathematical sense. The frequency description differs from the periodic one in that the various frequencies participating are not harmonics of some fundamental frequency.

Transformation of a signal from the time-domain into the frequency-domain and vice versa is commonly required for analysis and processing purposes. The transformation into the frequency-domain allows highlighting the frequency content of the signal, a feature barely difficult to quantify in its time-domain representation. The transformation from one domain to the other does not change the information content present in the signal.

2.12 Estimation of the Power Spectrum of Stationary Random Signals

Spectral analysis involves the characterization of the frequency content of a signal by means of a signal processing method [84]. Statistical analysis is used to assess the spectral content of noise present in signals. If the signal to be analyzed is treated as finite, as it

occurs in most real world signals, its underlying statistical characteristics are neither known nor can be determined in an exact way; only an estimate of its true spectrum can be obtained [69].

One useful and easy-to-implement way for estimating the power spectrum of a signal is the one originally proposed by Bartlett and known as the averaging periodogram method [20]. The method consists of transforming the coefficients of a discrete time signal $X(n)$ by obtaining its discrete Fourier transform $X(f)$

$$X(f) = T \sum_{n=0}^{N-1} X(n)e^{-i2\pi fnt}, \quad (2.38)$$

where N denotes the number of sample points of the discrete signal $X(n)$, T the sampling period and $n = 0, 1, 2, \dots, N - 1$. Once the Fourier transform is obtained the PSD of the signal at frequency f can be computed by the expression

$$P_x(f) = \frac{1}{NT} |X(f)|^2. \quad (2.39)$$

The periodogram method as proposed originally by Bartlett introduces bias in the computation of the PSD function. Welch [175] introduced a modification to reduce the bias. This modification consists on averaging certain overlapping portions of length- N input samples to compute the periodogram. Thus, an estimation of the PSD is obtained by calculating the average spectrum at all overlapping intervals. In the case of a stochastic process, described by an ensemble of records, the bias is reduced by computing the spectrum for each record and then averaging all the spectra.

Chapter 3

Methods of Nonlinear Analysis

3.1 Introduction

The description and analysis of mechanical systems by the linear systems approach is in many cases insufficient to describe the dynamic behavior of many systems such as the suspension and the component parts of a vehicle when it is subjected to strong road excitation. If the system behaves linearly and the excitation is stationary, the evaluation of the response statistics is straightforward; there are several techniques to obtain, in most cases, a closed form solution. However, when the magnitude of such excitation is high enough to drive the system to exhibit nonlinear behavior, or when the system parameters are changing, the dynamic analysis of the vehicle requires techniques which apply beyond the linear response range. Unlike linear vibration systems, when dealing with nonlinear vibration problems the superposition principle does not apply. However, since most linear analysis techniques make use of the superposition principle, many researchers have attempted to obtain alternative formulations to find a general solution for nonlinear analysis by superimposing particular solutions [139, 143]. Another limitation encountered in nonlinear systems is that, unlike a linear system subjected to Gaussian random excitation, a Gaussian random response is not obtained. Due to this limitation the second order statistics that give the complete definition of the probability distribution function of the response of a linear system for Gaussian excitation provide only partial information for a nonlinear system [140, 141, and 144].

In this chapter some of the most commonly used nonlinear methods are discussed along with their advantages and drawbacks. In general, for the analysis of nonlinear systems, exact solutions are not available and analysts have to resort to numerical techniques, and to analytical techniques to determine approximate solutions to the problems. Some of these methods are summarized below. A more detailed review can be found in the references provided [90, 91, 142, 148-150].

3.2 The Monte Carlo Method

Amongst the variety of methods available to treat nonlinear problems, the Monte Carlo method provides a general technique that is applicable to many tasks in engineering for estimating, within any desired level of confidence, the exact response statistics of randomly excited non-linear systems. In lieu of experimental data, Monte Carlo simulation is often the only tool available for assessing the accuracy of random vibration solutions generated by approximate methods of analysis [151, 152]. Therefore, due to its importance in nonlinear analysis a, detailed discussion about this technique is presented.

Monte Carlo simulation is based on random computation experiments [99, 152, 153, and 155]. The stochastic differential equations governing the motion of the system can be construed an infinite set of deterministic differential equations [152]. The input data generation process plays a pivotal part in the implementation of the method. It is important that the process ensures that the input sample excitation are representative of the real world. Therefore, the creation of time histories of random processes whose frequency content is compatible with a prescribed power spectrum is essential in the Monte Carlo simulation of a stochastic system. Note that at this stage of the process a set of pseudo-random numbers belonging to a population with a specified pdf must be generated. For each sample of the

random excitation the response may be computed by any of the commonly available numerical integration techniques of differential equations. When the set of response time histories is complete, they are ensemble averaged, and both, the statistical moments and the psd are estimated from the response time series. By increasing the number of sample responses the expected deviation of the obtained numerical values from the theoretical values of the response statistics is reduced, providing results within any confidence level. If determination of the probability density function of the system's response is needed, a greater number of response samples is required to achieve a reliable result. However, if the set of time histories corresponds to an ergodic process, the ensemble average can be determined from its temporal counterpart [145]. Under this condition only one, long, sample response function is required eliminating the need of a large number of sample functions.

The Monte Carlo Method allows the computation of the probability density function, the moments, and the spectral density of the response of a stochastic system. These statistical parameters are determined from an ensemble of deterministic solutions, which are created from realizations of the system's random parameters. If $y_i(t_j)$ denotes the system's response computed at each time step Δt or at time $t_j = j\Delta t$, where $j=1,2,\dots,N$, the estimates of statistical parameters such as the mean and the standard deviation can be obtained. If \hat{m}_y denotes mean response of m_y then an estimate of the mean is obtained by means of the expression

$$\hat{m}_y = \frac{1}{N} \sum_{j=1}^N y_i(t_j). \quad (3.1)$$

Similarly, an estimate $\hat{\sigma}_y$, of the standard deviation of the response, σ_y , can be computed by using

$$\hat{\sigma}_y = \sqrt{\frac{1}{N-1} \sum_{i=1}^N [y_i(t_j) - \hat{m}_y]^2}. \quad (3.2)$$

The Monte Carlo analysis requires numerous computations of the response of the system that is studied. The accuracy of the results improves as the number of deterministic solutions is increased. For every simulation that is conducted, an excitation time history must be computed. Thus, an efficient method to create these time histories is critical for the minimization of the computational time of the simulation. In the case of the determination of the probability density function, a greater number of solution samples is required in comparison with the number of samples needed to accurately estimate the mean value and mean square of the response.

The major advantage of Monte Carlo method is that reliable solutions can be obtained for any problem whose deterministic solution (either analytical or numerical) is unknown. However, the major drawback of the Monte Carlo method, as mentioned before, is the large number of sample records required for the estimation of the response statistics within confidence levels of accuracy, which makes the computation process time consuming. Even though the accuracy can be improved as much as required, it is important to bear in mind that accuracy is inversely proportional to \sqrt{N} , where N denotes the number of samples. Thus, it is necessary to increase the number of experiments by a factor of 100 to decrease the error by a factor of 10. Obviously, this method is quite inefficient from a computational point of view, especially when M-DOF systems are considered. Figure 3.1

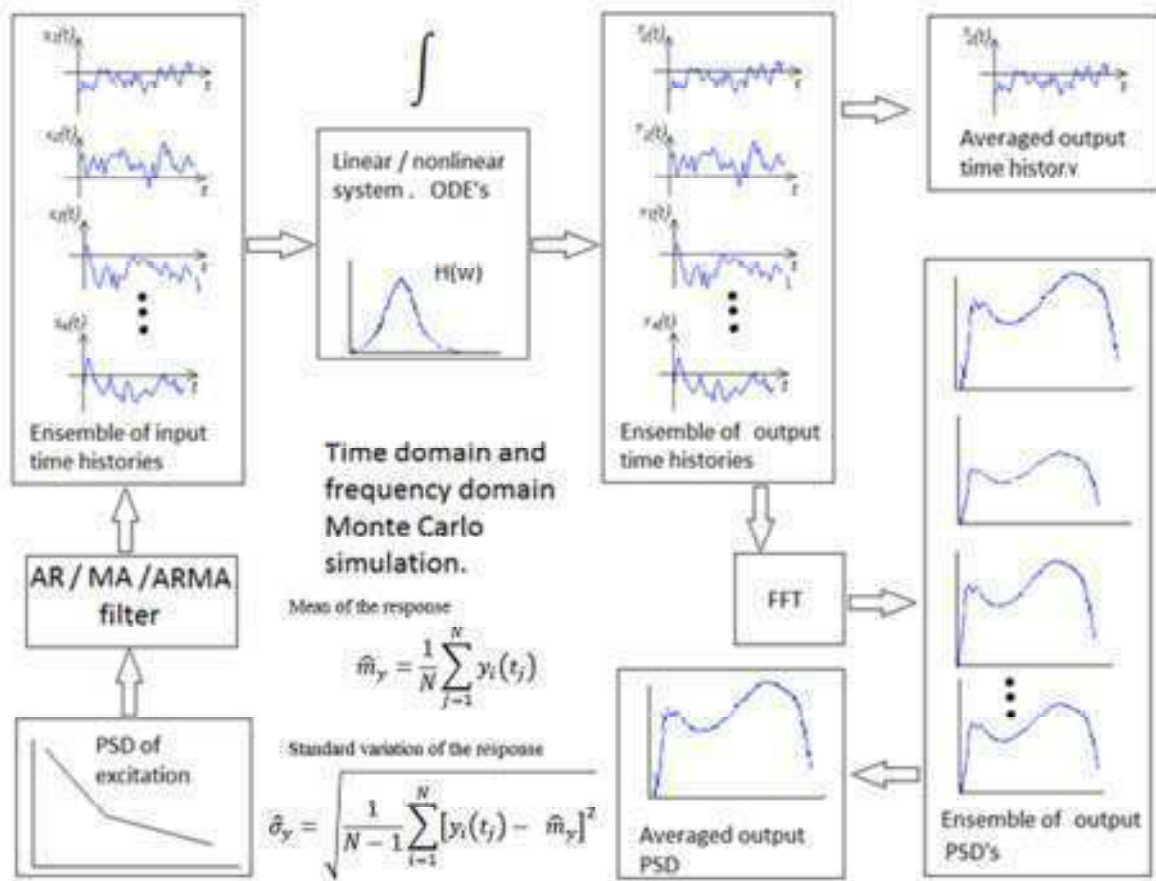


Fig. 3.1 Schematic representation of Monte Carlo method.

summarizes the steps involved in the Monte Carlo simulations carried out in either the time-domain or the frequency-domain.

3.3 Perturbation Methods

Perturbation methods or perturbation theory is a large collection of iterative methods for obtaining approximate solutions to problems involving a small parameter ε , which characterizes the magnitude of the nonlinear terms in these equations. The basic idea is to expand the solution to the nonlinear set of equations in terms of a nonlinearity scaling parameter ε in the form of a power series [138, 143, and 149]. Specifically, the perturbation

approach seeks to decompose a nonlinear problem into an infinite number of linear ones. Hence, perturbation theory is most useful when the first few steps capture the important features of the solution and the remaining ones yield small corrections.

In principle, the perturbation method can be used to estimate the response to any order. However, the calculations are usually lengthy and after the first order, the method may become impractical. Consequently, the perturbation method can only be applied effectively when weakly nonlinear systems are considered.

3.4 Closure Techniques

To characterize the probability density function of the response of a nonlinear system, computation of higher order moments is required. However, these statistical moments are governed by an infinite hierarchy of coupled equations; therefore, some form of a closure scheme has to be applied in order to make the set of moment equations solvable. In stochastic dynamics the term ‘closure’ refers to a procedure, by which an infinite hierarchy of equations governing the statistical moments of random quantities is truncated, and higher order moments are computed approximately. In other words, the moment equations are ‘closed’ by assumptions regarding the statistical structure of the response [99]. The simplest closure scheme is the Gaussian closure, in which higher moments are expressed in terms of the first-order and second-order moments as if the random processes involved were normally distributed. Gaussian closure leads to an associated linear system which excitation is Gaussian, and its response is then assumed to be an approximation to the response of the nonlinear system [152]. One limitation of Gaussian closure is that it only yields satisfactory results when the system under analysis possesses weak non-linearities. To improve accuracy, a higher non-Gaussian level of closure can be used. This

improvement can be achieved, for example, by neglecting all the cumulants moments [39] above certain order $n > 2$, where $n=2$ correspond to Gaussian closure. Of course, the complexity of the closed set of moment equations to be solved, increases with a higher order of closure. Although this greater complexity presented by non-Gaussian closure method makes it difficult to treat M-DOF systems and non-stationary problems with strong nonlinearities, it is certainly possible to apply the method to tackle these kinds of problems.

3.5 Markov Methods

Markov methods offer an alternative approach to the solution of non-linear random vibration problems. For many dynamic systems subjected to wide-band random excitation, the system's response can be modeled as a multi-dimensional Markov process, for which the probability density function of the response is governed by a partial differential equation, called the Fokker-Planck-Kolmogorov (FPK) equation [99, 134]. FPK equation should be solved under appropriate initial and boundary conditions. One important aspect of these methods is that the actual excitation processes are approximated as white noises. Pre-filters are used in those cases where the white noise approximation is not suitable. Despite the recent theoretical contributions to these methods, the type of non-linear random vibration problems for which the appropriate FPK equation can be solved exactly is still quite limited. For example, when applied to the analysis of M-DOF systems the numerical integration of the FPK equation becomes quickly quite cumbersome, because of the high dimension of the probability space that is to be discretized. Hence, in the case of M-DOF non-linear systems the applicability of Markov methods is restricted to the solution of the stationary response of the system. This limitation makes Markov Methods not readily applicable for a wide class of practical M-DOF systems.

3.6 Probability Density Evolution Method

Among the most recent methods proposed to tackle stochastic dynamic analysis problems is the Probability Density Evolution Method (PDEM). This method was proposed by Li and Chen [156] as an alternate way of analyzing nonlinear stochastic systems with random parameters. The method is applicable to either S-DOF systems or M-DOF systems. In the case of M-DOF systems, they can be described by the governing equation [157]

$$\mathbf{M}(\boldsymbol{\Theta})\ddot{\mathbf{X}} + \mathbf{C}(\boldsymbol{\Theta})\dot{\mathbf{X}} + \mathbf{f}(\boldsymbol{\Theta}, \mathbf{X}) = \mathbf{F}(t) \quad (3.3)$$

where $\mathbf{M}(\boldsymbol{\Theta})$ and $\mathbf{C}(\boldsymbol{\Theta})$ are, the $n \times n$ mass and damping random matrices respectively; $\boldsymbol{\Theta}$ is the $r \times 1$ random structural parameter vector with known probability density function (PDF) $p_{\boldsymbol{\Theta}}(\boldsymbol{\Theta})$ where $\boldsymbol{\Theta} = (\Theta_1, \Theta_2, \dots, \Theta_r)$; $\mathbf{f}(\boldsymbol{\Theta}, \mathbf{X})$ is the $n \times 1$ restoring nonlinear random vector, $\mathbf{F}(t)$ is the deterministic or random excitation.

The purpose of the PDEM is to estimate the instantaneous probability density function (PDF) and its evolution for the response of linear and nonlinear structures involving random parameters. The PDEM has also been applied for reliability evaluation [157, 159]. In order to apply the method it is necessary to know the joint probability density function (PDF) $p_{\boldsymbol{\Theta}}(\boldsymbol{\Theta})$ of the random parameters.

It seems that the PDEM is still in an early stage of development and validation. In the different papers written by Li and Chen about the PDEM, the authors address the case of nonlinear restoring force and consider Rayleigh's damping to simplify the problem, but no description on the treatment of other type of damping is further considered. There are also several numerical issues that must be addressed. For example, the PDEM is very sensitive to the way the representative discretized points in the domain $\Omega_{\boldsymbol{\Theta}}$ are selected; accuracy and

computational efficiency can be seriously compromised if an adequate selection of points is not achieved. To this end researchers are still working in numerical algorithms that allow the optimal selection of these points [157, 159, and 161]. One of these methods is based on cubature formulae [160], but careful attention to the use of these formulae is required, otherwise spurious results could still be obtained. The PDEM involves the use of difference schemes to evaluate the PDF. In principle any method could be used, however it has been found that the Lax-Wendroff difference scheme yields reliable results in many cases; still some problems preserving the non-negative nature of the PDF may arise. A modified Lax-Wendroff scheme has been proposed to overcome this difficulty [157].

Despite the numerical restrictions discussed above, the PDEM yields to reliable results in the problems discussed by Li and Chen to exemplify the applicability of the method. Juxtaposing the results obtained by the PDEM with those obtained via Monte Carlo simulation the authors found good agreement between both sets of results, and a much faster convergence than that obtained with Monte Carlo simulation.

Most applications of this method have been related to the study of the probabilistic response and reliability evaluation of structures subjected to earthquake excitation [156-161]. In the research about recent applications of the PDEM in other fields of mechanics, the author of this dissertation could not find references to the application of the PDEM in the analysis of the response of vehicles to random excitation. It is the author's opinion that this is due to the nature of many of the stochastic problems studied by researchers in the automotive field. In general, the dynamics of these systems are governed by ordinary differential equations that do not contain random parameters.

3.7 Statistical Linearization Method

The basic idea of the linearization approach is to replace the original nonlinear system by a linear one in such a way that the difference between the two systems is minimized in some statistical sense. In this way, the parameters of the linearized system are determined. The response of the equivalent linear system is used to approximate the response of the nonlinear system. By assuming Gaussian excitation the unknown statistics of the response are evaluated by approximating it as a Gaussian process. Roberts and Spanos provided a comprehensive account of statistical linearization [39].

A feature that differentiates statistical linearization from all approximate methods, discussed earlier, is its capacity to provide information on the power spectral density of the response quite easily. Moreover, once the actual linearization has been performed, the response statistics can be computed analytically. Consequently, the method is computationally quite efficient compared to numerical integration. The linearization approach can be applied for both white noise and non-white noise inputs. Therefore, it can be concluded that the linearization can be applied to problems with a wide variety of excitation forms. Furthermore, it is quite convenient in applications involving M-DOF systems.

Because of its versatility the method of statistical linearization will be used for the first time to study in the ensuing the nonlinear dynamic behavior of motorcycles. In this context the method is briefly reviewed in the next chapter.

Chapter 4

Statistical Linearization Method Applied to M-DOF Systems

4.1 Introduction

The statistical linearization method is based on the idea of substituting an original nonlinear system by an equivalent linear system (auxiliary system) in such a way that the difference between these two systems is minimized in a statistical sense. In general, the auxiliary system needs not necessarily be linear [39]. However, for the case of M-DOF systems only the response of linear systems is readily available. Several authors have shown that this method has fewer limitations as compared to other analytical methods [97-99].

The pioneer works of Krylov and Bogoliubov [94] on deterministic linearization set the theoretical foundation of the method of statistical linearization. The method is presented as such in the papers of Caughey [95], Iwan [96] and others with a probabilistic approach. A practical perspective of the method in engineering applications was first presented by Atalik and Utku [97], who made a great contribution to the applicability of the method by assuming a Gaussian behavior of all the state variables, and demonstrating that the Gaussian assumption greatly simplifies the computation of the linearization coefficients. Caughey was the first to apply the stochastic linearization technique to a restricted class of M-DOF systems with specific forms of nonlinearities in the stiffness terms and uncorrelated excitation vector [126, 127, and 129]. Iwan and Paparizos generalized the method to cover M-DOF systems with a fairly general type of nonlinearity in the damping and stiffness terms [117]. Later, the method was further generalized to include non-

stationary responses, and the conditions for existence and uniqueness of solutions generated by equivalent linearization were examined [99, 109]. Faravelli, Casciati, and Singh showed that the method was very reliable in the analysis of hysteretic systems [98]. Spanos and Iwan [99] studied the mathematical conditions required to ensure the existence and uniqueness of the equivalent linear system. The book by Roberts and Spanos [39] on computational techniques in nonlinear stochastic dynamics shows that among them, the statistical linearization method is the one that offers more advantages in terms of implementation, accuracy, applicability to M-DOF systems, systems with hysteretic behavior, and treatment of non-polynomial nonlinearities. The work by Bouc [101] on hysteretic systems presented a smooth and versatile model of hysteresis. This work along with the contributions by Wen and Eliopoulos [109] and others [110–112], motivated the diversification of the application of the method in many structural dynamics fields such as vibration of frames [113], steel and concrete structures [115,116], soil profiles [117], three dimensional frames [118], base isolation [119] and hybrid control [120].

4.2 General Formulation of Statistical Linearization Method

A brief overview of the method is given below. Only the general steps involved in the analysis of a M-DOF nonlinear system by the method of statistical linearization are presented. However, in chapter 6 the details related to the analysis of a 4-DOF motorcycle model subjected to road roughness and experiencing in-plane motion are discussed, along with the necessary implementation steps. A thorough treatment of this technique can be found in the book of Roberts and Spanos [39].

In the following discussion it is assumed that the excitation and response processes of concern are stationary, and the non-linear system is of the zero-memory type. Also, the assumption of Gaussianity for both, the excitation and the response is considered.

Consider a M-DOF nonlinear system which equations of motion have the following general matrix form

$$\mathbf{M}\ddot{\mathbf{q}} + \mathbf{C}\dot{\mathbf{q}} + \mathbf{K}\mathbf{q} + \mathbf{\Phi}(\mathbf{q}, \dot{\mathbf{q}}, \ddot{\mathbf{q}}) = \mathbf{F}(t), \quad (4.1)$$

where the $n \times n$ matrices \mathbf{M} , \mathbf{C} , and \mathbf{K} correspond to the system mass, damping, and stiffness matrices, respectively. \mathbf{q} is the system displacement vector, $\mathbf{F}(t)$ is the system force vector, and $\mathbf{\Phi}(\mathbf{q}, \dot{\mathbf{q}}, \ddot{\mathbf{q}})$ is a vector function containing the nonlinearities. According to the basic idea of the statistical linearization method, the nonlinear system described by Equation 4.1 is replaced by an equivalent linear system, the statistics of which are easily computed and may be used as approximations to the statistics of the output of the nonlinear system. This equivalent linear system has the form

$$(\mathbf{M} + \mathbf{M}_e)\ddot{\mathbf{q}} + (\mathbf{C} + \mathbf{C}_e)\dot{\mathbf{q}} + (\mathbf{K} + \mathbf{K}_e)\mathbf{q} = \mathbf{F}(t), \quad (4.2)$$

where the linearizing matrices \mathbf{M}_e , \mathbf{C}_e , and \mathbf{K}_e are obtained by minimizing the difference, or error $\boldsymbol{\varepsilon}$, between the actual and the equivalent linear system. That is

$$\boldsymbol{\varepsilon} = \mathbf{\Phi}(\mathbf{q}, \dot{\mathbf{q}}, \ddot{\mathbf{q}}) - \mathbf{M}_e\ddot{\mathbf{q}} - \mathbf{C}_e\dot{\mathbf{q}} - \mathbf{K}_e\mathbf{q}. \quad (4.3)$$

The difference $\boldsymbol{\varepsilon}$ can be minimized by keeping in mind that it is a random process, and then the expected value of the square of the error can be used as a criterion for minimization, i.e. require that $E\{\boldsymbol{\varepsilon}^T \boldsymbol{\varepsilon}\} = \text{minimum}$.

The previous condition is satisfied when [39]

$$\frac{\partial E\{\boldsymbol{\varepsilon}^T \boldsymbol{\varepsilon}\}}{\partial m_{ij}^e} = 0, \quad (4.4)$$

$$\frac{\partial E\{\boldsymbol{\varepsilon}^T \boldsymbol{\varepsilon}\}}{\partial c_{ij}^e} = 0, \quad (4.5)$$

$$\frac{\partial E\{\boldsymbol{\varepsilon}^T \boldsymbol{\varepsilon}\}}{\partial k_{ij}^e} = 0, \quad (4.6)$$

where m_{ij}^e , c_{ij}^e and k_{ij}^e are the (i, j) elements of the matrices \mathbf{M}_e , \mathbf{C}_e , and \mathbf{K}_e , respectively, and $i, j = 1, 2, \dots, n$.

Applying conditions (4.4), (4.5), and (4.6) to Eq (4.3) leads to

$$E\{\boldsymbol{\Phi}_i \hat{\mathbf{q}}\} = E\{\hat{\mathbf{q}} \hat{\mathbf{q}}^T\} \begin{bmatrix} \mathbf{k}_{i*}^{eT} \\ \mathbf{c}_{i*}^{eT} \\ \mathbf{m}_{i*}^{eT} \end{bmatrix}, \quad i = 1, 2, \dots, n \quad (4.7)$$

where

$$\hat{\mathbf{q}} = [\mathbf{q}, \dot{\mathbf{q}}, \ddot{\mathbf{q}}]^T, \quad (4.8)$$

and \mathbf{m}_{i*}^{eT} , \mathbf{c}_{i*}^{eT} , and \mathbf{k}_{i*}^{eT} are the i th rows of the matrices \mathbf{M}_e , \mathbf{C}_e , and \mathbf{K}_e , respectively.

From the previous results, and using Gaussian approximation, Kazakov [39] obtained the following simple expressions that allow the computation of the elements of the matrices \mathbf{M}_e , \mathbf{C}_e , and \mathbf{K}_e :

$$m_{ij}^e = E \left\{ \frac{\partial \Phi_i}{\partial \ddot{q}} \right\}, \quad (4.9)$$

$$c_{ij}^e = E \left\{ \frac{\partial \Phi_i}{\partial \dot{q}} \right\}, \quad (4.10)$$

and

$$k_{ij}^e = E \left\{ \frac{\partial \Phi_i}{\partial q} \right\}. \quad (4.11)$$

The set of equations (4.9), (4.10), and (4.11) can be used for both stationary and non-stationary random vibration analyses [39].

As mentioned earlier, the idea of substituting the actual nonlinear system by an equivalent linear one relates the fact that well established techniques exist to analyze linear problems. Depending on the nature of the information which is being sought, the analyst chooses among the various methods of analysis available, the one that suits particular needs. Once the elements of the linearizing matrices \mathbf{M}_e , \mathbf{C}_e , and \mathbf{K}_e are found, the auxiliary linear system is defined and ready to be used to determine its statistics, which should be the best approximation of the statistics of the nonlinear system. At this point note that instead of a single-step procedure, what is established is an iterative process that leads to the optimal values for the elements of the matrices \mathbf{M}_e , \mathbf{C}_e , and \mathbf{K}_e . In this regard, Equation (4.7) leads to a unique set of equations for \mathbf{M}_e , \mathbf{C}_e , and \mathbf{K}_e , if and only if, the matrix $E\{\hat{\mathbf{q}}\hat{\mathbf{q}}^T\}$ is non-singular. Spanos and Iwan [99] have shown that in general, this is the case and it can be assumed that $q_1, \dots, q_n, \dot{q}_1, \dots, \dot{q}_n, \ddot{q}_1, \dots, \ddot{q}_n$ are linearly independent, which ensures that a unique set of equations for the matrices \mathbf{M}_e , \mathbf{C}_e , and \mathbf{K}_e exists, corresponding to the minimization of the error defined by equation (4.3).

4.3 Spectral Approach Solution Procedure

The spectral approach is one of the methods for conducting linear vibration analyses. In this method the corresponding spectral density matrix of the response process $\mathbf{S}_q(\omega)$ is sought.

Consider a nonlinear system described by

$$\mathbf{M}\ddot{\mathbf{q}} + \mathbf{C}\dot{\mathbf{q}} + \mathbf{K}\mathbf{q} + \mathbf{g}(\mathbf{q}, \dot{\mathbf{q}}) = \mathbf{Q}(t), \quad (4.12)$$

in which the non-linearity $\mathbf{g}(\mathbf{q}, \dot{\mathbf{q}})$ depends only on displacements and velocities, and is assumed to be antisymmetric. The input excitation $\mathbf{Q}(t)$ is a zero-mean stationary random process with spectral density matrix $\mathbf{S}_Q(\omega)$.

The matrix $\mathbf{S}_q(\omega)$ of the response random process can be determined via the equivalent of Equation (2.31). That is,

$$\mathbf{S}_q(\omega) = \mathbf{H}(\omega)\mathbf{S}_Q(\omega)\mathbf{H}(\omega)^{T*}, \quad (4.13)$$

which involves the spectral density matrix $\mathbf{S}_Q(\omega)$ of the excitation $\mathbf{Q}(t)$ and the matrix of the frequency response functions $\mathbf{H}(\omega)$ of the equivalent linear system

$$\mathbf{H}(\omega) = [-\omega^2\mathbf{M} + i\omega(\mathbf{C} + \mathbf{C}_e) + (\mathbf{K} + \mathbf{K}_e)]^{-1}, \quad (4.14)$$

which is associated to the auxiliary system

$$\mathbf{M}\ddot{\mathbf{q}} + (\mathbf{C} + \mathbf{C}_e)\dot{\mathbf{q}} + (\mathbf{K} + \mathbf{K}_e)\mathbf{q} = \mathbf{Q}(t). \quad (4.15)$$

It is clear that in order to compute $\mathbf{H}(\omega)$ it is necessary to compute the elements of the matrices \mathbf{C}_e and \mathbf{K}_e first. This step is accomplished by applying the relations (4.10) and (4.11) obtained previously.

Next, the variance of the response can be calculated by using the indexed version of Equation (2.27)

$$E\{\mathbf{q}_{ij}^2(t)\} = \int_{-\infty}^{\infty} \mathbf{S}_{q_{ij}}(\omega) d\omega, \quad (4.16)$$

where $i = 1, \dots, n$; and $j = 1, \dots, n$.

The iterative process can be set next by using equations (4.10), (4.11), (4.13), and (4.14). A detailed scheme with the steps of implementation will be provided in the next chapter while applying the method to the analysis of the stochastic dynamics of a motorcycle.

Chapter 5

Road Profile Modeling and Synthetic Road Realization

5.1 Introduction

This chapter is divided in three parts. The first part is a description of some studies to characterize road roughness as a stationary random process. The second part is devoted providing an introduction to the methods of synthetic road realization. The third part features a study of AR filters showing that they are suitable computational tools that allow the synthesis of reliable time histories compatible with a given road spectrum. A comparison between the power spectrum of the AR filter output time histories and the target road spectrum is presented. Also the stochastic properties of the time histories and how well their target spectrum is fitted are assessed.

5.2 Characterization of Road Roughness

To analyze in the time-domain the dynamic response of a vehicle, such as a motorcycle, moving on an uneven road surface, the excitation due to the road profile must be modeled as a time series, or a realization of a stochastic process. The appropriate synthesis of road roughness profiles, compatible with certain power spectrum, is the basis for conducting riding comfort studies, among others (see section 1.1) in which the dynamic behavior of the motorcycle must be understood. Thus, a reliable characterization of the road profiles is required. Roughness is a measure of the deviations from a true planar surface in a road. It is responsible for vehicle vibrations which affect vehicle dynamics and ride comfort, and can be described effectively in a statistical sense, usually in terms of power spectral density [200].

The definition of roughness is kept intentionally general because roughness is a relative term. The effects on vehicle dynamics and ride comfort depend strongly on the geometrical and physical characteristics of the vehicle, and on the velocity at which it is moving on the ground. For instance, what could seem to be a smooth road for a passenger on a heavy large vehicle could be experienced as an uncomfortable vibration for another passenger on a small light vehicle, regardless of the fact that both vehicles traverse the same section of the road at the same constant velocity [164]. For these reasons, any description of the geometrical features of a road must be linked to the vehicle characteristics to be meaningful in ride and comfort studies. However, to have a practical description of roughness that can be operational, models of roughness must be simple in its mathematical form and must involve a limited number of parameters.

Road elevation profiles can be measured either by using high-speed profilometers, or by performing close interval rod and level surveys [93]. The first attempts of characterizing roughness from a statistical point of view dates back to the late 1950's. Bekker [164] provides a historical overview of this kind of studies. As an example, one of the first significant results that were obtained is shown in Figures 5.1, 5.2, and 5.3.

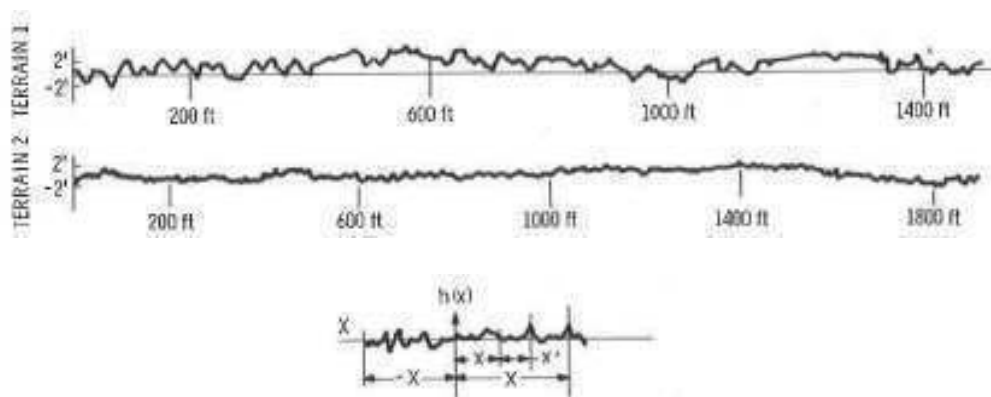


Figure 5.1 Terrain profiles measured in off-road locomotion studies [164].

Figure 5.1 shows the profiles of two different proving grounds [201]. Measurements were taken every two feet, and the elevation was measured to the nearest one-hundredth of a foot. Since roughness is a spatial disturbance, the power spectral density function is defined in terms of spatial frequency Ω (radians per foot).

Figures 5.2 and 5.3 show the corresponding power spectra of these profiles plotted in log-log format, which has been of common usage in the automotive field. Both curves present the characteristic decaying versus frequency behavior of this type of spectra. Higher amplitudes imply rougher roads and vice versa. The PSD corresponding to Terrain 1, which presents pronounced profile irregularities, exhibits higher values than those exhibited by the PSD of terrain 2, which has a smoother profile. Noted can also be a waviness at the tail of both spectra, which was of concern for the researchers, since they initially expected a smoother behavior at the tail. Problems related with aliasing, and elimination of bumps and potholes needed to be resolved prior to deriving smoother PSDs. Also methods and equipment for collecting data needed to be improved [164]. Blackman and Tuckey [85] provided descriptions of the computations of the PSD and estimates of errors involved.

Based on the idea of the exponential equation, Dodds and Robson [67] proposed a simple power formula that fits experimental data in most of the operational range of frequencies (0.5-20 Hz) required for motorcycle studies. This model is widely used in dynamics studies, and is discussed more in detail in section 5.15.

Other approaches and models have been proposed. Kropác and Mucka [128] presented a road model that, besides describing ground roughness, it incorporates potholes and obstacles associated with deteriorated roads. Öijer and Edlund [74] also presented a model to describe a combination of random roughness and transient obstacles that allow analysis of vehicles

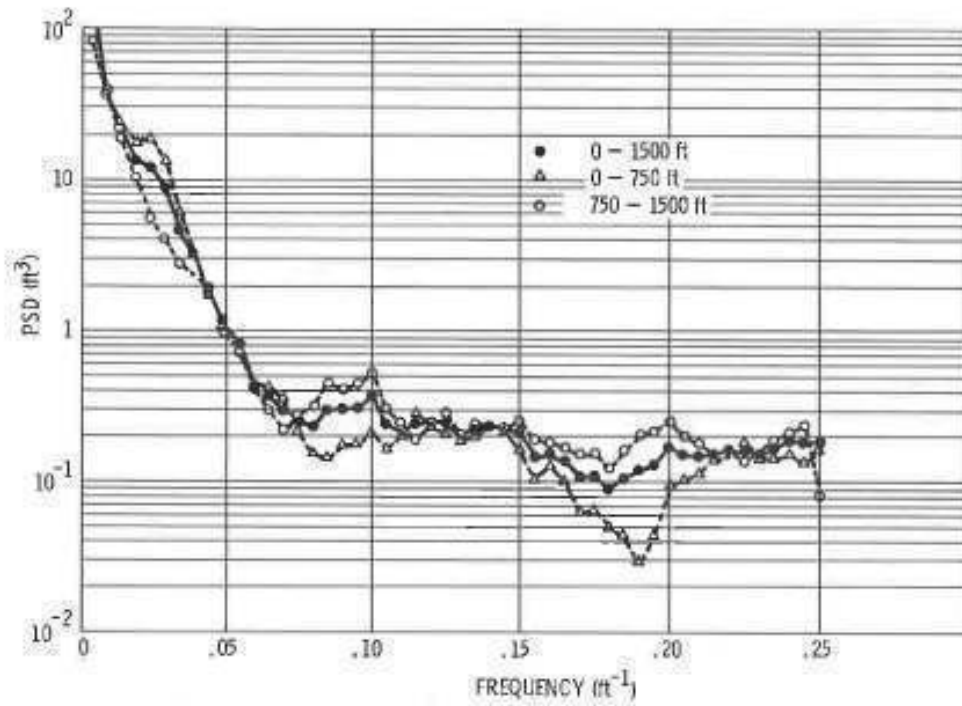


Figure 5.2 Power spectral density of terrain 1 [164].

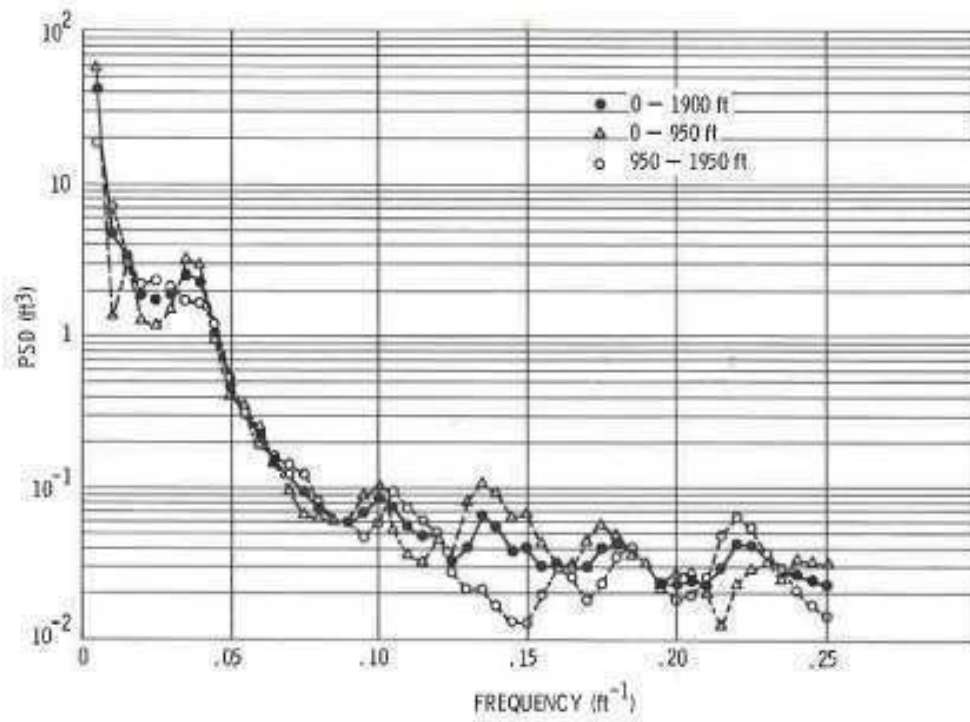


Figure 5.3 Power spectral density of terrain 2 [164].

subject to non-stationary excitation. Sprinc et.al [77] discussed the practical aspects of gathering roughness data and proposed the use of a device called DYNVIA, which allows acquiring reliable roughness data at a lower cost compared to other devices. Xu et.al [79] proposed the use of a non-contact acoustical transducer, and also a roughness model of exponentially decaying form. Bogsjö and Forsén [86] analyzed fatigue due to road roughness, and suggested the use of a road model which is the sum of Gaussian noise and of transient events such as holes and bumps.

5.2.1 General Considerations on the Characterization of Roughness

When characterizing road roughness it is commonly assumed that it is a zero-mean, stationary and ergodic Gaussian process [67]. These assumptions, by virtue of the Central Limit Theorem (section 2.2), can be considered reasonably reliable. They allow the complete characterization of this kind of random processes in terms of their second-order moments; namely the mean and variance, which are obtained from the time histories of the excitations, as discussed in section 2.2.

In the frequency domain, under the same assumptions, road profiles can be adequately described by a power spectral density function. This approach is suitable for analyzing both linear and non-linear systems, and allows the study of the motorcycle response, given its traversal speed and its dynamical characteristics [36].

As it has been indicated previously, the PSD of road roughness is described as a function of the wave number (cycle/m, or cycle/ft), but it can also be described as a function of frequency with units in either radians per second (rad/s) or cycles per second (Hz). The last form is particularly useful in vehicle dynamics because the velocity of the vehicle appears as a parameter in the PSD roughness function [68]. In addition, there exist

several ways of expressing the PSD of a road profile; see for example references [41], [68] and [87], and no agreement among authors exists on what definition must be used. Moreover, in many publications it is not clearly stated which definition of PSD is considered, making it often difficult to compare reported data.

The problem of the variety of definitions for a PSD and the generated confusion has been addressed by Davis and Thompson [68], who have summarized the different ways of defining a road profile PSD and have provided insight in the use of the units involved. In this thesis, the Wiener-Khinchine relations (equations (2.11) and (2.12)) and the PSD of both, the road and the motorcycle's response, are defined following the convention used by Newland [41]. The relation between the so called *two-sided power spectrum* S_x and the *one-sided experimental power spectrum* W is given by Equation (2.16), reproduced here again for convenience

$$W(f) = 4\pi S_x(\omega) \quad (2.16)$$

It is important to point out that the *two-sided power spectrum* S_x is expressed as a function of the angular frequency ω while the *one-sided experimental power spectrum* W is expressed as a function of frequency in Hz.

5.3 Road Roughness Model

In the first stage of the work of this thesis the model presented in [67] known as the *split-power law*, was adopted. This power spectrum gives the magnitude of the surface irregularities as a function of their *wavelength* λ . It is described by the equation

$$S_{rr}(k) = S_0 \left(\frac{k}{k_0} \right)^{-n} \begin{cases} n = n_1 & k \leq k_0 \\ n = n_2 & k > k_0, \end{cases} \quad (5.1)$$

where $k_0 = \frac{1}{2\pi}$ is the *cut-off wavenumber*, n_1 and n_2 are exponents, and S_0 is a constant that depends on the quality of the road; k is the *wavenumber* defined as

$$k = \frac{2\pi}{\lambda}, \quad (5.2)$$

which can be interpreted as the number of wavelengths λ contained in a distance of 2π .

Table 5.1 shows the values of these parameters for various road types as presented by Dodds and Robson [67].

Table 5.1 Road quality constants (adapted from reference [67])

Road class	S_0 [$\times 10^{-6}$ m ³ /cycle]		n_1		n_2	
	Road Quality	Range	Mean	Standard deviation	Mean	Standard deviation
Motorways	Very good	2-8	1.945	0.464	1.360	0.221
	Good	8-32				
Principal roads	Very good	2-8	2.05	0.487	1.440	0.266
	Good	8-32				
	Average	32-128				
	Poor	128-512				
Minor roads	Average	32-128	2.28	0.534	1.428	0.263
	Poor	128-512				
	Very poor	512-2048				

The experimental power spectrum of a typical road, along with two approximations is shown in Figure 5.4. The solid line corresponds to the split-power law approximation Equation (5.1), and the dotted line shows an *integrated white noise approximation*, the latter is explained in reference [88].

Assuming that the motorcycle travels at constant speed V , the power spectrum given by Eq (5.1), which is expressed in terms of the wavenumber k can be rewritten in terms of time. To this end the following relations are useful [41]

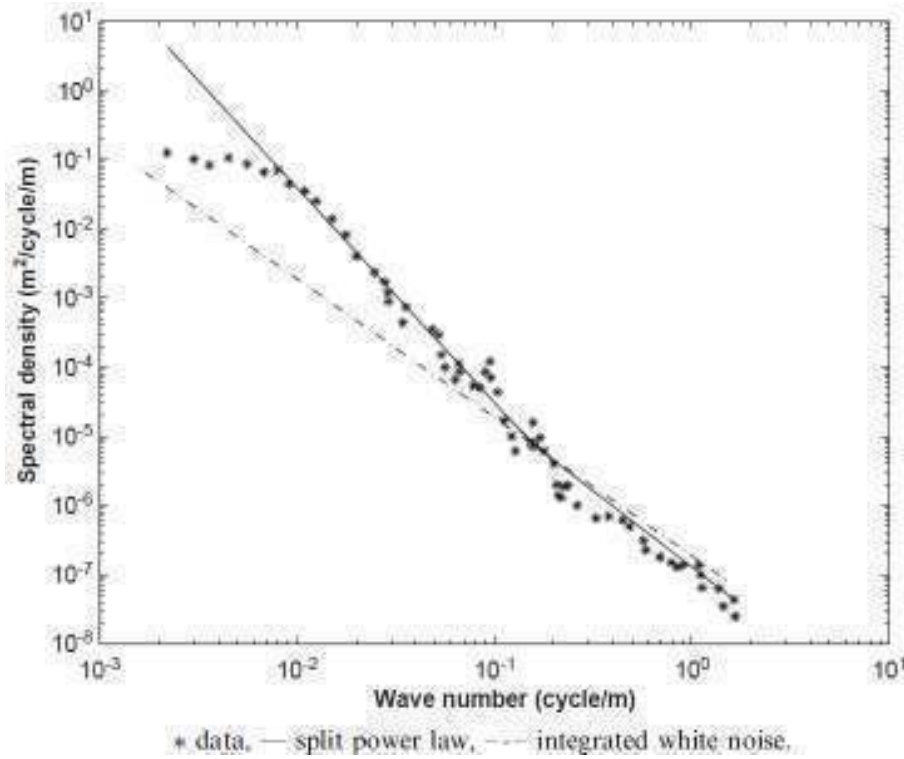


Figure 5.4 Typical power spectrum of road profile and two approximations [88].

$$\omega = Vk, \quad (5.3)$$

and

$$S_{rr}(\omega = Vk) = \frac{1}{V} S_{rr}(k). \quad (5.4)$$

Combining equations (5.1), (5.2) and (5.3) the following expression is obtained

$$S_{rr}(\omega, V) = \frac{S_0}{V} \left(\frac{\omega}{Vk_0} \right)^{-n} \begin{cases} n = n_1 & \frac{\omega}{V} \leq k_0 \\ n = n_2 & \frac{\omega}{V} > k_0. \end{cases} \quad (5.5)$$

In this case, due to the transformation, $k_0 = 1$. Thus, $S_{rr}(\omega, V)$ has units m^2/Hz .

Several PSD's for an average quality road profile were obtained using Equation (5.5). The curves, corresponding to various speeds are shown in Figure 5.5. The values used for generating these curves are $n_1=2$, $n_2=1.5$, $S_0=64 \times 10^{-6} \text{ m}^2/\text{rad m}^{-1}$.

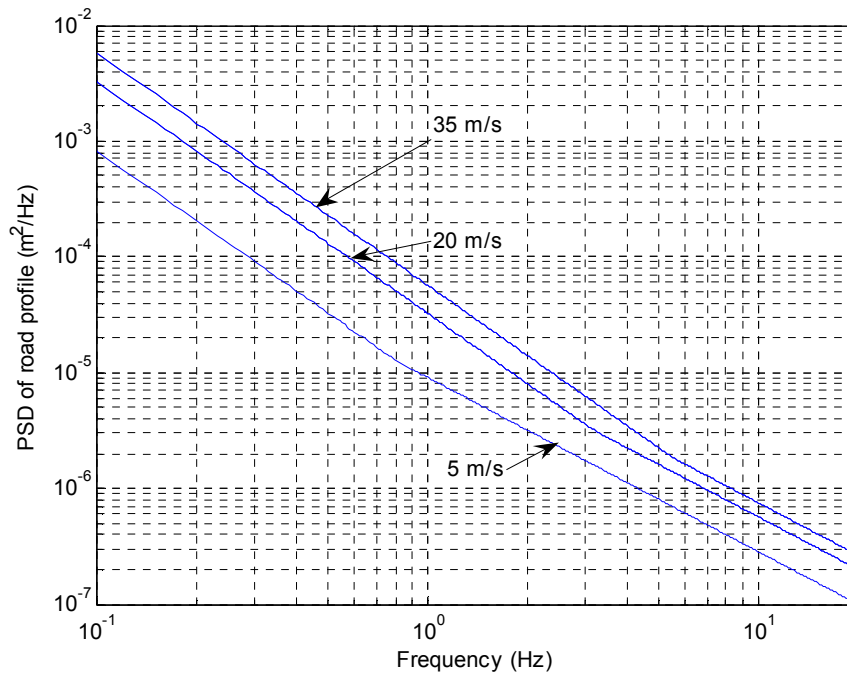


Figure 5.5 Power spectra for an average quality road.

Although the split power formula provides a simple way to fit a road power spectrum, it cannot be generated by linear filters. This problem has been reported by Turkey and Akcay [88]. They discarded the split power formula and applied a *subspace-based frequency-domain algorithm* [89] to approximate an experimental spectrum. The author of this thesis also experienced the same problem when tried to generate time histories based on this PSD model. The problem observed is that, since the split power formula is unbounded at the zero frequency, the signals generated using AR filters, contain low frequency components with large amplitudes which are not part of the real signals compatible with the given power spectrum. As it will be discussed later, depending on how the model is formulated, absolute coordinates or relative coordinates, the analysis of the response of a motorcycle, involve the use of the velocities and accelerations imposed by the road profile. The velocity and acceleration PSD's are computed by means of Equations

(2.18) and (2.19), which involve the road profile PSD. Hence, when these time histories are synthesized by using Equation (5.5), through Equations (2.18) and (2.19), without any modification the results obtained are not good representation of the true signals. Therefore, this model is not suitable for simulating the response of the motorcycle. Yet, this model gives a good approximation within the regions B and C shown in Figure 5.6. Thus, instead of discarding Equation (5.5), a complimentary function was used to approximate the road PSD within region A of the same figure. The model used by Narayanan and Senthil [78] can be used to accomplish this goal. It provides a good approximation for the road PSD within the regions A and B of Figure 5.6, but fails in region C.

The model has the form

$$S_h(\omega) = \frac{\sigma^2 a V}{\pi(\omega^2 + (aV)^2)} \quad (5.6)$$

where $S_h(\omega)$ is the psd of the road surface, σ^2 denotes the variance of the road, V is the vehicle velocity, and a represents the quality of the road. A plot of a road PSD and its approximation is shown in Figure 5.7.

The single values reported of a and σ^2 to approximate the PSD shown in Figure 5.7, were used to estimate the order of the constants needed for different values of speed and road quality; since these data are not provided by the authors. Thus, by using equations (5.5) and (5.6) the entire road profile PSD can be approximated. Figure 5.8 shows one PSD obtained applying this approach.

Time histories were generated from the new PSD's. An improvement was observed in the quality of the signals generated and also in the response PSD's obtained. These results are discussed in detail in section 5.18.

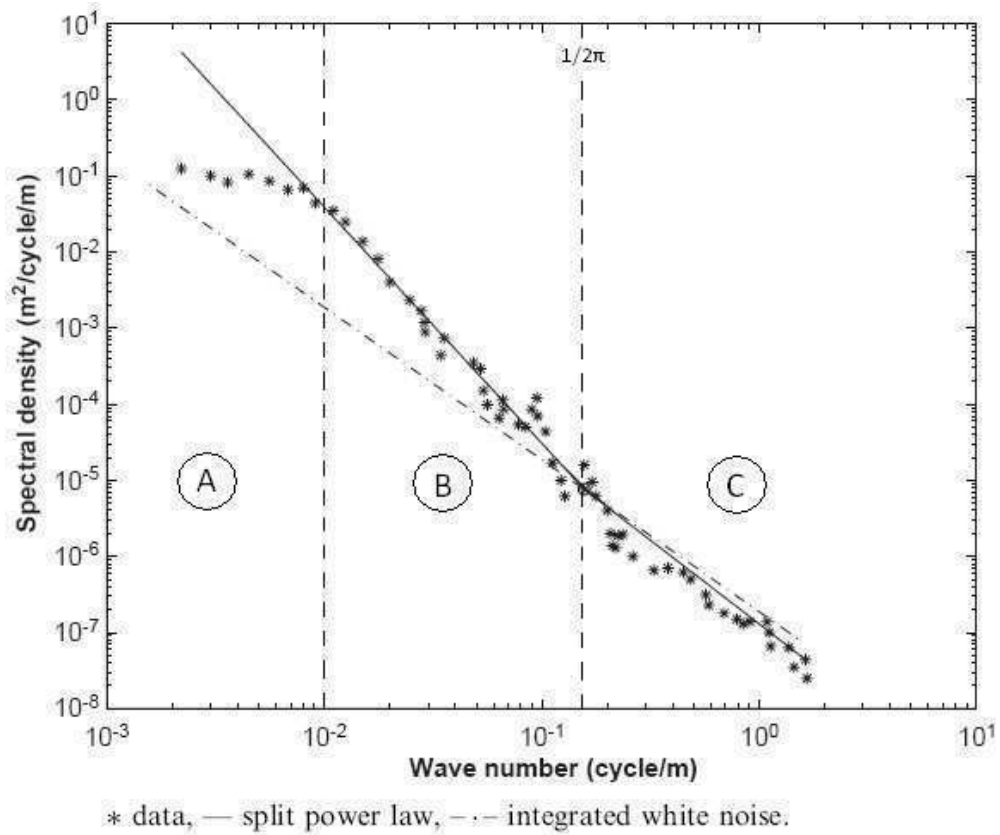


Figure 5.6 Sections of power spectrum fitted by two different roughness models.

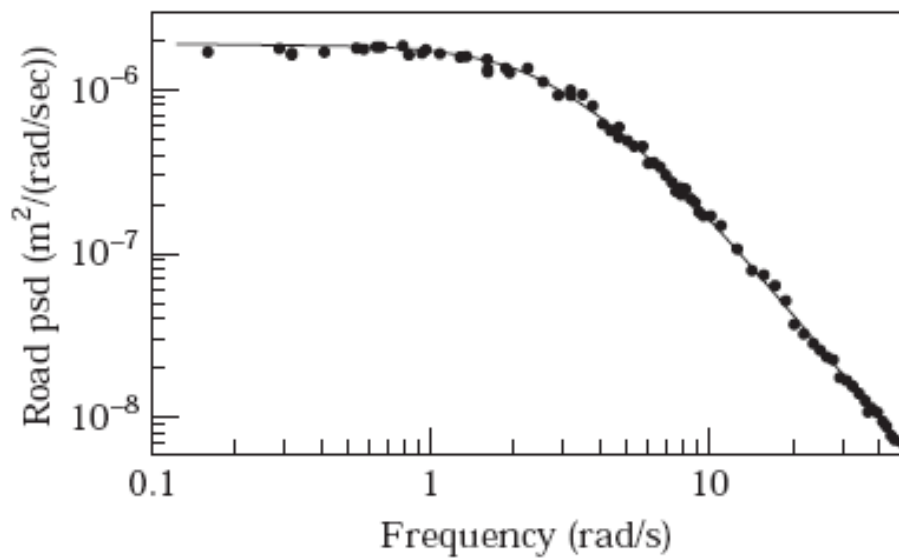


Figure 5.7 Power spectrum of road roughness and fitting (from reference [78]).

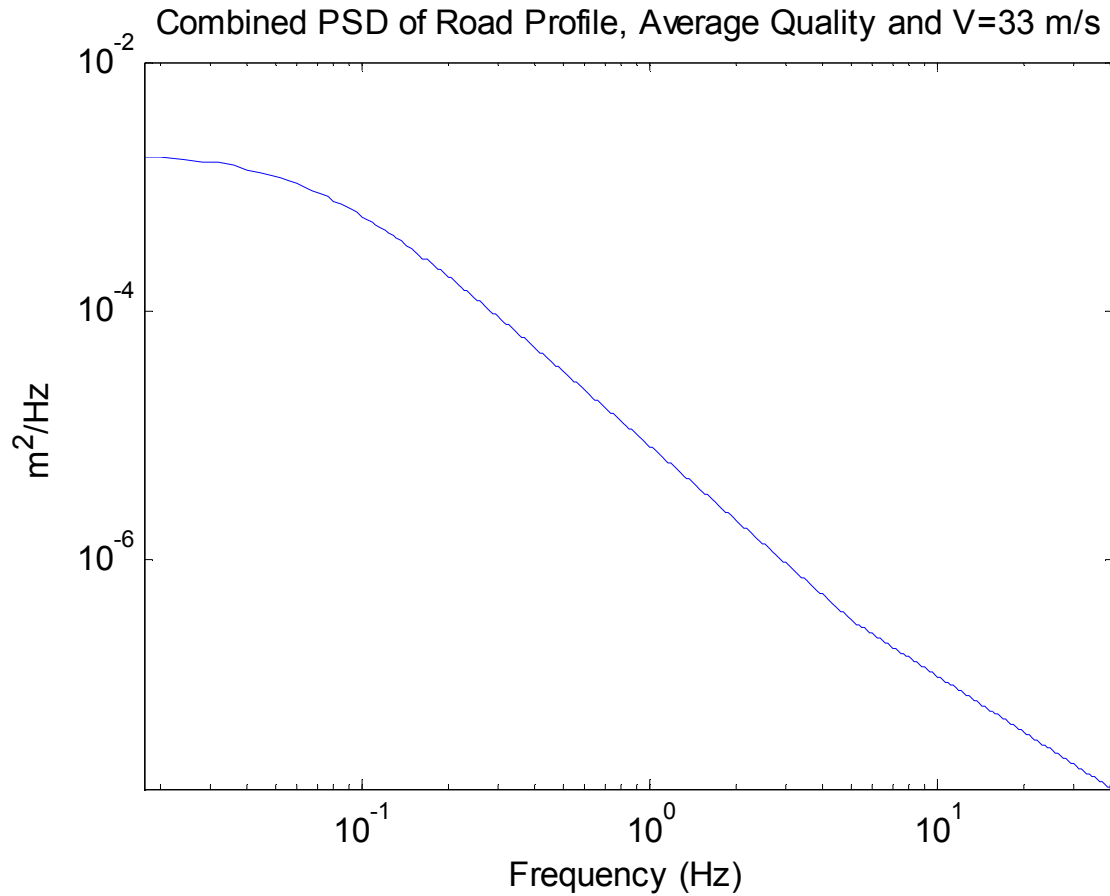


Figure 5.8 Combined PSD obtained with two different models.

As mentioned in the preceding section, the analysis of the response of the motorcycle model, expressed in terms of relative coordinates, requires the use of acceleration realizations as the excitation to the system. Equation (2.19), allows the computation of the necessary acceleration power spectrum in a very straight forward manner. For the road profile PSD of Figure 5.8, the corresponding acceleration PSD is shown in Figure 5.9.

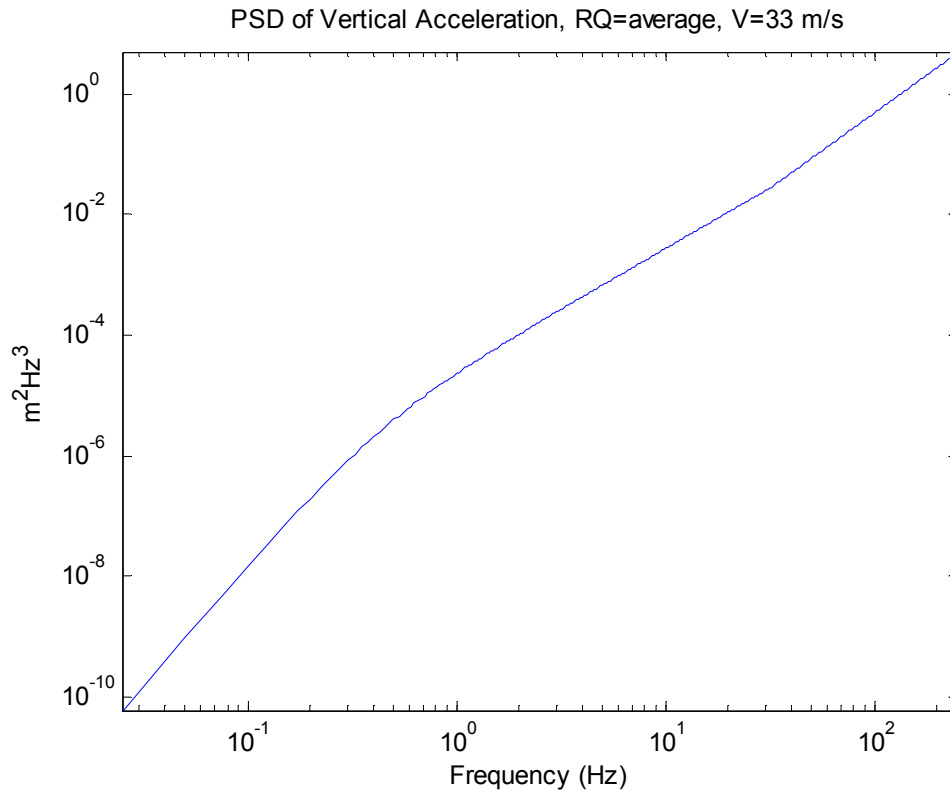


Figure 5.9 Acceleration power spectrum.

5.4 Synthesis of Road Realizations

Nowadays a number of methods for simulating stationary random processes which are compatible with a specified (target) power spectrum have been proposed. Borgman [199] used superposition of sinusoidal functions in the simulation of ocean surface elevation by choosing the frequency in such a way that the amplitude of each sinusoidal function was an equal portion of the target spectrum. A method for simulating several simultaneous time series by passing white noise through filters was also presented in the same publication. Cuong et. al. [154], generated random sequences with applications in marine dynamics by using a method based on the Fast Fourier Transform (FFT). Shinozuka [131] introduced the harmonic superposition method. It is a technique that simulates a random process by a

series of cosine functions with random frequency. It employs Monte Carlo method and works well with many kinds of PSD. Although the technique is of easy implementation it is computationally costly. The harmonic superposition method has been widely accepted and applied in various branches of engineering including vehicle dynamics. Later, Shinozuka and Deodatis [63] presented an upgraded version of the method which features the use of the FFT technique to reduce the cost of digitally generating sample functions of the simulated stochastic process. Yonglin and Jiafan [83] present the method of linear filtration, which the authors found to be computationally more efficient than the method of harmonic superposition. However, the analyses of results presented are based on a visual evaluation of a single time history instead of a more formal analysis of the statistical characteristics of the generated series, thus casting doubts on the effectiveness of the method. Spanos and Hansen [64] proposed an alternative method based on linear prediction theory (LPT), or autoregressive (AR) filter, for the numerical simulation of sea wave records obtained as the output of a recursive digital filter to a white noise input. In a later publication, Spanos [65] reviewed the applicability of LPT on the simulation of ocean waves and extended the study by examining the moving average (MA) and the autoregressive moving average (ARMA) algorithms as options for this problem, showing the good capabilities of these algorithms in fitting the Pierson-Moscowitz spectrum. Further, Spanos [66] showed the applicability of the three algorithms in other engineering branches, in particular in the spectral characterization of high frequency space shuttle lift-off data.

5.5 The Autoregressive Approximation

In an autoregressive (AR) approximation of order m , the n -th sample time history $\hat{f}(n)$ is computed as a linear combination of the m previous samples and a white noise process

$w(n)$ (with power spectrum equal to one), defined in the frequency band $[-\omega_{co}, \omega_{co}]$, where ω_{co} is the cut-off frequency. Thus, the n -th time history $\hat{f}(n)$ can be computed as follows

$$\hat{f}(n) = - \sum_{k=1}^m a_k \hat{f}(n-k) + Gw(n), \quad (5.7)$$

where a_k and G are parameters to be determined.

The parameters a_k can be obtained by minimizing the ratio between the areas of the target (known) power spectrum $S_0(\omega)$ and the power spectrum $\hat{S}_{AR}(\omega)$ of the synthesized time histories [64]

$$E_{AR} = \int_{-\omega_{co}}^{\omega_{co}} \frac{S_0(\omega)}{S_{AR}(\omega)} d\omega, \quad (5.8)$$

leading to the Toeplitz matrix equation

$$\begin{bmatrix} R_0 & R_1 & R_2 & R_{m-1} \\ R_1 & R_0 & \dots & R_{m-2} \\ R_2 & R_1 & & \\ \vdots & \vdots & & \\ R_{m-1} & R_{m-2} & \dots & R_0 \end{bmatrix} \begin{bmatrix} a_1 \\ a_2 \\ \vdots \\ a_m \end{bmatrix} = - \begin{bmatrix} R_1 \\ R_2 \\ \vdots \\ R_m \end{bmatrix}. \quad (5.9)$$

Each element R_k ($k = 0, \dots, m$) can be computed using Equation (2.15). In this case

$$R_k(n) = \int_{-\omega_{co}}^{\omega_{co}} S_0(\omega) \cos(k\omega T) d\omega. \quad (5.10)$$

Once the R_i elements are computed, the parameters a_k can be obtained by solving the system given by Equation (5.9).

The parameter G can be determined by equalizing the areas under the curves of the output spectrum \hat{S}_{AR} and the target power spectrum S_0 . That is require,

$$\int_{-\omega_{co}}^{\omega_{co}} S_0(\omega) d\omega = \int_{-\omega_{co}}^{\omega_{co}} S_{AR}(\omega) d\omega, \quad (5.11)$$

which leads to [64]

$$G^2 = \frac{T}{2\pi} \left(R_0 + \sum_{k=1}^m a_k R_k \right). \quad (5.12)$$

The Nyquist criterion defines the time step to be used in terms of the cut-off frequency ω_{co} . That is

$$\Delta t = \frac{\pi}{\omega_{co}}. \quad (5.13)$$

The power spectrum S_{AR} can be computed using the equation

$$S_{AR}(\omega) = \frac{G^2}{\left| 1 + \sum_{k=1}^m a_k e^{-ik\omega T} \right|^2}. \quad (5.14)$$

5.6 AR Fitting of a Combined Dodds-Narayanan Road Power Spectrum

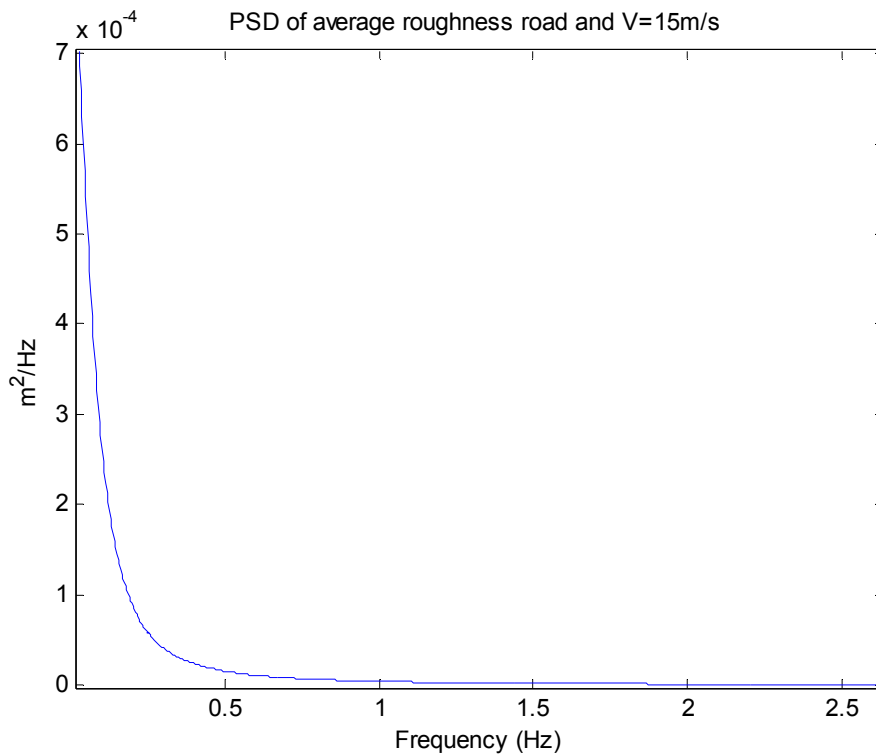
This section presents the results obtained by fitting an AR model to the roughness PSD corresponding to an average quality road with an associated velocity of 15m/s. Table 5.2 shows the required formulae and parameters. Figure 5.10 shows the linear-linear plot of the PSD.

The linear-linear representation is helpful to appreciate the real shape of the road PSD. A steep decaying behavior is observed. It can also be observed that the greater amplitudes are concentrated in a narrow-low-frequency band within 0 and 0.5 Hz, approximately.

Table 5.2 Parameters and equations for average quality roughness PSD with $V=15\text{m/s}$, and $\omega_{co} = 250 \text{ rad/s}$.

Branch of PSD	Formula used	Domain	Parameters
Right	Equation (5.6)	$\omega \in [0, V/K]$	$\sigma = 0.0835, \quad a = 0.0835,$
Left	Equation (5.5)	$\omega \in (\frac{V}{K}, \omega_{co}]$	$S_0 = 128 \times 10^{-6}, \quad n_1=2.0, \quad n_2=1.5, \quad k_0 = 1$

However, the order of magnitude of the amplitudes beyond 0.5 Hz is difficult to estimate. The decaying behavior and the very low amplitudes can be enhanced with the aid of a log-log representation of the PSD, as shown in Figure 5.11. With the aid of this graph it is easier to acquire a better graphical description of the distribution of amplitudes along the operational frequency range, although the shape of the PSD now appears distorted. Once the PSD (target PSD) is computed, the AR filter can be used to fit the target PSD and generate the excitation time histories.

**Figure 5.10** Linear-linear plot of PSD of average road profile.

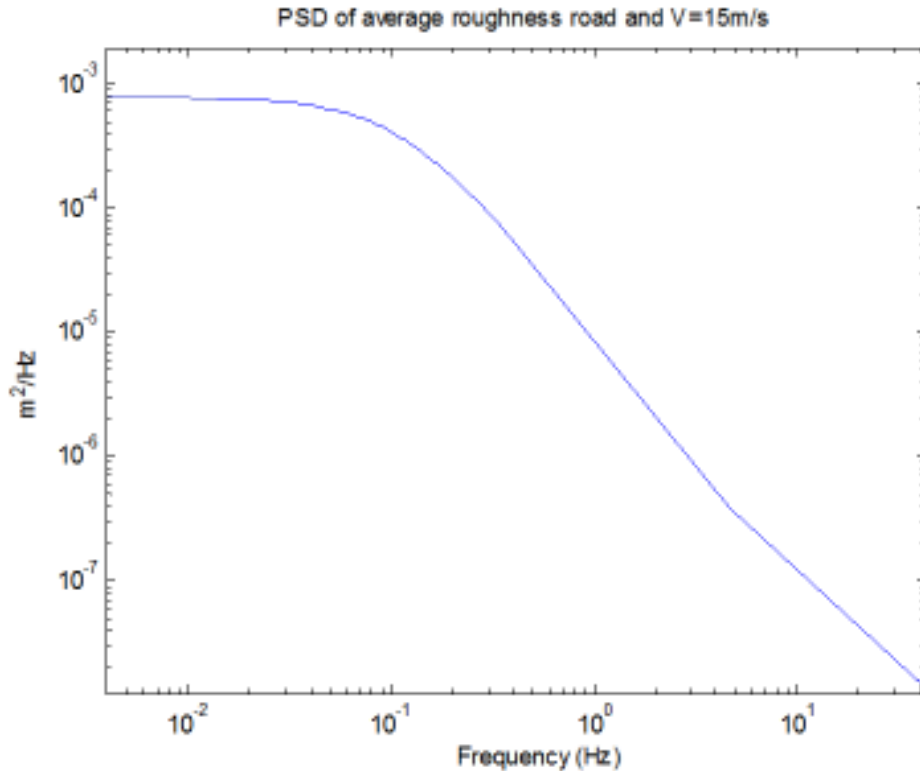


Figure 5.11 Log-log plot of PSD of average road profile.

The AR filter was implemented in MATLAB. In general, a good fitting of the target spectrum was found with an ensemble of $n_{th}=250$ realizations and an order of 45 (denoted AR(45)). According to the criterion given by Spanos and Hansen [64], who suggest a minimum value of the cut-off frequency ω_{co} , equal to twice the frequency range where the PSD is defined, the cut-off frequency was set in 40 Hz ($\cong 251 \text{ rad/s}$); since the range of frequencies of interest is 20 Hz.

In the present work, the value of ω_{co} is used as the minimum value required, since this value has to be adjusted by an algorithm developed to match the time step between two consecutive realization values, the time step of integration of the equations of motion; and the time lag between the front wheel and rear wheel input, the latter depending on the ratio p/V . This algorithm is explained in Chapter 6.

5.7 Analysis of Results. Target Power Spectrum Fitting

The evaluation of correct fitting of the target spectrum by the PSD of the AR(45) filter is carried out by the following tests: visual inspection, computation of area under target spectrum ($A1$), computation of area under spectrum from AR filter ($A2$), and computation of area under spectrum of time histories ($A3$).

The last spectrum computed serves as a further validation. It is obtained by applying the Welch method (section 2.13) [81], [84], which is implemented in Matlab as the pwelch function. Figures 5.12 and 5.13 show the target spectrum along with the PSD obtained from the AR(45) filter, and the PSD obtained with the Matlab function pwelch.

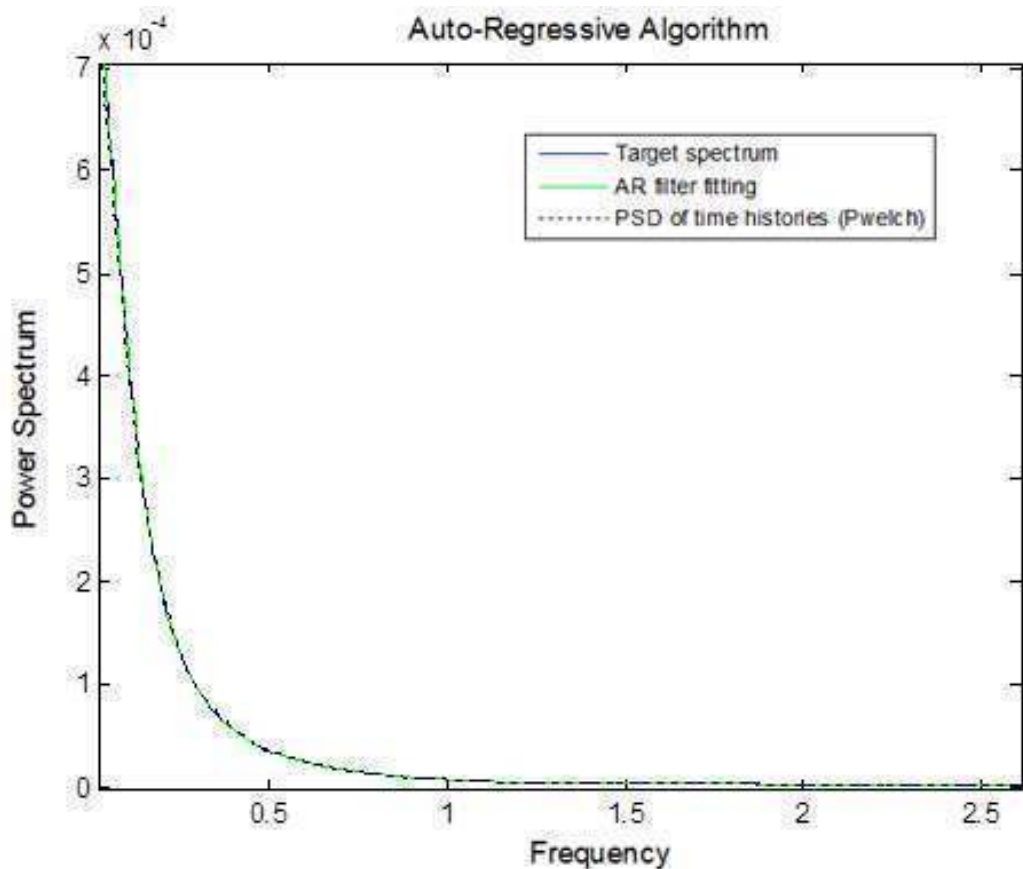


Figure 5.12 PSD of road profile obtained from AR(45) filter and target PSD.

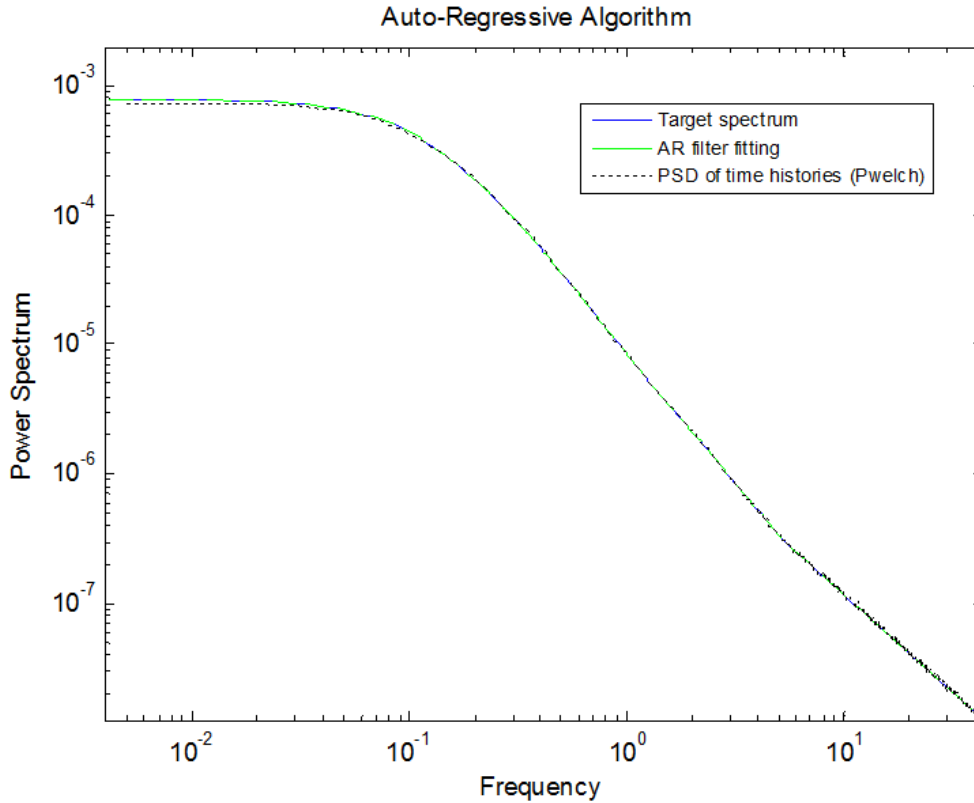


Figure 5.13 Log-log of road profile obtained from AR(45) filter and target spectrum.

The area under each spectrum is computed within the same frequency interval. Besides the computation and comparison of areas $A1$, $A2$, and $A3$; information from the time histories is obtained by:

- I. Computation of autocorrelation of time histories evaluating $R_x(\tau = 0)$, which according to Equation (2.8) equals the variance of the signal (v_S); and by Equation (2.13), equals the area under the power spectral density curve.

and

- II. Analysis of the behavior of the autocorrelation function as $R_x(\tau \rightarrow \infty)$ of the time histories generated by the AR(45) filter. According to Equation (2.9), this analysis allows verification that a zero-mean stationary process is being obtained.

Table 5.3 Areas under PSD's of Figures 5.12 and 5.13.

A1 Target spectrum	A2 AR(45) spectrum	A3 Pwelch spectrum	v_s Variance of t. h.
2.6988e-004	2.6351e-004	2.6342e-004	2.5697e-004
% Error	2.36	2.39	4.78

Table 5.3 presents the computed areas of each PSD presented in Figures 5.12 and 5.13, along with the computed value of the variance of the time histories. From the results of Table 5.3 it can be seen that the fitting is very good. Only the variance exhibits a greater percentage error, which is acceptable, but it may be even improved by increasing the order of the filter. However, the reduction in error of just one or two percent points perhaps is not worth the greater computational effort required.

5.8 Analysis of Results. Generation of Time Histories

An ensemble consisting of 250 time histories was created. One sample time history compatible with the displacement PSD is shown in Figure 5.14. Note the presence of small amplitude components at high frequencies versus the high amplitude components at low frequencies. This behavior is in accord with the shape of the PSD of Figure 5.13.

The analysis of the behavior of the autocorrelation of the PSD, Figure 5.15, is based on the detailed explanations presented in [92] and [145], for the analysis of AR type signals. The slowing decaying behavior shows that successive samples of the time histories are similar, which occur when the poles of the AR filter are real and positive, and are located close to the unit circle. The graph of the autocorrelation corresponds to a low-pass spectrum, which is the case corresponding to the displacement PSD used.

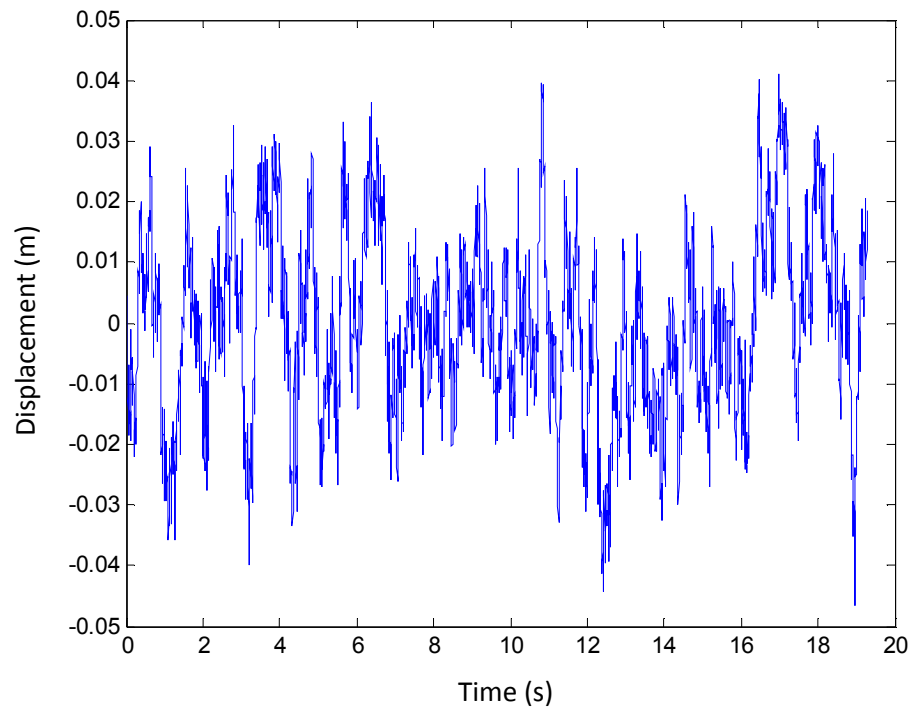


Figure 5.14 Sample time history of the excitation.

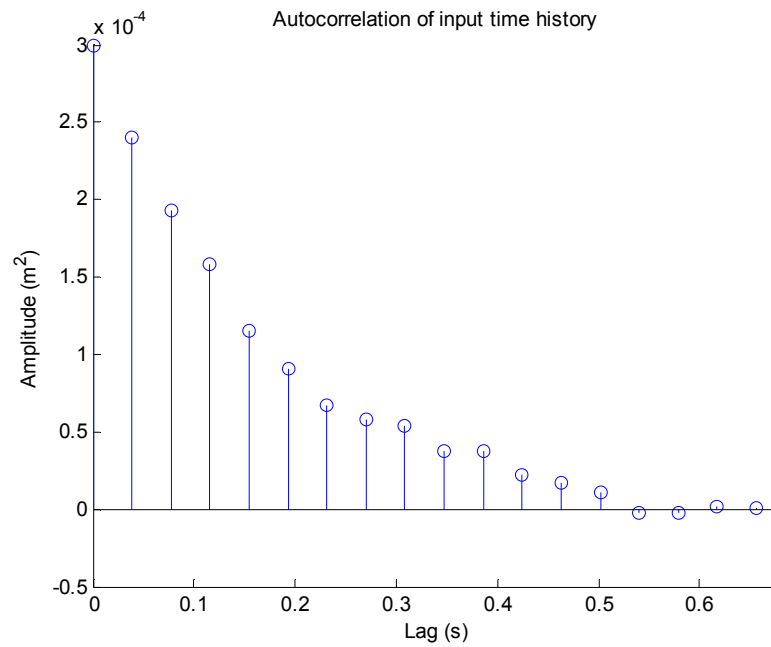


Figure 5.15 Autocorrelation of time history.

5.8.1 Fitting of an Acceleration Power Spectrum

The acceleration PSD was obtained from the displacement PSD with the aid of equation (2.19). The resulting PSD is shown in linear-linear format in Figure 5.16 along with the PSD of the AR(45) filter, and the PSD of the time histories. The same information is presented in Figure 5.17 in log- log format. As in the previous analysis, a number of 250 time histories was generated and used to determine the PSD of the ensemble using the pwelch function of Matlab. The same procedure used to validate the preceding results is used herein.

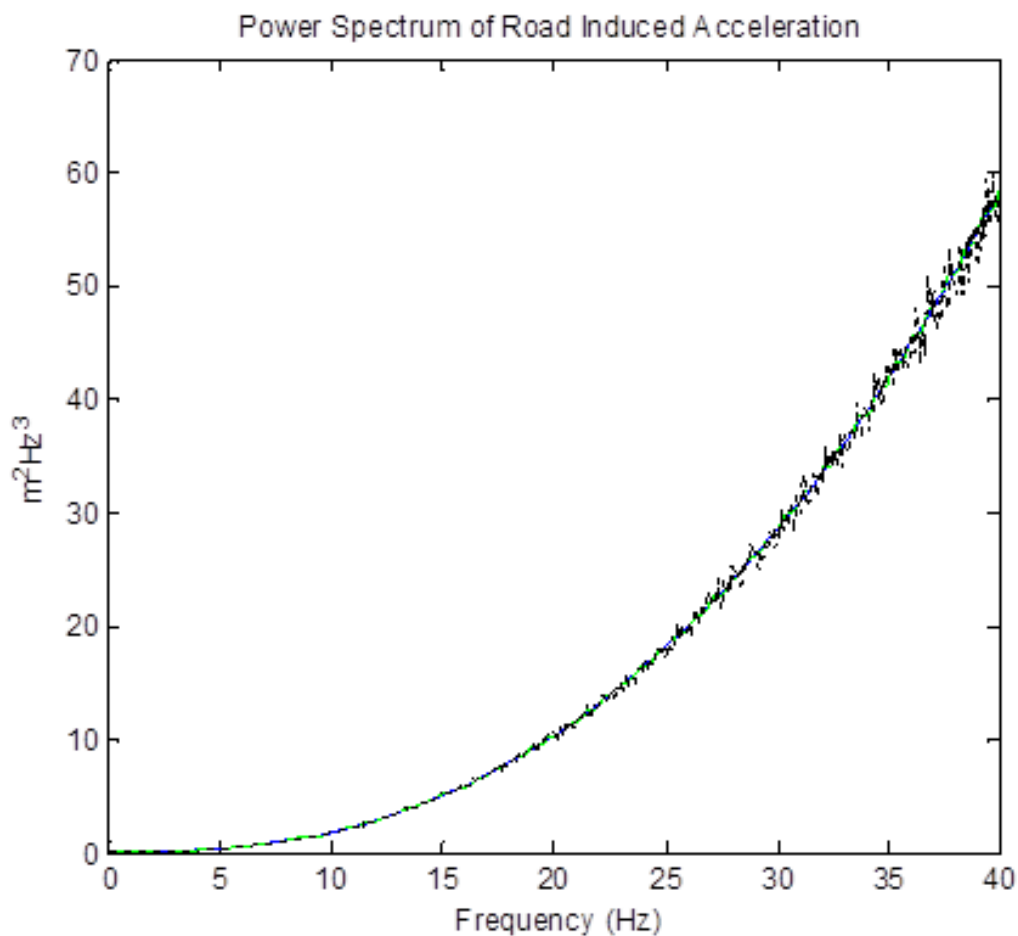


Figure 5.16 PSD of induced acceleration and AR(45) power spectrum.

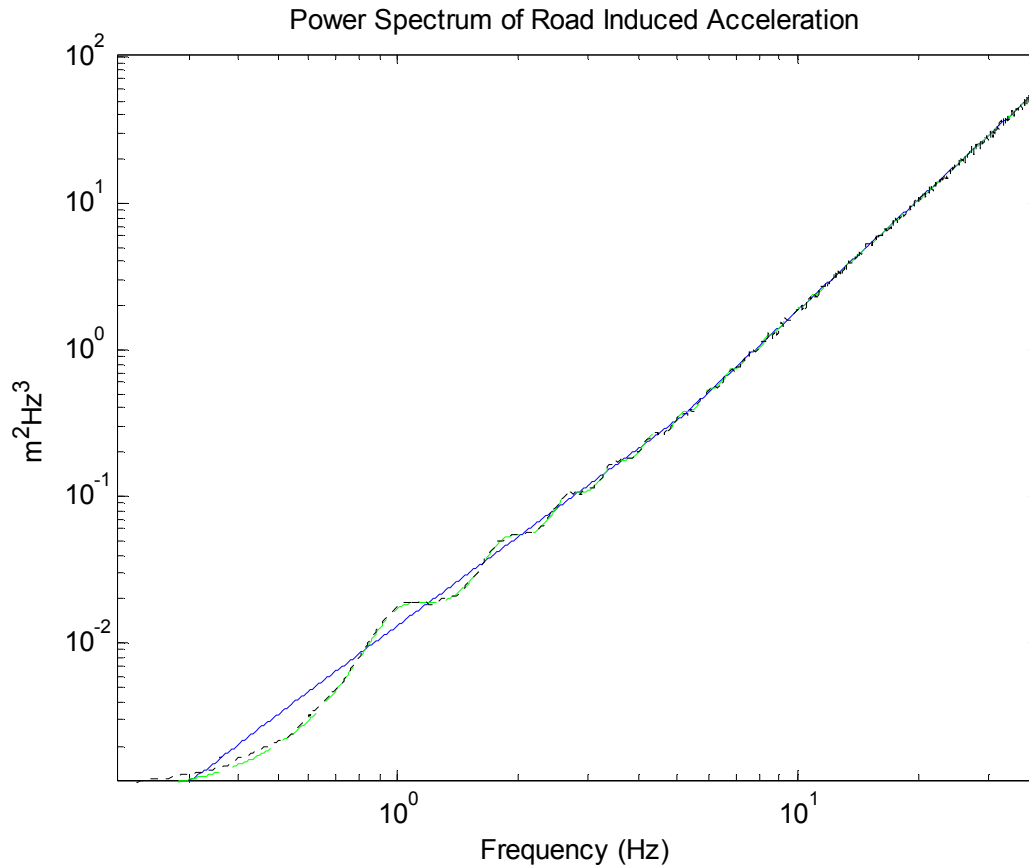


Figure 5.17 Log-log graph of PSD of induced acceleration and AR(45) power spectrum.

A good fitting is seen in Figures 5.16 and 5.17. Small fluctuations around the target spectrum are observed at the high frequencies in Figure 5.16; while Figure 5.17 shows a soft wavy fluctuation in the low frequencies.

Table 5.4 Areas under PSD's of Figures 5.16 and 5.17.

A1 Target spectrum	A2 AR(45) spectrum	A3 Pwelch spectrum	v_S Variance of t. h.
1.4937e+003	1.4936e+003	1.4897e+003	1.4892e+003
% Error	0.0067	0.2678	0.3013

Despite these fluctuations about the target spectrum, the numerical results summarized in Table 5.4, show that the AR filter is capable of fitting quite accurately the acceleration spectrum and of generating reliable signals. With only 250 time histories and an order of 45 the maximum percent error is less than 0.5%.

A sample time history of acceleration is shown in Figure 5.18. In contrast to the time history of the displacement PSD; Note the presence of large amplitude components at high frequencies, in accord with the shape of the acceleration PSD of Figure 5.16.

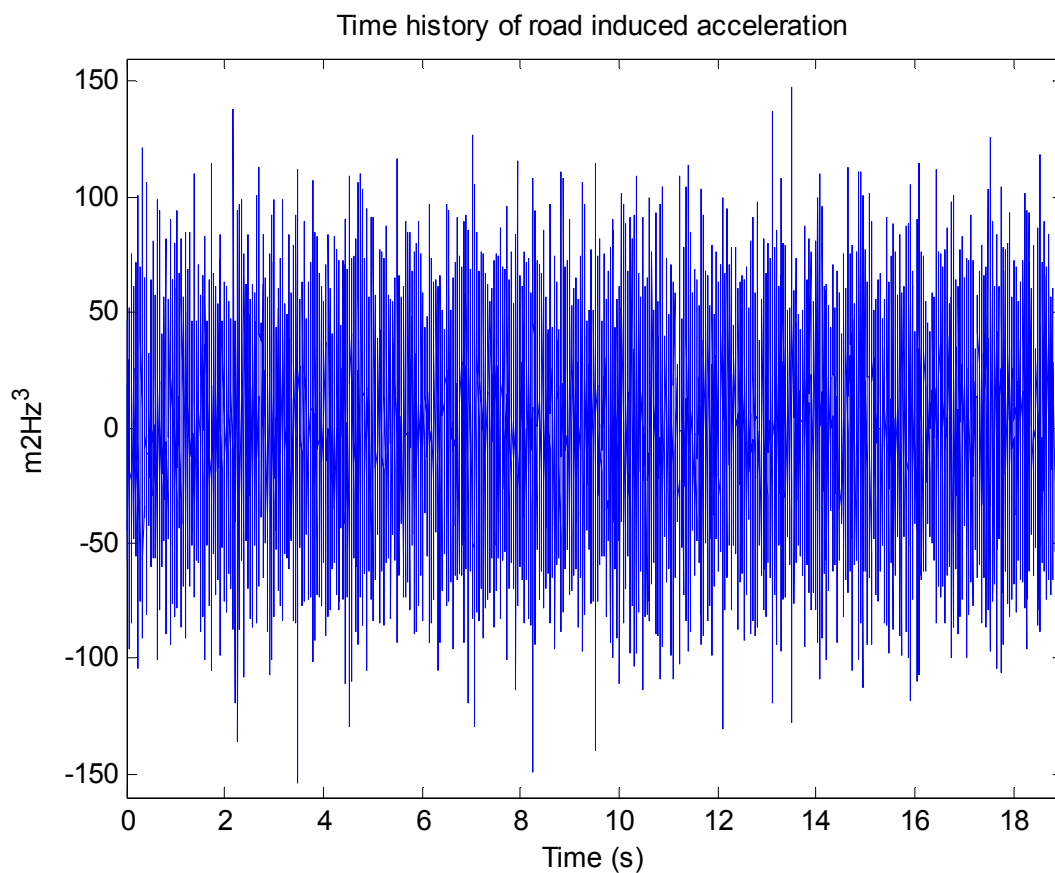


Figure 5.18 Sample time history of acceleration.

The autocorrelation of the acceleration time histories is shown in Figure 5.19. Contrary to the slowly decaying behavior of the displacement PSD autocorrelation, the autocorrelation in Figure 5.19 presents a sudden drop and an alternate change of sign. This behavior is directly related to the rapidly oscillating sequence shown in Figure 5.18., which in turn is related to a high-pass spectrum that has negative real poles close to the unit circle.

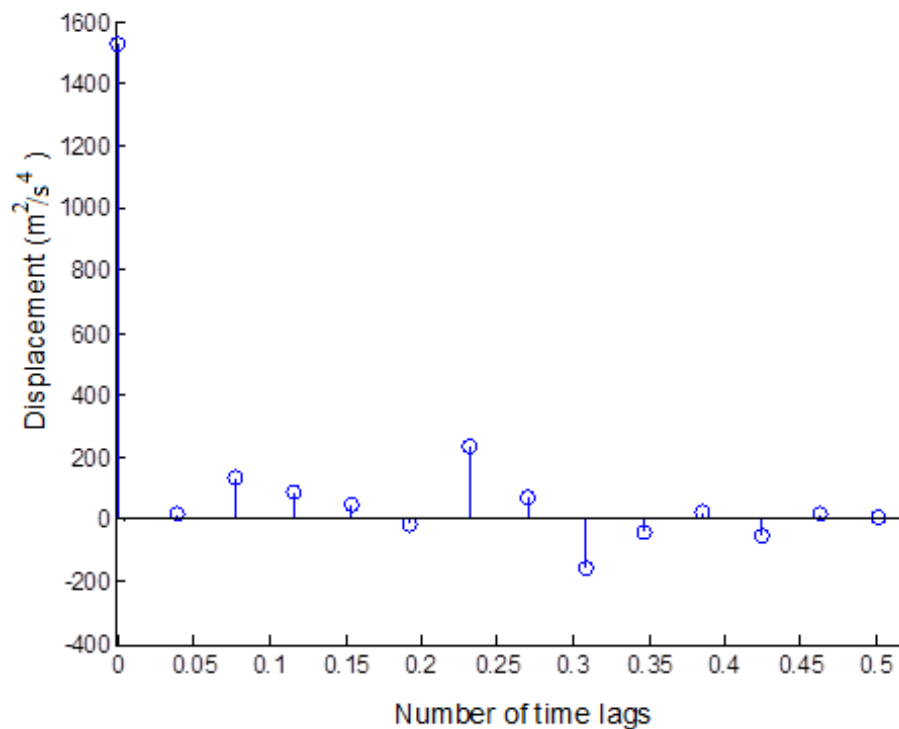


Figure 5.19 Autocorrelation of acceleration.

The preceding road profile models are used in ensuing chapters as input in the dynamic analysis of nonlinear motorcycle models.

Chapter 6

Modeling of Motorcycle Dynamics

6.1 Introduction

A motorcycle, as many ground vehicles, must comply with comfort and safety criteria. To accomplish these goals it is necessary to analyze the dynamical behavior of the motorcycle. Depending on the particular study, certain assumptions can lead to a quite simplified model that may be used to obtain pertinent and accurate information about the motorcycle's behavior. To that end it is necessary, as a first step, to define the main elements and parameters used to model and analyze motorcycles. Also, it is important to specify the conditions in which the motorcycle behavior is studied so that the correct simplifying assumptions may be made. In this regard, two general kinds of motion define the conditions and parts of the motorcycle to be considered in the analysis [43]:

- I. *In-plane motion*, which occurs when the motorcycle travels in a straight path and is lying all the time in the vertical plane. The *in-plane modes* involve frame, suspension, and wheels motion in the vertical plane,
- II. *Out-of-plane motion*, which presents *the out-of-plane modes*, and involves roll, yaw, steering angles and steering head lateral displacement.

The in-plane modes are related to ride comfort and road holding, whereas the out-of-plane modes are related to vehicle stability. In straight running, in-plane and out-of-plane modes are uncoupled and they can be examined separately [33].

Once the motorcycle's elements and parameters are identified an appropriate model is derived. Several configurations are possible. For example, for the analysis of in-plane

motion common examples include: the one-degree-of-freedom (1-DOF) model, the 2-DOF model, and the 4-DOF model [43].

In this study the analysis of the dynamical response of a motorcycle to road roughness as it moves at constant speed in a vertical plane, with respect to the ground is considered. For that purpose the motorcycle is modeled as a 4-DOF system. Thus, only those geometrical parameters that are relevant to the description of the in-plane model are explained in detail. However, for a more complete description of out of plane motion the reader can consult references [12, 20, 23, 29, and 43].

6.2 General Description of a Motorcycle

Basically two complimentary approaches are used to describe a motorcycle [206]:

- I. The *kinematic approach*, which involves a description of position and orientation of the motorcycle and especially of the locations of the points of application of contact point forces;
- II. The *dynamic approach*, which involves the forces and moments acting on the motorcycle and those generated between interconnected elements.

The kinematic description of the motorcycle is important because it is the way in which the various relationships between the motion variables, according to the geometrical properties of the motorcycle, are determined. The dynamical approach allows however, determining the governing equations of motion of the motorcycle. To a first degree of approximation, the kinematical description can be made assuming non-deformable elements, and deformations may be taken into account in the dynamical analysis [43].

6.2.1 Kinematic Description of a Motorcycle

To simplify the kinematic description, the motorcycle is assumed to comprise four main rigid bodies [43], Figure 6.1:

- I. the *rear assembly*, which includes the frame, saddle, tank, and motor-gear group;
 - II. the *rear wheel*,
 - III. the *front assembly*, comprised by the fork, the steering head and the handlebars,
- and
- IV. the *front wheel*.

Considering non-deformable tires and their pure rolling motion, each wheel can only rotate about:

- I. the contact point on the wheel plane (forward motion),
- II. the intersection axis of the motorcycle and road planes (roll motion),
- III. the axis passing through the contact point and the center of the wheel (spin).

Assuming that the tires move without slippage the number of degrees of freedom required to describe the motion of a motorcycle is 3 [43]:

- I. *forward motion* of the motorcycle (represented by the rear wheel rotation);
 - II. *roll motion* around the straight line which joins the tire contact points on the road plane;
- and
- III. *steering rotation*.

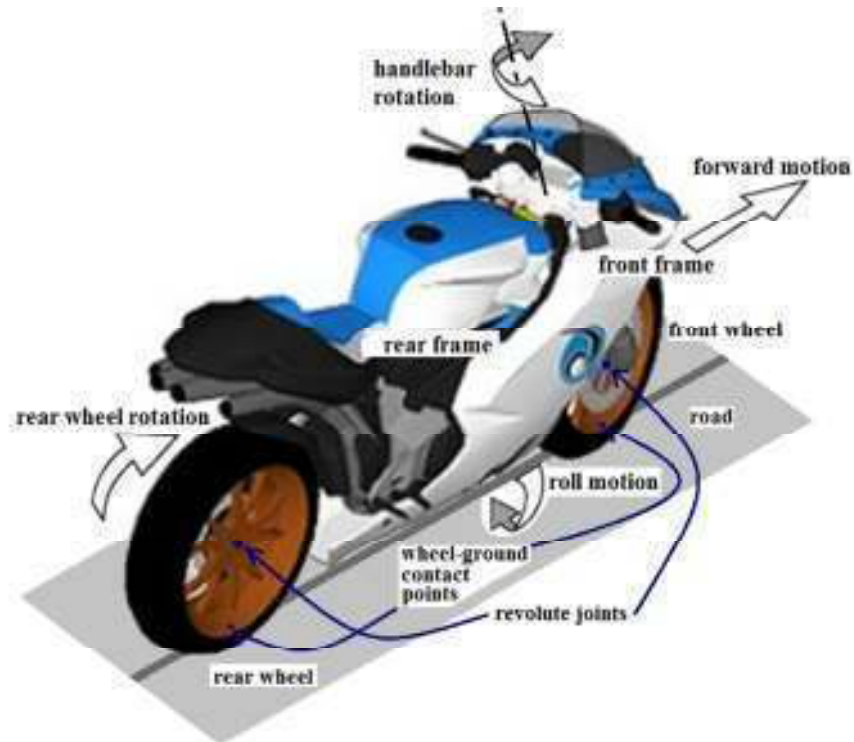


Figure 6.1 Kinematic description of a motorcycle (Adapted from [205]).

A more realistic motion can be considered if slippage is taken into account; due to the generation of longitudinal (driving and braking) and lateral forces a set of four degrees of freedom can be added to the previous set. That is

- I. *longitudinal slippage of the front wheel* (braking),
 - II. *longitudinal slippage of the rear wheel* (thrust or braking),
- and
- III. *lateral slippage of the rear wheel*.

Thus, in terms of kinematics there are seven degrees of freedom to completely describe the motorcycle's motion.

6.2.2 Geometric Parameters of a Motorcycle

Assuming that the motorcycle is a rigid body with no suspension and non-deformable toroidal tires, the following parameters can be used to geometrically it [43]:

- I. p wheelbase,
- II. d fork offset,
- III. ε caster angle,
- IV. R_r radius of the rear wheel,
- V. R_f radius of the front wheel,
- VI. t_r radius of the rear tire cross section,
- and
- VII. t_f radius of the front tire cross section.

These parameters are shown in Figure 6.2.

The *wheelbase* is the distance between the contact points of the tires on the road; the *caster angle* is the angle between the vertical axis and the rotation axis of the front section (the axis of the steering head); the *fork offset* is the distance between the axis of the steering

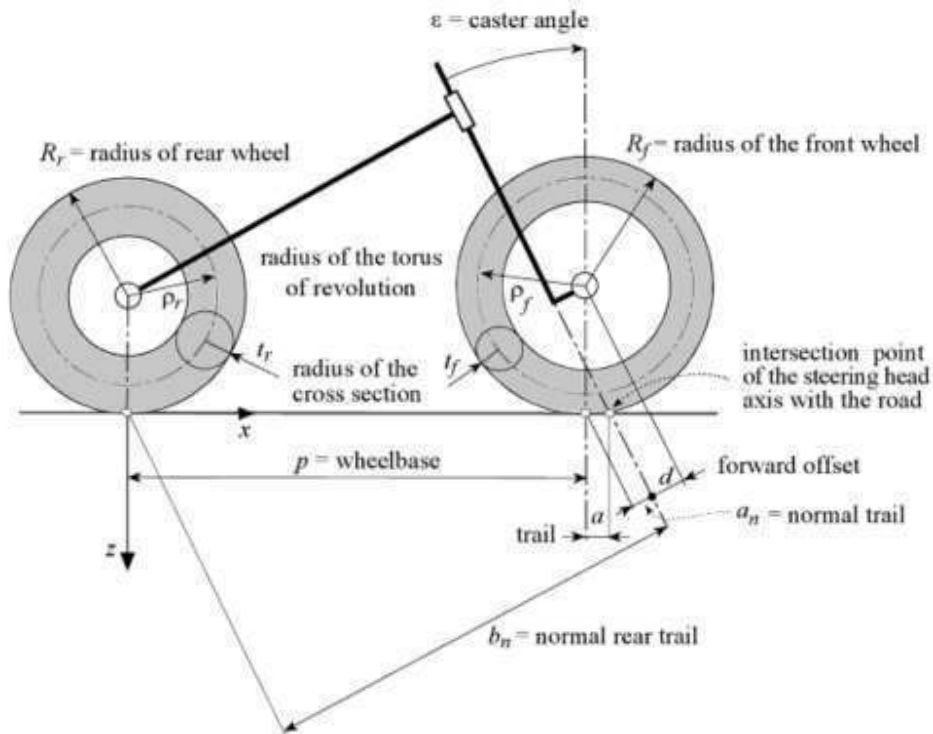


Figure 6.2. Geometry of a motorcycle (From reference [43])

head and the center of the front wheel; and the *trail* is the distance between the contact point of the front wheel and the intersection point of the steering head axis with the road. It is considered positive if the contact point of the front wheel is behind the intersection point of the steering head axis and the road.

Two parameters are expressed in terms of the previous ones. Specifically the *normal trail* a_n , is

$$a_n = R_f \sin(\varepsilon) - d, \quad (6.1)$$

And the *mechanical trail* a , is

$$a = a_n / \cos(\varepsilon). \quad (6.2)$$

The geometric parameters usually needed to describe the kinematic and dynamic behavior of a motorcycle are the wheelbase, the trail, and the caster angle.

The wheelbase is important in this analysis because it has a great influence in the in-plane modes of vibration of the motorcycle. The value of the wheelbase varies according to the kind of motorcycle. Usually it ranges from 1.20 m up to 1.6 m, but in some cases it can be greater.

The caster angle also varies according to the type of motorcycle: from 19° to 33°.

The value of the trail depends on the type of motorcycle and its wheelbase. It ranges from 75 mm to 120 mm or even greater in some cases. The trail plays an important role in the stability of the motorcycle, especially in rectilinear motion, when the effect of lateral forces is considered. The greater the value of a positive trail the more stable the motorcycle is in rectilinear motion, but less maneuverable.

From these parameters, only the wheelbase is used in the present study, the other two do not have a considerable effect in the description of in plane motion [43].

6.3 Simplifying Criteria for Obtaining a 4-DOF In-Plane Model

For modeling purposes, a motorcycle with suspension can be regarded as a rigid body (*sprung mass*) connected to the wheels with elastic systems (front and rear suspension). The masses attached to the wheels are called *unsprung masses*. The degrees of freedom involved in the 4-DOF model are associated with two modes of vibration, namely the *in-plane* and *out-of-plane* modes; they are characterized by their respective natural frequencies.

6.3.1 In-plane Vibration Modes of a Motorcycle

The in-plane modes are decoupled from the out-of-plane ones. The first mode, called the *bounce mode*, is a pure vertical translation, while the second mode, called the *pitch mode*, is a pure rotation around the center of gravity. These modes are shown in Figure 6.3. For in-plane motion these two modes are uncoupled. *Front hop mode*, *rear hop mode* correspond to the vertical motion of each unsprung mass.

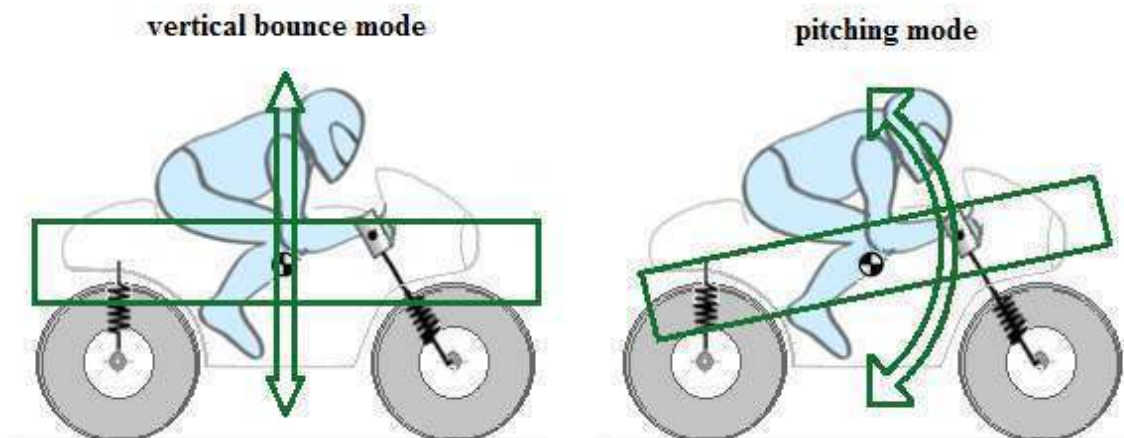


Figure 6.3. Typical modes of vibration of an in-plane motorcycle model.

6.3.2 Simplified Model of Motorcycle Suspension

6.3.2.1 Suspension Modeling

Motorcycle suspension plays an important role in braking, shock absorption, and rider comfort by allowing the wheels to follow the profile of the road without transmitting excessive vibration to the rider. The suspension is also intended to provide wheel grip on the road plane to transmit the required driving and braking forces.

Ride quality is an important aspect of vehicle-road interaction and increasing attention has been devoted by motorcycle researchers to the area of rider comfort [7-9, and 36]. This is not only because there exists a demand from riders of more comfortable motorcycles; but because there is also a close connection between comfort and rider's handling capacity.

Another important consequence of improving comfort in motorcycles is an increase in rider's safety. These considerations have also motivated an active research in the field of design and analysis of motorcycle suspension systems; the following contributions exemplify this trend.

Jennings [4] carried out experimental work with suspension dampers in order to investigate the effect of suspension damping on cornering weave and concluded that the damping characteristics of the suspension greatly affected the motorcycle stability, and that the rear suspension damping is important in controlling cornering weave instability. Basso et al. [189] used a 2-DOF model to analyze the dynamic behavior of the front suspension of a motorcycle which travels at different speeds. They also carried out experimental measurements which showed close agreement with simulation results, leading the authors to conclude that the 2-DOF model provided a good representation of the suspension system. Evangelou [190] introduced a variable geometry rear mono-shock suspension

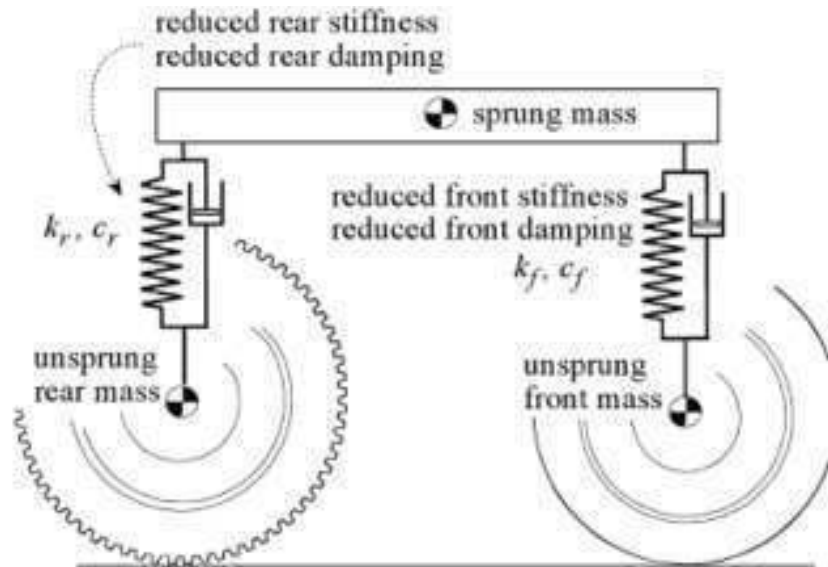


Figure 6.4 Reduced suspension model (from [43])

system that can be used to control high performance motorcycles. The results show that this suspension design renders improvements on the dynamic properties of the weave mode for a range of working regimes. Other relevant contributions can be found in references [78, 166, 176-179]

6.3.2.2 Reduced Stiffness of the Suspension

Since several configurations of suspension are available, the in-plane dynamics study requires the real suspension to be reduced to an equivalent suspension, represented by two vertical spring-damper units that connect the unsprung masses to the sprung mass [43]. Figure 6.4 depicts this abstraction.

The parameters defining the equivalent suspension are the reduced stiffness, and the reduced damping.

With reference to Figure 6.2, if k denotes the real stiffness of the front suspension, the reduced stiffness k_f can be computed by the equation

$$k_f = \frac{k}{\cos^2(\varepsilon)}. \quad (6.3)$$

The value of the reduced stiffness of the front suspension varies according to the weight of the motorcycle and its use. Values range from about 10,000 N/m for light motorcycles to values around 20,000 N/m for heavy motorcycles.

The reduced stiffness of the rear suspension involves the geometric parameters of the particular type of suspension. Thus, a general formula [43] provides is

$$k_r \cong k\tau_{m,YC}^2, \quad (6.4)$$

where $\tau_{m,YC}^2$ represents the ratio between the deformation velocity of the spring and the wheel vertical velocity.

Values of the reduced stiffness of the rear suspension range from about 18,000 N/m for light motorcycles to values around 30,000 N/m for heavy motorcycles.

6.3.2.3 Reduced Damping of the Suspension

With reference to Figure 6.2, if the damping constant of the fork is denoted by c , the equivalent damping of the front suspension c_f is

$$c_f = \frac{c}{\cos^2(\varepsilon)}. \quad (6.5)$$

The velocity ratio depends on the geometric characteristics of the rear suspension mechanism and varies with the vertical wheel travel.

The reduced damping of the rear suspension is

$$c_r \cong c\tau_{m,YC}^2. \quad (6.6)$$

6.4 Motorcycle Tires

Tires are one of the most important elements in motorcycles. Due to their deformability, tires allow contact between the wheel and the road; improve the adherence and the comfort of the ride, and influence the stability of the vehicle.

6.4.1 Tire Modeling

As mentioned before, the early motorcycle models did not take into account the effect of the tire. The paper presented by Sharp in 1971 [2] introduced another important improvement in motorcycle modeling with the inclusion of a model for the tires, addressing sources of steady state forces and moments due to side-slip and camber angle.

An improvement to Sharp's 1971 model was achieved by Sharp and Pacejka [25]. A more detailed study of the generation of shear forces in the contact patch area was presented. In this regard, other notable contributions are the works of Cossalter and Doria [165], Cossalter et al. [187], Lot [169], and Tezuka et al. [171]. All these studies present tire models that have found application in the analysis of the motorcycle stability and handling, especially at cornering.

Motorcycle tires present a real challenge for modeling purposes. This is the reason why, depending on the type of study, different approaches have been employed by researchers. Indeed, there is no consensus on a single model that describes all the possible tire features. However, some contributions have aimed to present models that can practically cover any dynamic situation in which the lateral and longitudinal interaction of the tire and the road is considered. The model most widely used is Pacejka's "magic formula" [198]. Other important contribution in this field is the model presented by Cossalter and Lot [29]. Note

that these tire models consider the road as flat; in general, non-flat road profiles are not included in these formulations.

6.4.2 Vibration Modes of Tires

The modes of vibration of motorcycle tires can be classified in two kinds: in-plane modes, and out-of-plane modes. However, mixed modes can also occur.

With regard to in-plane dynamics, tires have a direct influence in shock absorption and braking. *In-plane modes* are characterized by radial and/or circumferential displacement of the points located in the symmetry plane of the wheel. In-plane modes occur in a range of 300-400 Hz, while *out-of-plane modes* occur in a range of 100-200 Hz.

Although out-of plane-modes have an excitation frequency range lower than in-plane modes, the latter are in general, the most often excited. This is due to the fact that during rectilinear motion or steady turning, the resultant of tire forces remains, approximately, on the symmetry plane of the wheel. Also, loss factors influence the presence of both vibration modes.

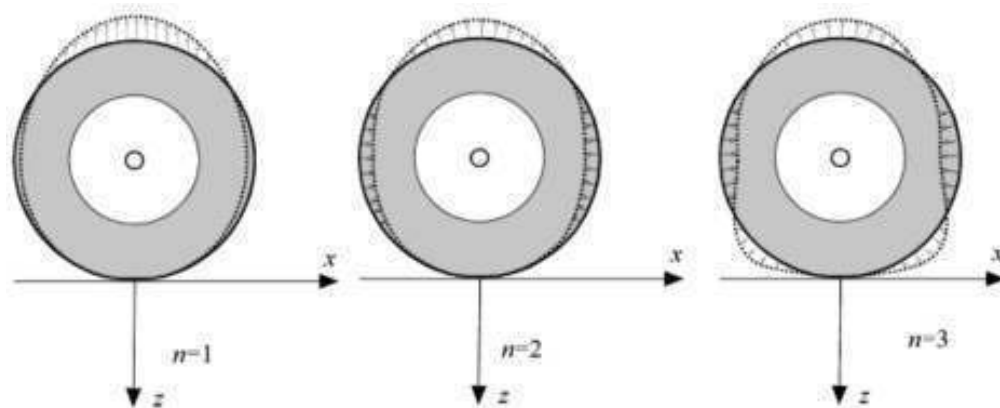


Figure 6.5 In-plane tire's mode of vibration (Adapted from [43])

For out-of-plane modes these losses are higher than those of in-plane-modes, and as a consequence out-of-plane modes fade away faster than in-plane-modes.

Since the sensation of discomfort experienced by the driver while traveling on a rough road is mainly due to vertical vibration [200], the preponderant excitation force to consider acting on the motorcycle is vertical as well. As a consequence, for studies related to comfort an in-plane motion is commonly assumed [164]. This assumption simplifies the analysis allowing the use of vertical tire/road models that define the vertical force provided by the tire. This force is mainly given by the tire's vertical stiffness and is also dependent of the ground profile [182]. These models may comprise a spring stiffness only, or a combination of tire stiffness and damping [162].

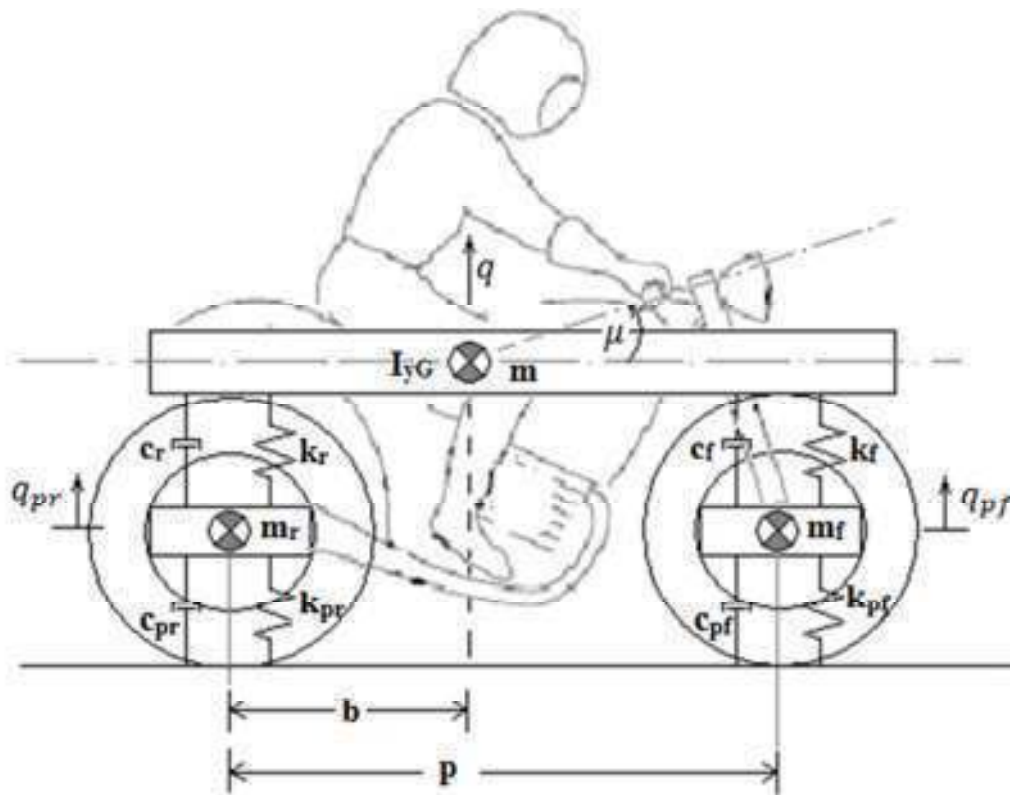


Figure 6.6. 4-DOF In Plane Model (Adapted from [43])

6.5 The Linear 4-DOF In-Plane Model

6.5.1 General Assumptions and Nomenclature

The motorcycle moves in a straight path in its plane of symmetry (in-plane motion) at constant speed. The driver is attached to the motorcycle with no possibility of getting separated from it. This assumption is reasonably valid for straight motion at constant speed. Further, the driver's mass, the rear assembly of the motorcycle (frame, saddle, tank, and motor-gear group), and the front assembly (the fork, the steering head and the handlebars) are all represented by a homogeneous, rectangular, prismatic bar (sprung mass) with its weight acting on its center of gravity (C.G.), refer to Figure 6.6.

Each tire with its corresponding brake system is represented by a single mass, the *unsprung mass*, which also accounts for the suspension elements' masses. Then the whole motorcycle is represented by three rigid bodies: the sprung mass and the rear and front unsprung masses whose vibrating motion is described by four independent coordinates: the vertical displacement of the sprung mass center q , the pitching rotation of the sprung mass μ , and the vertical displacements of the two unsprung masses q_{pf} and q_{pr} . The tires' stiffnesses k_{pf} and k_{pr} , and damping c_{pf} and c_{pr} are represented by the pair of spring-dashpot attached to the ground.

Drag forces are not considered. It is also assumed that the tires always keep contact with the road and that there is no slipping.

6.5.2 Motorcycle Data

The motorcycle values shown in Table 6.1 are reported in reference [43], and they are used in this thesis.

Table 6.1 Motorcycle data sheet.

Motorcycle characteristics	
Wheelbase p [m]	1.40
Distance from the center of gravity to the rear wheel b [m]	0.70
Sprung mass (The masses of the chassis, engine and rider) m [kg]	200
Front unsprung mass m_f [kg]	15.0
Rear unsprung mass m_r [kg]	18.0
Pitch moment of inertia I_{yG} [kgm ²]	38.0
Reduced stiffness of the front suspension k_f [N/m]	15,000
Reduced stiffness of the rear suspension k_r [N/m]	24,000
Reduced damping of the front suspension c_f [Ns/m]	500
Reduced damping of the rear suspension c_r [Ns/m]	750
Front tire stiffness k_{pf} [N/m]	180,000
Rear tire stiffness k_{pr} [N/m]	180,000
Front tire damping c_{pf} [Ns/m]	0
Rear tire damping c_{pr} [Ns/m]	0

6.5.3 Derivation of the Linear Model of Motion in Absolute Coordinates

To derive the equation of motion of the motorcycle in absolute coordinates, sum up forces in the Z-direction. This yields

$$m\ddot{q} + (c_f + c_r)\dot{q} - c_f\dot{q}_{pf} - c_r\dot{q}_{pr} + [c_f(p - b) - c_r b]\dot{\mu} + (k_f + k_r)q + [k_f(p - b) - k_r b]\mu - k_r q_{pr} - k_f q_{pf} = 0. \quad (6.7)$$

Similarly summing up moments about the center of gravity yields

$$I_G\ddot{\mu} + [c_f(p - b) - c_r b]\dot{q} - c_f(p - b)\dot{q}_{pf} + c_r b\dot{q}_{pr} + [c_r b^2 + c_f(p - b)^2]\dot{\mu} + [k_f(p - b) - k_r b]q - k_f(p - b)q_{pf} + k_r b q_{pr} + [k_r b^2 + k_f(p - b)^2]\mu = 0. \quad (6.8)$$

Also considering the rear unsprung mass one obtains

$$m_r \ddot{q}_{pr} - c_r \dot{q} + (c_r + c_{pr}) \dot{q}_{pr} + c_r b \dot{\mu} + (k_r + k_{pr}) q_{pr} - k_r q + k_r b \mu = 0, \quad (6.9)$$

and considering the motion of the front sprung mass one derives

$$m_f \ddot{q}_{pf} - c_f \dot{q} + (c_f + c_{pf}) \dot{q}_{pf} + c_f (p - b) \dot{\mu} + (k_f + k_{pf}) q_{pf} - k_f q + k_f (p - b) \mu = 0. \quad (6.10)$$

The preceding four equations can be grouped in the form

$$\begin{bmatrix} m & 0 & 0 & 0 \\ 0 & I_G & 0 & 0 \\ 0 & 0 & m_r & 0 \\ 0 & 0 & 0 & m_f \end{bmatrix} \begin{bmatrix} \ddot{q} \\ \ddot{\mu} \\ \ddot{q}_{pr} \\ \ddot{q}_{pf} \end{bmatrix} + \begin{bmatrix} c_f + c_r & c_f(p - b) - c_r b & -c_r & -c_f \\ c_f(p - b) - c_r b & c_r b^2 + c_f(p - b)^2 & c_r b & -c_f(p - b) \\ -c_r & c_r b & c_r + c_{pr} & 0 \\ -c_f & -c_f(p - b) & 0 & c_f + c_{pf} \end{bmatrix} \begin{bmatrix} \dot{q} \\ \dot{\mu} \\ \dot{q}_{pr} \\ \dot{q}_{pf} \end{bmatrix} + \begin{bmatrix} k_f + k_r & k_f(p - b) - k_r b & -k_r & -k_f \\ k_f(p - b) - k_r b & k_r b^2 + k_f(p - b)^2 & k_r b & -k_f(p - b) \\ -k_r & k_r b & k_r + k_{pr} & 0 \\ -k_f & -k_f(p - b) & 0 & k_f + k_{pf} \end{bmatrix} \begin{bmatrix} q \\ \mu \\ q_{pr} \\ q_{pf} \end{bmatrix} = \begin{bmatrix} 0 \\ 0 \\ 0 \\ 0 \end{bmatrix}. \quad (6.11)$$

Or in a symbolic notation

$$\mathbf{M} \ddot{\mathbf{q}} + \mathbf{C} \dot{\mathbf{q}} + \mathbf{K} \mathbf{q} = \mathbf{0}, \quad (6.12)$$

where \mathbf{M} is the mass matrix given by the equation

$$\mathbf{M} = \begin{bmatrix} m & 0 & 0 & 0 \\ 0 & I_G & 0 & 0 \\ 0 & 0 & m_r & 0 \\ 0 & 0 & 0 & m_f \end{bmatrix}, \quad (6.13)$$

\mathbf{C} corresponds to the damping matrix

$$\mathbf{C} = \begin{bmatrix} c_f + c_r & c_f(p - b) - c_r b & -c_r & -c_f \\ c_f(p - b) - c_r b & c_r b^2 + c_f(p - b)^2 & c_r b & -c_f(p - b) \\ -c_r & c_r b & c_r + c_{pr} & 0 \\ -c_f & -c_f(p - b) & 0 & c_f + c_{pf} \end{bmatrix}, \quad (6.14)$$

and \mathbf{K} denotes the stiffness matrix

$$\mathbf{K} = \begin{bmatrix} k_f + k_r & k_f(p - b) - k_r b & -k_r & -k_f \\ k_f(p - b) - k_r b & k_r b^2 + k_f(p - b)^2 & k_r b & -k_f(p - b) \\ -k_r & k_r b & k_r + k_{pr} & 0 \\ -k_f & -k_f(p - b) & 0 & k_f + k_{pf} \end{bmatrix}. \quad (6.15)$$

Further, \mathbf{q} denotes the vector of generalized displacements

$$\mathbf{q} = \begin{bmatrix} q \\ \mu \\ q_{pr} \\ q_{pf} \end{bmatrix}. \quad (6.16)$$

6.5.4 Equations of Motion in Relative Coordinates

In many situations it may be convenient to express the model in relative coordinates, as shown in Figure 6.7. This is the case, for example, for the dynamical analysis of a suspension where forces in the spring elements need to be computed.

The following transformations relate the absolute and the relative systems

$$z_r = q - \mu b - q_{pr}, \quad (6.17a)$$

$$z_f = q - \mu a - q_{pf}, \quad (6.17b)$$

$$z_{pr} = q_{pr} - w_r, \quad (6.17c)$$

and

$$z_{pf} = q_{pf} - w_f. \quad (6.17d)$$

This set of transformation equations can be expressed in the convenient matrix form

$$\mathbf{z} = \mathbf{A}^{-1} \mathbf{q} - \mathbf{w}, \quad (6.18)$$

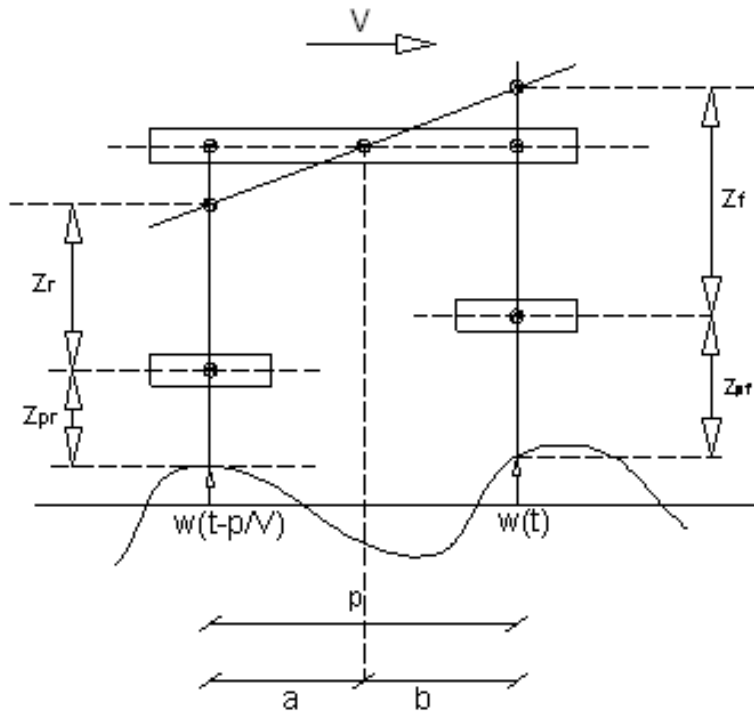


Figure 6.7. 4-DOF In Plane Model in relative coordinates.

where

$$\mathbf{A}^{-1} = \begin{bmatrix} 1 & -b & -1 & 0 \\ 1 & a & 0 & -1 \\ 0 & 0 & 1 & 0 \\ 0 & 0 & 0 & 1 \end{bmatrix}, \quad (6.19)$$

and

$$\mathbf{A} = \frac{1}{d} \begin{bmatrix} a & b & a & b \\ -1 & 1 & -1 & 1 \\ 0 & 0 & d & 0 \\ 0 & 0 & 0 & d \end{bmatrix}. \quad (6.20)$$

The last expression allows expressing the model in terms of absolute coordinates according to the relation

$$\mathbf{q} = \mathbf{A}(\mathbf{z} + \mathbf{w}). \quad (6.21)$$

Applying Equation (6.17a-d) to the system in Equation (6.12), the equations of motion take the form

$$\bar{\mathbf{M}}\ddot{\mathbf{z}} + \bar{\mathbf{C}}\dot{\mathbf{z}} + \bar{\mathbf{K}}\mathbf{z} = \mathbf{0}, \quad (6.22)$$

where the mass, damping and stiffness matrices, $\bar{\mathbf{M}}$, $\bar{\mathbf{C}}$, and $\bar{\mathbf{K}}$, respectively; in terms of relative coordinates are expressed as

$$\bar{\mathbf{M}} = \frac{1}{p} \begin{bmatrix} am & bm & am & bm \\ -I_G & I_G & -I_G & I_G \\ 0 & 0 & pm_r & 0 \\ 0 & 0 & 0 & pm_r \end{bmatrix}, \quad (6.23)$$

$$\bar{\mathbf{C}} = \begin{bmatrix} c_r & c_f & 0 & 0 \\ -bc_r & ac_f & 0 & 0 \\ -c_r & 0 & c_{pr} & 0 \\ 0 & -c_f & 0 & c_{pf} \end{bmatrix}, \quad (6.24)$$

$$\bar{\mathbf{K}} = \begin{bmatrix} k_r & k_f & 0 & 0 \\ -bk_r & ak_f & 0 & 0 \\ -k_r & 0 & k_{pr} & 0 \\ 0 & -k_f & 0 & k_{pf} \end{bmatrix}, \quad (6.25)$$

and

$$\bar{\mathbf{z}} = \begin{bmatrix} z_r \\ z_f \\ z_{pr} \\ z_{pf} \end{bmatrix}. \quad (6.26)$$

6.5.5 Free Vibration

The natural vibration frequencies of the 4-DOF system described by Equation (6.12) are:

$$f_{n1} = 2.03 \text{ Hz}$$

$$f_{n2} = 3.42 \text{ Hz}$$

$$f_{n3} = 16.98 \text{ Hz}$$

$$f_{n4} = 18.16 \text{ Hz}$$

$$\omega_{n1} = 12.76 \text{ rad/s}$$

$$\omega_{n2} = 21.48 \text{ rad/s}$$

$$\omega_{n3} = 106.70 \text{ rad/s}$$

$$\omega_{n4} = 114.11 \text{ rad/s}$$

6.6. Motorcycle Response to Road Profile. Frequency Domain Approach

If the motorcycle moves at constant speed V the dynamic equilibrium is described by the set of second order differential equations in absolute coordinates

$$\mathbf{M}\ddot{\mathbf{q}} + \mathbf{C}\dot{\mathbf{q}} + \mathbf{K}\mathbf{q} = \tilde{\mathbf{C}}\dot{\mathbf{w}} + \tilde{\mathbf{K}}\mathbf{w}, \quad (6.27)$$

where \mathbf{w} is the vector of road unevenness that excites the front and the rear wheels and is expressed as

$$\mathbf{w} = \begin{Bmatrix} 0 \\ 0 \\ w_r \\ w_f \end{Bmatrix}. \quad (6.28)$$

The symbols $\tilde{\mathbf{C}}$ and $\tilde{\mathbf{K}}$ denote the superimposed motion damping and stiffness matrices given by the equations

$$\tilde{\mathbf{C}} = \begin{bmatrix} 0 & 0 & 0 & 0 \\ 0 & 0 & 0 & 0 \\ 0 & 0 & c_{pr} & 0 \\ 0 & 0 & 0 & c_{pf} \end{bmatrix}, \quad (6.29)$$

and

$$\tilde{\mathbf{K}} = \begin{bmatrix} 0 & 0 & 0 & 0 \\ 0 & 0 & 0 & 0 \\ 0 & 0 & k_{pr} & 0 \\ 0 & 0 & 0 & k_{pf} \end{bmatrix}. \quad (6.30)$$

In relative coordinates Equation (6.27) takes the form

$$\bar{\mathbf{M}}\ddot{\mathbf{z}} + \bar{\mathbf{C}}\dot{\mathbf{z}} + \bar{\mathbf{K}}\mathbf{z} = -\bar{\mathbf{M}}\ddot{\mathbf{w}}. \quad (6.31)$$

6.6.1 Frequency Response Function Matrix

The vertical accelerations can be obtained by transforming the system of Equations (6.27) into the frequency domain for analysis in the absolute coordinates, or the system of Equations (6.31) for analysis in relative coordinates.

6.6.1.1 Frequency Response Function Matrix in Absolute Coordinates

Transformation of Equations (6.27) into the frequency domain leads to

$$\mathbf{H}_q(\omega) = [-\omega^2 \mathbf{M} + i\omega \mathbf{C} + \mathbf{K}]^{-1} [i\omega \tilde{\mathbf{C}} + \tilde{\mathbf{K}}]. \quad (6.32)$$

The two excitations at the wheels correspond to the same excitation, but with a time lag p/V . Thus the excitation vector Equation (6.28) can be expressed as

$$\mathbf{w} = \begin{Bmatrix} 0 \\ 0 \\ w(t - p/V) \\ w(t) \end{Bmatrix}. \quad (6.33)$$

This, in turn can be expressed in the frequency domain as

$$\mathbf{W}(\omega, V) = \begin{Bmatrix} 0 \\ 0 \\ e^{-i\omega(p/V)} \\ 1 \end{Bmatrix} W(\omega) = \mathbf{T}(\omega, V) W(\omega), \quad (6.34)$$

where the wheel-base filtering vector $\mathbf{T}(\omega, V)$ is given by

$$\mathbf{T}(\omega, V) = \begin{Bmatrix} 0 \\ 0 \\ e^{-i\omega(p/V)} \\ 1 \end{Bmatrix}. \quad (6.35)$$

Taking into consideration Equation (6.34) the FRF given by Equation (6.32) takes the form

$$\hat{\mathbf{H}}_q(\omega, V) = [-\omega^2 \mathbf{M} + i\omega \mathbf{C} + \mathbf{K}]^{-1} [i\omega \tilde{\mathbf{C}} + \tilde{\mathbf{K}}] \mathbf{T}(\omega, V). \quad (6.36)$$

Considering the form of Equations (6.29), Equation (6.36) can be recast in form

$$\hat{\mathbf{H}}_q(\omega, V) = \begin{bmatrix} 0 & 0 & \hat{H}_{qqpr} & \hat{H}_{qqpf} \\ 0 & 0 & \hat{H}_{\mu qpr} & \hat{H}_{\mu qpf} \\ 0 & 0 & \hat{H}_{qprqpr} & \hat{H}_{qprqpf} \\ 0 & 0 & \hat{H}_{qpfqpr} & \hat{H}_{qpfqpf} \end{bmatrix} \begin{Bmatrix} 0 \\ 0 \\ e^{-i\omega(p/V)} \\ 1 \end{Bmatrix}, \quad (6.37)$$

or

$$\hat{\mathbf{H}}_q(\omega, V) = \begin{bmatrix} \hat{H}_{qqpr} e^{-i\omega(p/V)} + \hat{H}_{qqpf} \\ \hat{H}_{\mu qpr} e^{-i\omega(p/V)} + \hat{H}_{\mu qpf} \\ \hat{H}_{qprqpr} e^{-i\omega(p/V)} + \hat{H}_{qprqpf} \\ \hat{H}_{qpfqpr} e^{-i\omega(p/V)} + \hat{H}_{qpfqpf} \end{bmatrix}. \quad (6.38)$$

Each element of $\hat{\mathbf{H}}_q(\omega, V)$ in Equation (6.38) defines a correlated FRF's of a mode.

Specifically, the sprung mass bounce (q) mode is

$$\hat{H}_{qr} = \hat{H}_{qqr} e^{-i\omega(p/V)} + \hat{H}_{qqf}. \quad (6.39a)$$

The sprung mass pitch (μ) mode is

$$\hat{H}_{\mu r} = \hat{H}_{\mu qr} e^{-i\omega(p/V)} + \hat{H}_{\mu qf}. \quad (6.39b)$$

The rear unsprung mass hop (q_{pr}) mode is

$$\hat{H}_{q_{pr}r} = \hat{H}_{q_{pr}q_r} e^{-i\omega(p/V)} + \hat{H}_{q_{pr}q_f}. \quad (6.39c)$$

And the front unsprung mass hop (q_{pf}) mode is

$$\hat{H}_{q_{pf}r} = \hat{H}_{q_{pf}q_r} e^{-i\omega(p/V)} + \hat{H}_{q_{pf}q_f}. \quad (6.39d)$$

6.6.1.2 Frequency Response Function Matrix in Relative Coordinates

Transforming Equations (6.31) into the frequency domain leads to

$$\hat{\mathbf{H}}_z(\omega, V) = [-\omega^2 \bar{\mathbf{M}} + i\omega \bar{\mathbf{C}} + \bar{\mathbf{K}}]^{-1} [\omega \bar{\mathbf{M}}] \mathbf{T}(\omega, V). \quad (6.40)$$

This can be recast as

$$\hat{\mathbf{H}}_z(\omega, V) = \begin{bmatrix} \hat{H}_{z_r z_r} & \hat{H}_{z_r z_f} & \hat{H}_{z_r z_{pr}} & \hat{H}_{z_r z_{pf}} \\ \hat{H}_{z_f z_r} & \hat{H}_{z_f z_f} & \hat{H}_{z_f z_{pr}} & \hat{H}_{z_f z_{pf}} \\ \hat{H}_{z_{pr} z_r} & \hat{H}_{z_{pr} z_f} & \hat{H}_{z_{pr} z_{pr}} & \hat{H}_{z_{pr} z_{pf}} \\ \hat{H}_{z_{pf} z_r} & \hat{H}_{z_{pf} z_f} & \hat{H}_{z_{pf} z_{pr}} & \hat{H}_{z_{pf} z_{pf}} \end{bmatrix} \left\{ \begin{array}{c} 0 \\ 0 \\ e^{-i\omega(p/V)} \\ 1 \end{array} \right\}, \quad (6.41)$$

or

$$\hat{\mathbf{H}}_z(\omega, V) = \begin{bmatrix} \hat{H}_{z_r z_{pr}} e^{-i\omega(p/V)} + \hat{H}_{z_r z_{pf}} \\ \hat{H}_{z_f z_{pr}} e^{-i\omega(p/V)} + \hat{H}_{z_f z_{pf}} \\ \hat{H}_{z_{pr} z_{pr}} e^{-i\omega(p/V)} + \hat{H}_{z_{pr} z_{pf}} \\ \hat{H}_{z_{pf} z_{pr}} e^{-i\omega(p/V)} + \hat{H}_{z_{pf} z_{pf}} \end{bmatrix}. \quad (6.42)$$

Again, each element of $\hat{\mathbf{H}}_z(\omega, V)$ in Equation (6.42) defines a correlated FRF's of a mode.

Specifically the relative bounce (z_r) between rear end of sprung mass and rear-unsprung mass is

$$\hat{H}_{z_r} = \hat{H}_{z_r z_{pr}} e^{-i\omega(p/V)} + \hat{H}_{z_r z_{pf}}. \quad (6.43a)$$

The relative bounce (z_f) between front end of sprung mass and front-unsprung mass is

$$\hat{H}_{z_f} = \hat{H}_{z_f z_{pr}} e^{-i\omega(p/V)} + \hat{H}_{z_f z_{pf}}. \quad (6.43b)$$

The relative hop (z_{pr}) between rear unsprung mass and the ground is

$$\hat{H}_{z_{pr}} = \hat{H}_{z_{pr} z_{pr}} e^{-i\omega(p/V)} + \hat{H}_{z_{pr} z_{pf}}. \quad (6.43c)$$

And the relative hop (z_{pf}) between front unsprung mass and the ground is

$$\hat{H}_{z_{pf}} = \hat{H}_{z_{pf} z_{pr}} e^{-i\omega(p/V)} + \hat{H}_{z_{pf} z_{pf}}. \quad (6.43d)$$

6.6.2 Computation of the Frequency Response Function Matrix

Using the values given in Table 6.1, and Equation (6.40) the FRF's of the 4-DOF were computed for several values of forward speed. These functions are shown in Figure 6.8a to Figure 6.8d. From these graphs it can be seen that the pitch, bounce, and hop frequencies are barely sensitive to speed variation. The computed natural frequency for rear bounce of the sprung mass is 12.76 rad/s, while its front bounce natural frequency is 21.48 rad/s. The

hop natural frequency for the rear unsprung mass is 106.70 rad/s, and the front hop natural frequency is 114.11 rad/s.

In Figure 6.8a and Figure 6.8b it can be observed that, for each graph corresponding to a certain speed, at low frequencies the amplitude increases quite rapidly until it reaches a maximum near the rear bounce mode natural frequency of the sprung mass. A second peak appears near the front bounce mode natural frequency of the sprung mass. These graphs also show a third maximum at 110 rad/s, which is between the two hop frequencies: the rear hop frequency at 106.7 rad/s, and the front hop frequency at 114.11 rad/s.

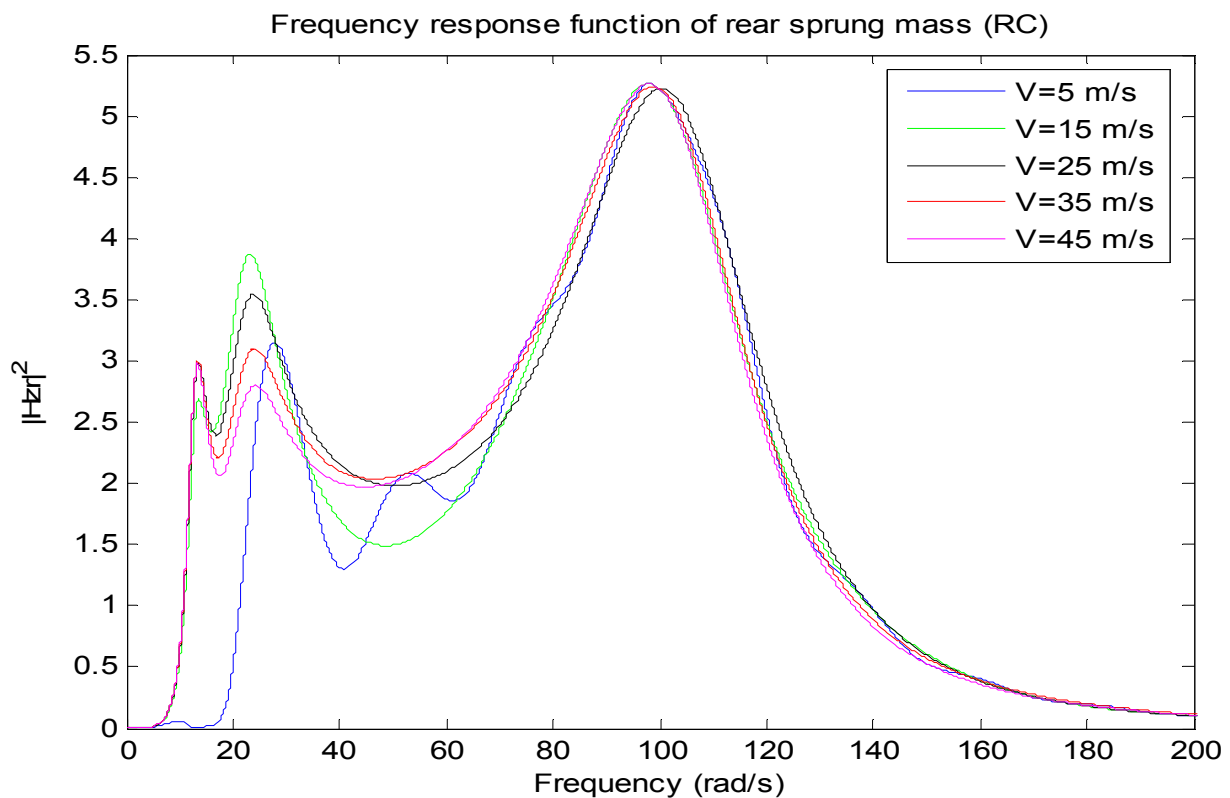


Figure 6.8a FRF's of rear sprung mass of 4-DOF linear model for several speeds.

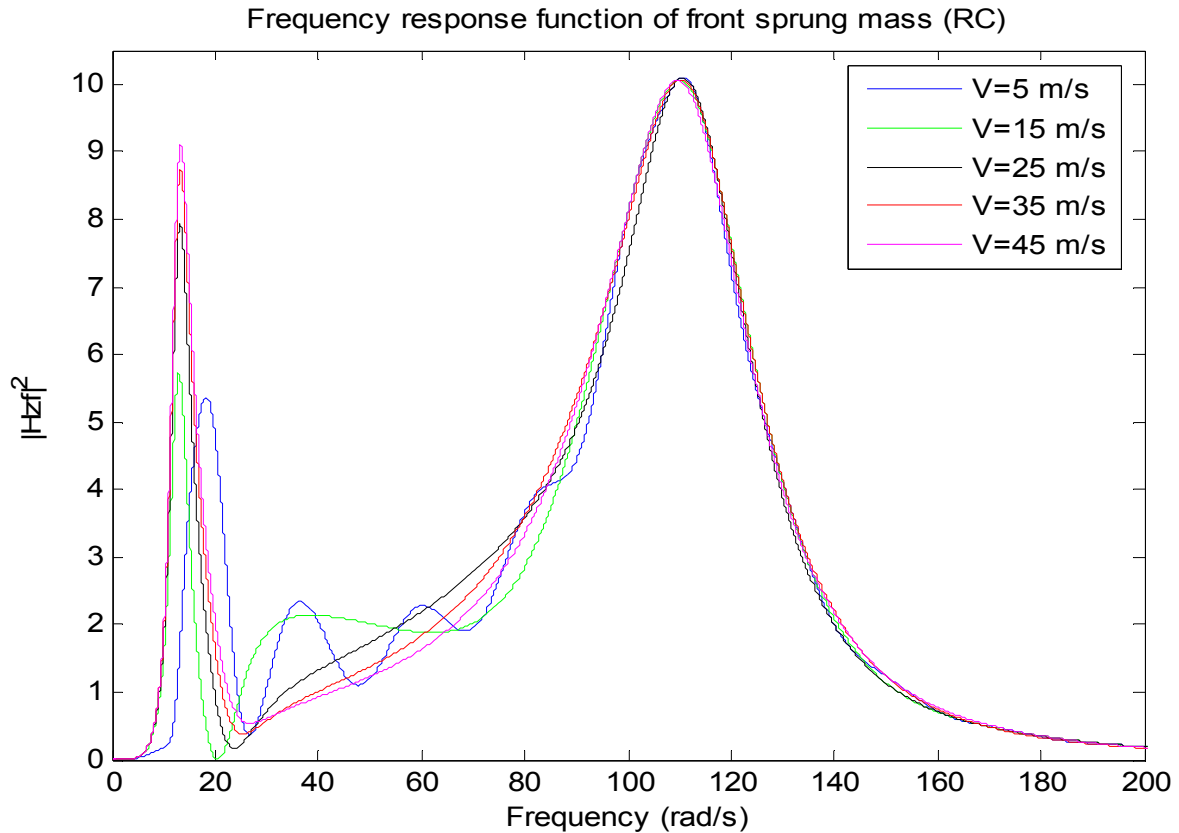


Figure 6.8b FRF's of front sprung mass of 4-DOF linear model for several speeds.

From Figures 6.8a and 6.8b it can also be seen that the peak corresponding to the rear bounce mode natural frequency of the sprung mass is located farther to the left of this value and its amplitude is sensitive to speed changes. Also the peak corresponding to the front bounce mode natural frequency appears located farther to the right from the reference value.

Figures 6.8c and 6.8d show a more constant behavior for various speeds. The front and rear bounce modes of the sprung mass are practically eliminated. A strong presence of the front and rear hop modes is shown with a more pronounced variation of the maxima.

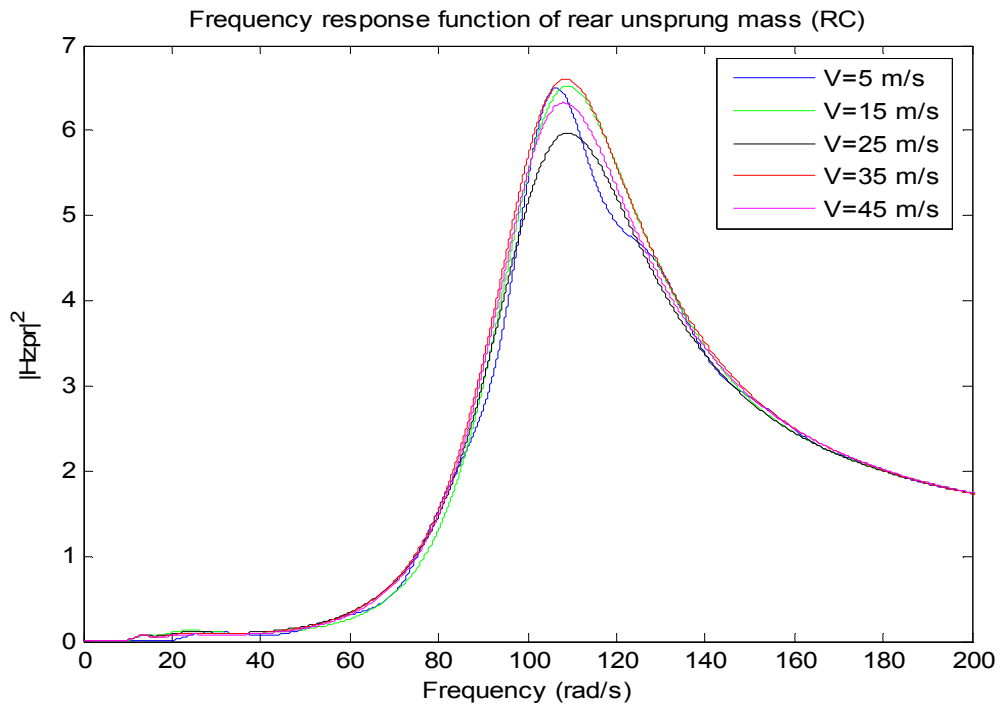


Figure 6.8c FRF's of rear unsprung mass of 4-DOF linear model for several speeds.

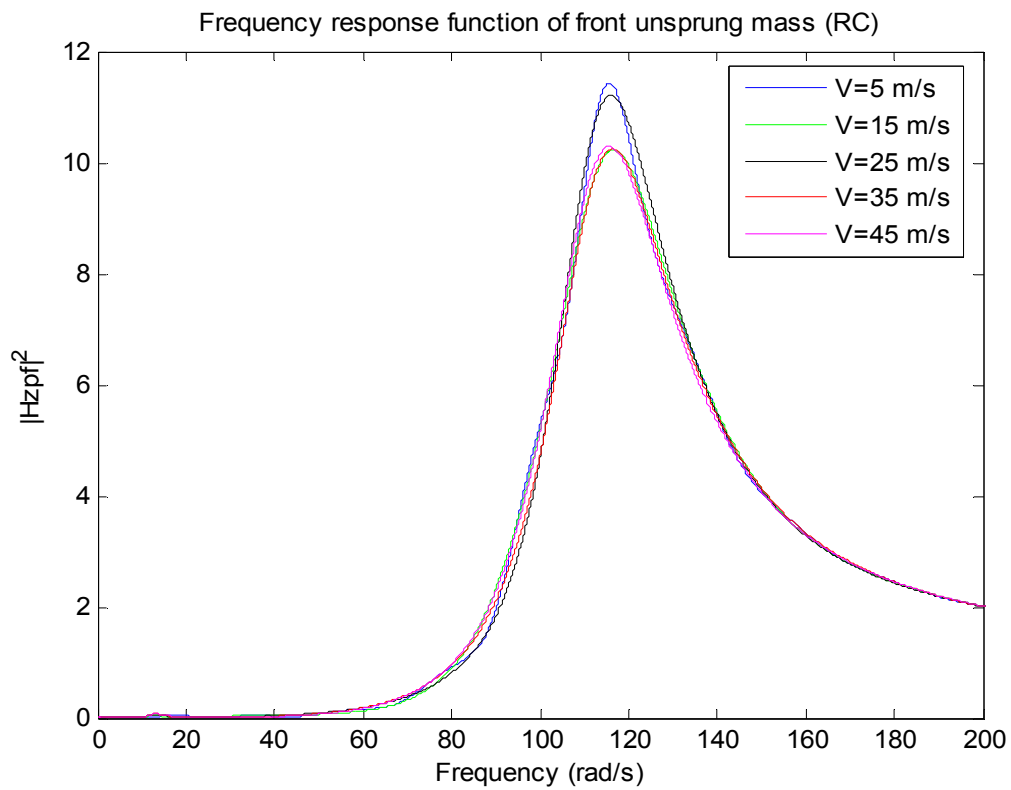


Figure 6.8d FRF's of front unsprung mass of 4-DOF linear model for several speeds.

6.7 Dynamical Analysis by Monte Carlo Simulation

To establish the correct implementation of the Monte Carlo method to be used for the dynamic analysis of the nonlinear 4-DOF model, first a numerical simulation is carried out using a linear 4-DOF motorcycle model. Subsequently, this numerical solution is compared with the analytical solution of the linear model obtained by using the frequency domain method. The case of a motorcycle traveling at 15 m/s on a regular quality road is considered. The motorcycle parameters are those specified in Table 6.1.

6.7.1 Validating Solution (Frequency Domain Method)

Once the FRF's of the model are computed it is possible to compute the PSD of the response with the aid of Equation (2.26). Specifically, for the relative coordinates,

$$S_{zr}(\omega) = |H_{zr}(\omega)|^2 S_x(\omega), \quad (6.44)$$

$$S_{zf}(\omega) = |H_{zf}(\omega)|^2 S_x(\omega), \quad (6.45)$$

$$S_{zpr}(\omega) = |H_{zpr}(\omega)|^2 S_x(\omega), \quad (6.46)$$

and

$$S_{zpf}(\omega) = |H_{zpf}(\omega)|^2 S_x(\omega) \quad (6.47)$$

hold. The power spectrum of the excitation is obtained as discussed in Chapter 3, by combining the individual PSD's specified with Equations (3.5) and (3.6). The resulting input PSD's for the road profile and the accelerations induced on the motorcycle are shown in Figure 6.9a, and Figure 6.9b.

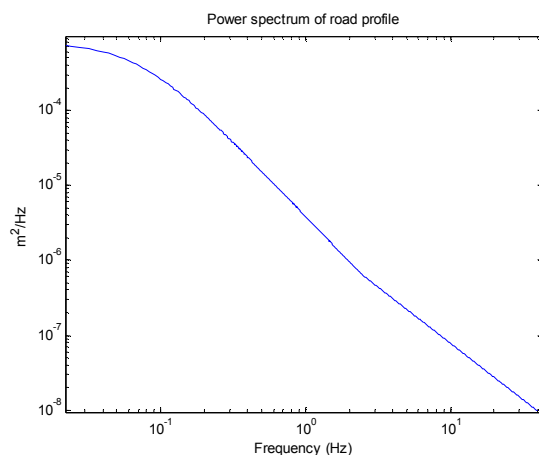


Figure 6.9a Power spectrum of road profile.

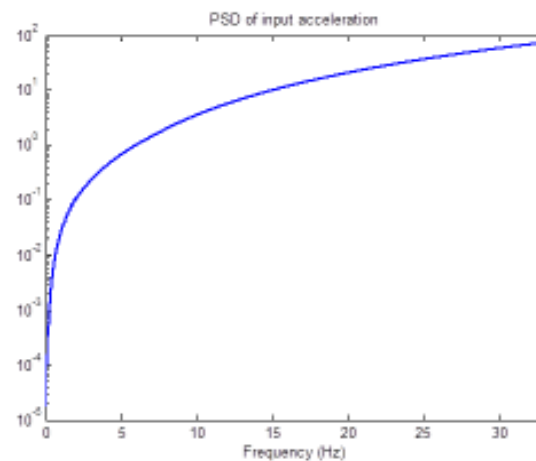


Figure 6.9b Power spectrum of accelerations.

The power spectrum of the road profile is used, in combination with Equations (6.44-6.47), to determine the analytical (frequency-domain) solution to the motorcycle response. However, the power spectrum of the acceleration is used in conjunction with an AR(45) filter to synthesize the input time histories required for the Monte Carlo simulation. The frequency response functions of the 4-DOF model, for a constant velocity of $V=15$ m/s are shown in Figures 6.10a-d.

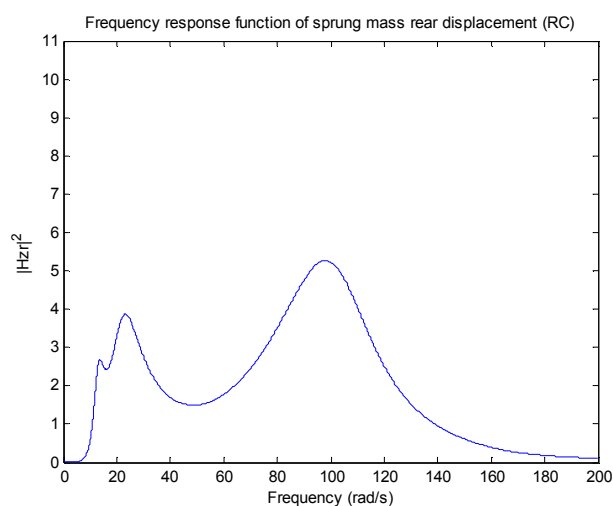


Figure 6.10a FRF of the Zr coordinate.

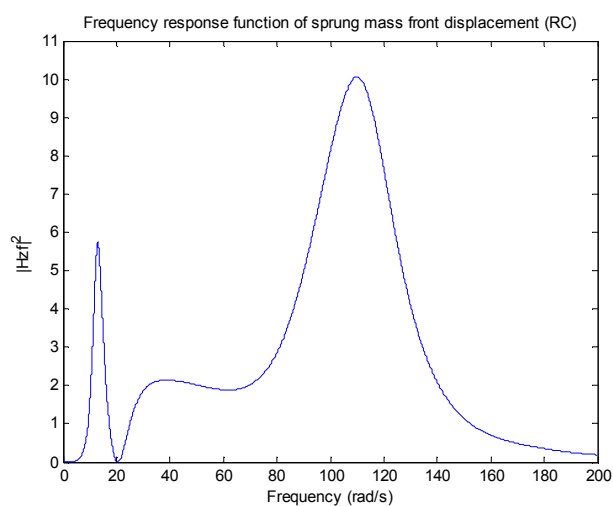


Figure 6.10b FRF of the Zf coordinate.

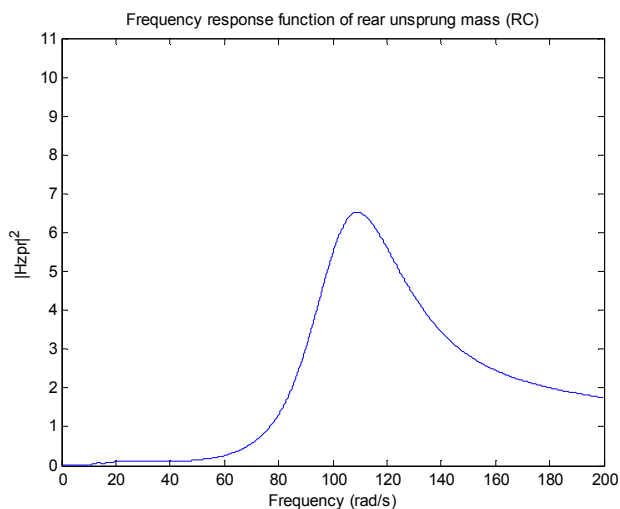


Figure 6.10c FRF of the Z_{pr} coordinate.

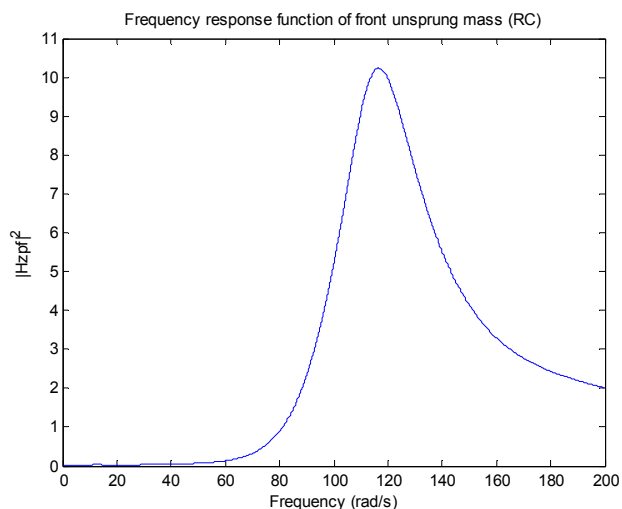


Figure 6.10d FRF of the Z_{pf} coordinate.

The power spectra of the response are shown in Figures 6.11a-d. These PSD's, along with those for the acceleration PSD's are those to be incorporated in the Monte Carlo simulation.

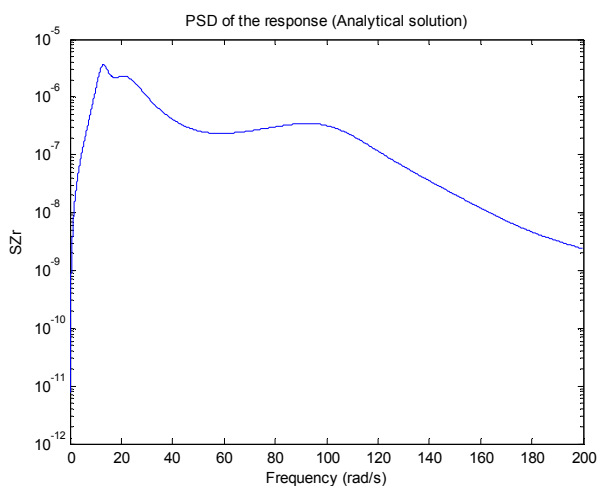


Figure 6.11a PSD of Response for Z_r coordinate.

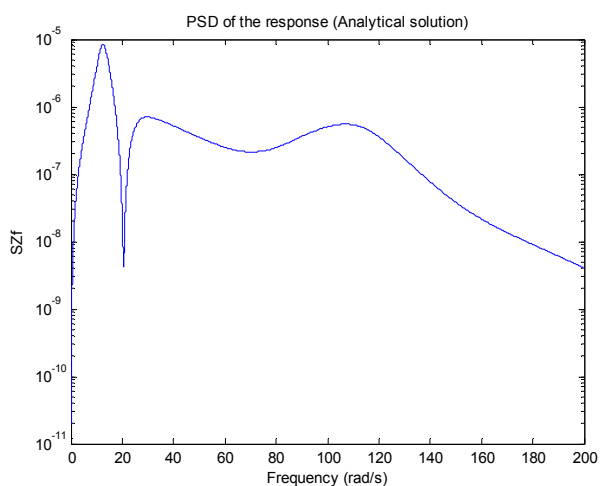


Figure 6.11b PSD of Response for Z_f coordinate.

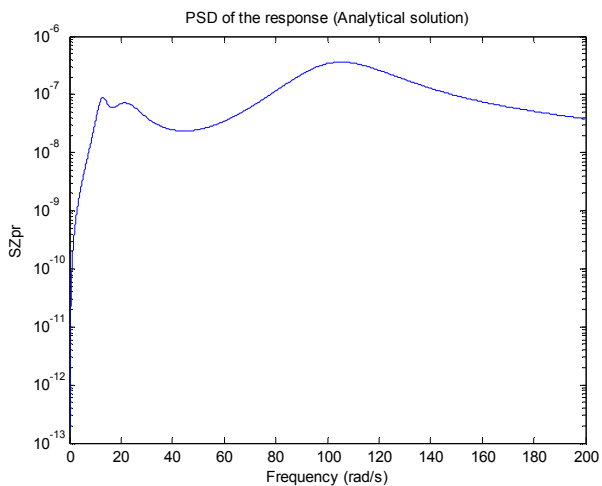


Figure 6.11c PSD of Response for Z_{pr} coordinate.

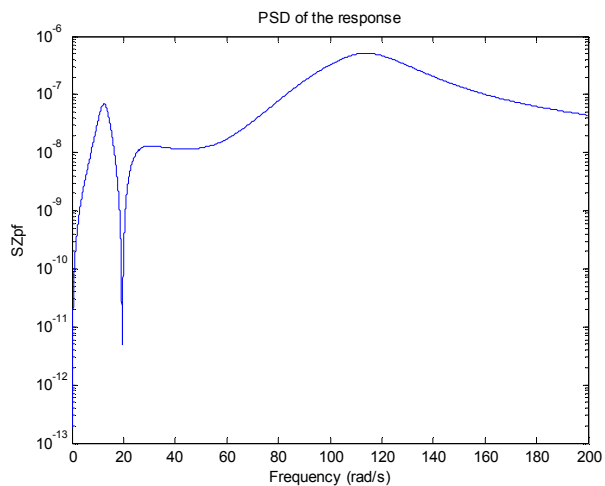


Figure 6.11d PSD of Response for Z_{pf} coordinate.

The acceleration PSD's of the response are shown in Figures 6.12a-d. These PSD's are obtained by using the equations

$$S_{\ddot{x}}(\omega) = \omega^4 S_x(\omega) = \omega^2 S_{\dot{x}}(\omega). \tag{2.19}$$

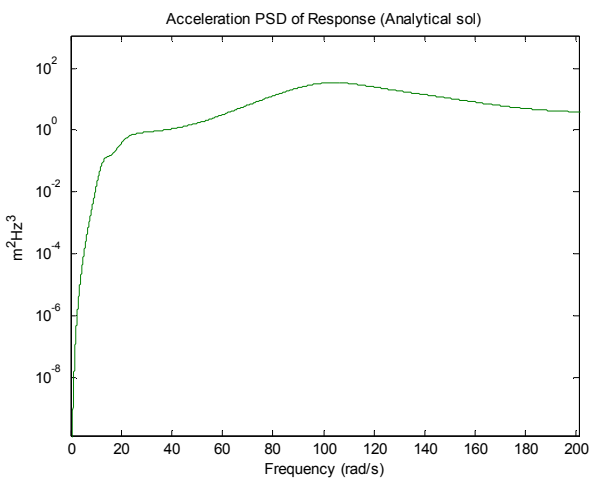


Figure 6.12a PSD of Response for \ddot{Z}_r coordinate.

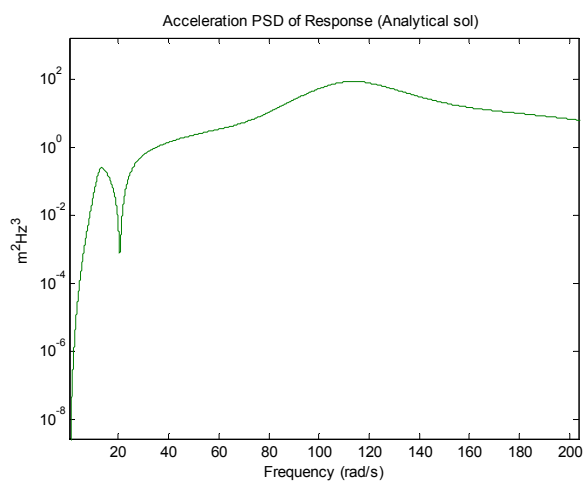


Figure 6.12b PSD of Response for \ddot{Z}_f coordinate.

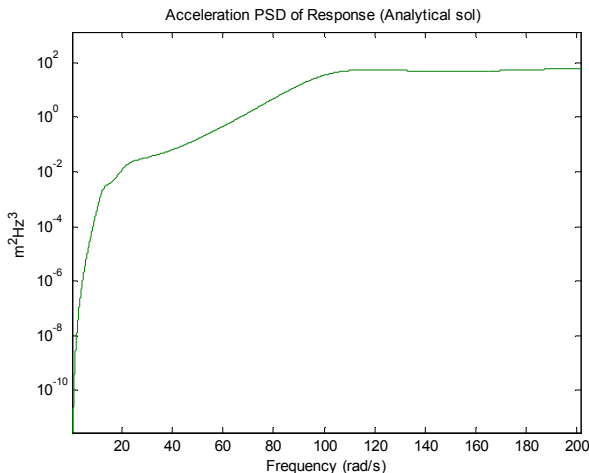


Figure 6.12c PSD of Response for \ddot{Z}_{pr} coordinate.

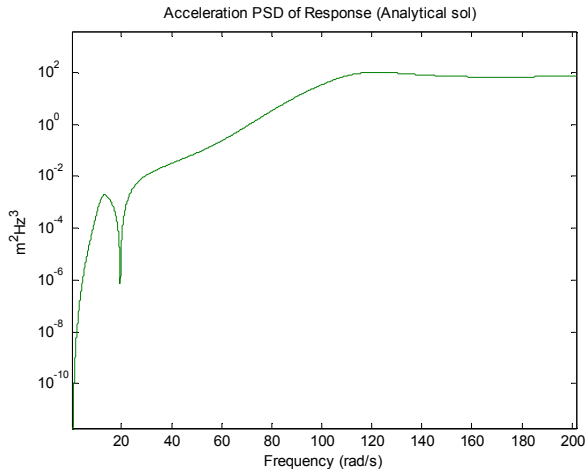


Figure 6.12d PSD of Response for \ddot{Z}_{pf} coordinate.

6.7.2 Response Power Spectrum Fitting by Monte Carlo Simulation

A satisfactory fitting of the target spectrum was obtained with 800 time histories for both the response in terms of displacements, and the response in terms of accelerations. Figures 6.13a to 6.13d present the results obtained.

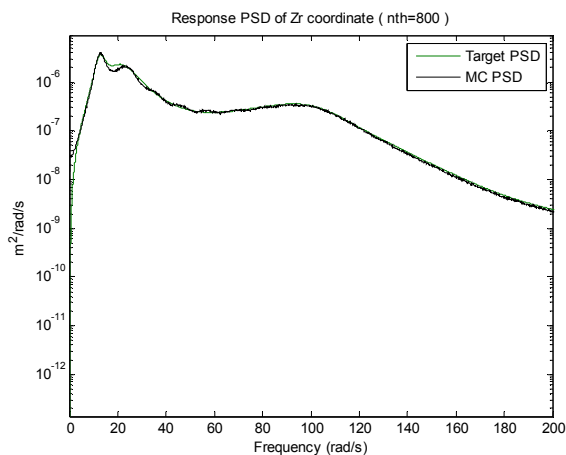


Figure 6.13a Approximation of PSD of Response for Zr coordinate using 800 time hist.

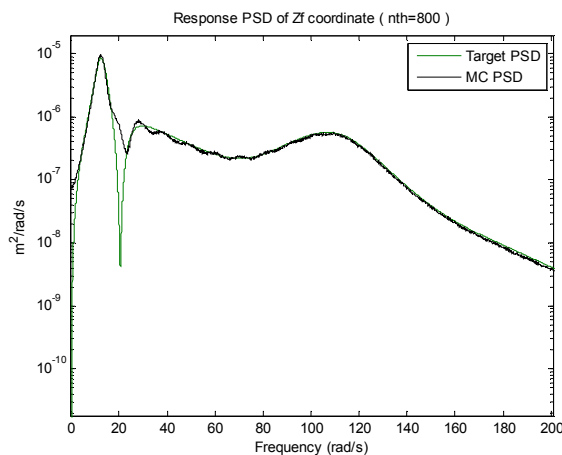


Figure 6.13b Approximation of PSD of Response for Zf coordinate using 800 time hist.

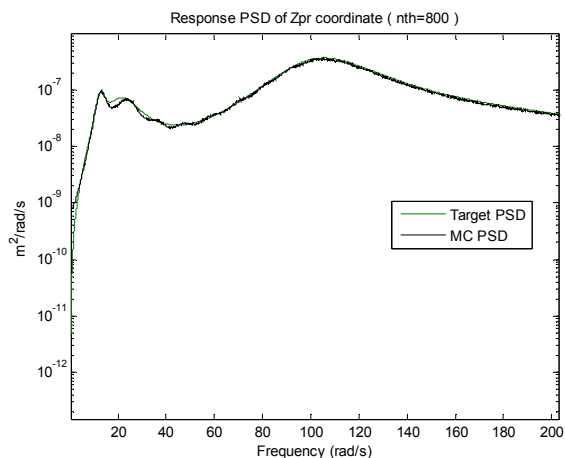


Figure 6.13c Approximation of PSD of Response for Z_{pr} coordinate using 800 time hist.

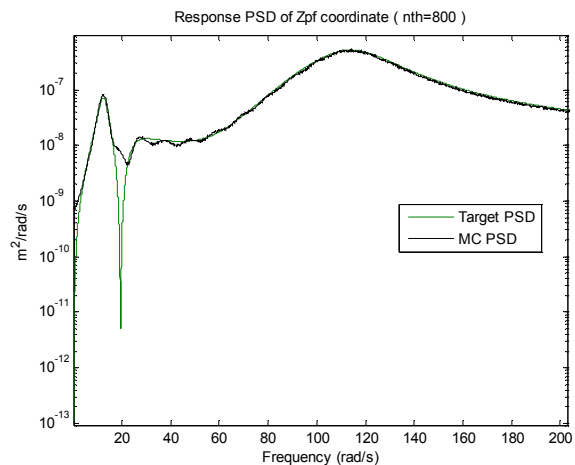


Figure 6.13d Approximation of PSD of Response for Z_{pf} coordinate using 800 time hist.

Similarly, the results for the response acceleration PSD's are shown in Figures 6.14a-d, and Table 6.3.

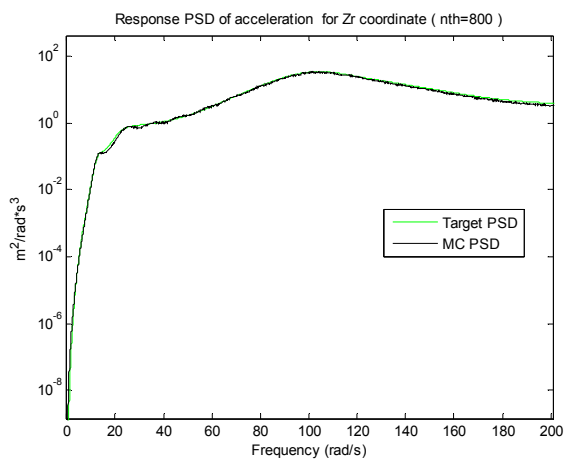


Figure 6.14a Approximation of PSD of response for \ddot{Z}_r coordinate using 800 time hist.

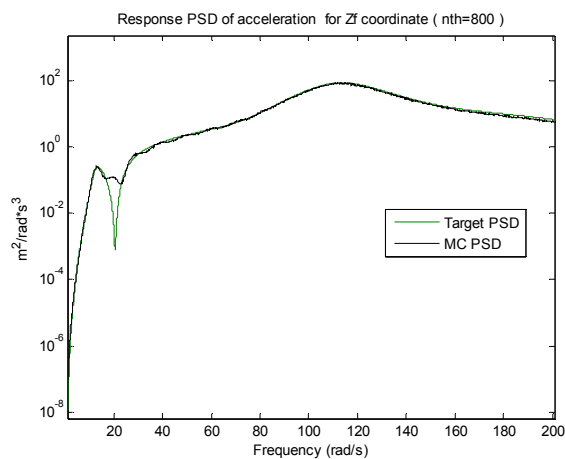


Figure 6.14b Approximation of PSD of response for \ddot{Z}_f coordinate using 800 time hist.

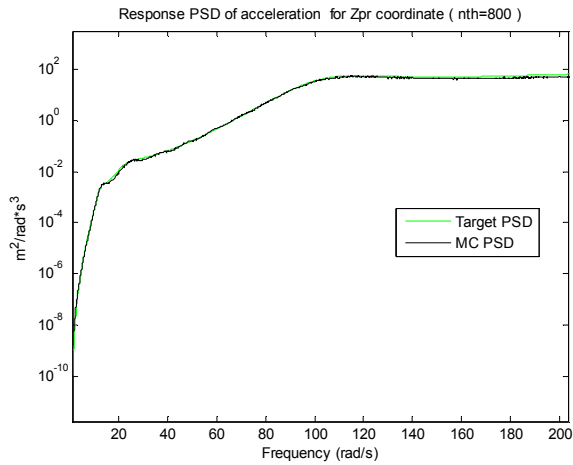


Figure 6.14c Approximation of PSD of response for \ddot{Z}_{pr} coordinate using 800 time hist.

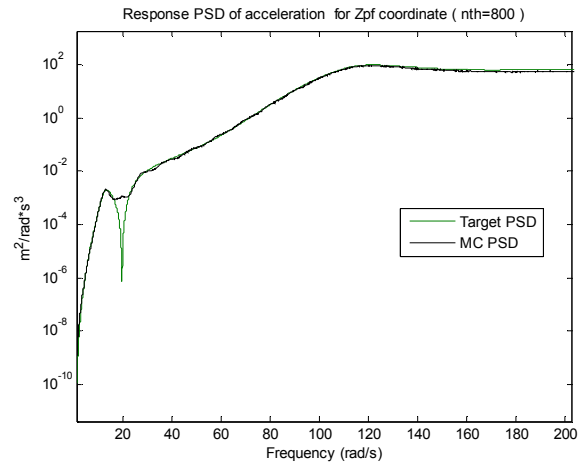


Figure 6.14d Approximation of PSD of response for \ddot{Z}_{pf} coordinate using 800 time hist.

Table 6.2 rms values of responses (accelerations) for the analytical and MC simulation

rms value acceleration	Analytical solution m/s^2	Monte Carlo simulation m/s^2
\ddot{Z}_r	0.2998	0.2924
\ddot{Z}_f	0.4141	0.4030
\ddot{Z}_{pr}	0.6172	0.6087
\ddot{Z}_{pf}	0.6937	0.6830

As can be seen from the graphs the Monte Carlo simulation is quite reliable.

Chapter 7

Statistical Linearization of the Nonlinear 4-DOF Motorcycle

Model

7.1 Introduction

The main drawback of incorporating nonlinear behaving devices in a passive motorcycle suspension model relates to the difficulty of solving the system of nonlinear differential equations governing the motion of the motorcycle, unless a Monte Carlo simulation is performed. In this sense, the statistical linearization method discussed in chapter 4 represents a powerful alternative tool for stochastic analysis of the nonlinear motorcycle dynamics model.

7.2 The Nonlinear 4-DOF Motorcycle Model

In the linear system model, the suspensions and the tires have been modeled by using simple Kelvin-Voigt models, whose parameters take into account both the constitutive law of real devices and their geometrical position in the motorcycle. This leads to the linear differential equations of motion Equation (6.27).

The nonlinear system assumes the presence of additional nonlinear devices. In general, the main source of nonlinearities is the suspension friction and the shock absorber behavior.

Figure (7.1) shows all the possible nonlinearities considered in the nonlinear model. As it can be seen in this figure the nonlinearities are related to the relative coordinates system, which exhibits some advantages over the absolute coordinates system, for formulation purposes. From this general scheme different configurations can be obtained.

Thus, the dynamic equilibrium equations of the nonlinear system in absolute coordinates are

$$\mathbf{M}\ddot{\mathbf{q}} + \mathbf{C}\dot{\mathbf{q}} + \mathbf{K}\mathbf{q} + \mathbf{g}(\mathbf{q}, \dot{\mathbf{q}}, \mathbf{w}, \dot{\mathbf{w}}) + \mathbf{p} = \tilde{\mathbf{C}}\dot{\mathbf{w}} + \tilde{\mathbf{K}}\mathbf{w}, \quad (7.1)$$

where the vector \mathbf{p} is given by the equation

$$\mathbf{p} = \begin{bmatrix} m_g \\ 0 \\ m_r g \\ m_f g \end{bmatrix}. \quad (7.2)$$

Further, the vector $\mathbf{g}(\mathbf{q}, \dot{\mathbf{q}}, \mathbf{w}, \dot{\mathbf{w}})$ contains all the nonlinear terms and, in general, comprises terms involving the excitation because of the absolute coordinate formulation. However, a relative formulation may reduce the dependence of the nonlinear vector to only the state variables of the dynamic system.

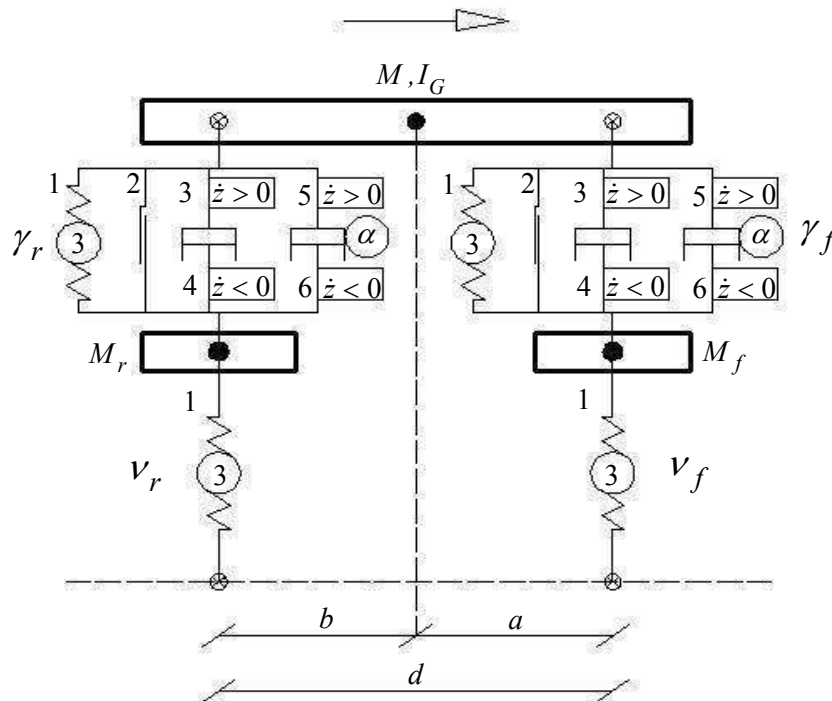


Figure 7.1. Schematic representation of a generalized nonlinear motorcycle system. All the possible nonlinear elements are indicated, but different configurations can be defined from this model.

The nonlinear vector $\mathbf{g}(\mathbf{q}, \dot{\mathbf{q}}, \mathbf{w}, \dot{\mathbf{w}})$ of the nonlinear system in Equation (7.1) can be defined in terms of a generic relative coordinate z_i , and its derivative with respect to time \dot{z}_i , i.e. $\bar{\mathbf{g}}(\mathbf{z}, \dot{\mathbf{z}})$.

Specifically, using the relations given by Equations (5.17a-d), the dynamic equilibrium of the nonlinear motorcycle model in relative coordinates can be cast in the form

$$\bar{\mathbf{M}}\ddot{\mathbf{z}} + \bar{\mathbf{C}}\dot{\mathbf{z}} + \bar{\mathbf{K}}\mathbf{z} + \bar{\mathbf{g}}(\mathbf{z}, \dot{\mathbf{z}}) + \mathbf{p} = -\bar{\mathbf{M}}\ddot{\mathbf{w}}, \quad (7.3)$$

where the square matrices $\bar{\mathbf{M}}$, $\bar{\mathbf{C}}$, and $\bar{\mathbf{K}}$ are defined according to Equations (5.23), (5.24), and (5.25).

Next the vector $\bar{\mathbf{g}}(\mathbf{z}, \dot{\mathbf{z}})$ is independent of the excitation and depends only on the nonlinear function of the relative coordinate \mathbf{z} and their time derivative $\dot{\mathbf{z}}$. Figure 5.6 depicts the 4-DOF system described in relative coordinates.

The types of nonlinearity considered and their mathematical representation are summarized in Table 7.1. According to this nomenclature the nonlinearities considered in this study, in both suspensions and tires, can be expressed in terms of z_i and \dot{z}_i . These are, a cubic stiffness z_i^3 ; a friction term $sign(\dot{z}_i)$; an additional linear dashpot having different coefficients in traction $U(\dot{z}_i)\dot{z}_i$, and in compression $U(-\dot{z}_i)\dot{z}_i$; and a nonlinear dissipating factor having different coefficients in traction $\dot{z}_i|\dot{z}_i|^\beta U(\dot{z}_i)$, and in compression $\dot{z}_i|\dot{z}_i|^\beta U(-\dot{z}_i)$. The symbol $U(\)$ denotes the unit step function.

The coefficients of the nonlinear terms represented in Figure 7.1 have been labeled γ for the suspensions, and ν for the tires. A first subscript denotes the rear (r) or front (f) part of the motorcycle, while the second subscript denotes the kind of nonlinearity

numbered from 1 to 6 as indicated in table 7.1. Thus, for instance, the coefficient γ_{f5} describes the strength of the nonlinear damping function in the front suspension.

The coefficients of nonlinearities are chosen to be proportional to their linear counterpart. For instance, the coefficients γ_{r1}, γ_{f1} of the cubic elastic suspension are scaled, by the parameter ε_1 , to the stiffnesses k_r, k_f respectively; the coefficients γ_{r2}, γ_{f2} of the frictional term are scaled, by the parameter ε_2 , to one twentieth of the sprung weight ($Mg/20$); the coefficients γ_{rj}, γ_{fj} ($j = 3, \dots, 6$) of the nonlinear viscous part are scaled by the parameters ε_j , to the damping coefficients c_r, c_f respectively; and the coefficients ν_{r1}, ν_{f1} of the cubic elastic term in the tires are scaled, by the parameter ε_1 , to the stiffness k_{pr}, k_{pf} respectively.

Table 7.1 Six kinds ($j=1\dots 6$) of nonlinear sources

Cubic stiffness	(j=1) $\gamma_{i1} z_i^3; i = r, f, pr, pf$
Coulomb friction	(j=2) $\gamma_{i2} \text{sign}(\dot{z}_i); i = r, f$
Additional linear dashpot having different coefficient in	(j=3) Traction $\gamma_{i3} \dot{z}_i U(\dot{z}_i); i = r, f$
	(j=4) Compression $\gamma_{i4} \dot{z}_i U(-\dot{z}_i); i = r, f$
Additional nonlinear dissipating devices having different coefficient in	(j=5) Traction $\gamma_{i5} \dot{z}_i \dot{z}_i ^\beta U(\dot{z}_i); i = r, f$
	(j=6) Compression $\gamma_{i6} \dot{z}_i \dot{z}_i ^\beta U(-\dot{z}_i); i = r, f$
$U()$ is the unit step function	

7.3 The Statistical Linearization Solution

7.3.1 Motorcycle Offset

Equation (7.3) captures the dynamic equilibrium of the nonlinear motorcycle model subjected to the gravity force and excited by the effects of the ground motion. The ground is modeled as a zero mean stationary process characterized by the power spectrum $S_W(\omega)$, for a given speed as V , reported in Equation (5.6).

The response of this system is not a zero mean process. As is well known, the response of a linear system under gravity can be assumed as the sum of a zero mean process and constant mean. This is nothing but the static equilibrium position, or, alternatively, the offset of the linear system. Further, the offset of a linear system does not depend on the excitation (amplitude, frequency content of the excitation, etc.) [136].

A nonlinear system in general requires some more considerations. In fact, the presence of a nonlinearity complicates the search of a static equilibrium position. Moreover, the adoption of asymmetric nonlinear devices creates an excitation-dependent offset [202, 203]. This means that, for a given road roughness, experienced by the motorcycle at various velocities, the nonlinear model will yield several offsets, complicating significantly the design of suspensions.

Consider the response \mathbf{z} of the nonlinear motorcycle as the sum of a stationary zero mean component $\hat{\mathbf{z}}$ and a constant mean \mathbf{m}_z . That is set

$$\mathbf{z} = \hat{\mathbf{z}} + \mathbf{m}_z; \quad (7.4)$$

where $\mathbf{m}_z = (m_r, m_f, m_{pr}, m_{pf})^T$ is the offset vector, and the generic process \hat{z}_i ($i = r, f, pr, pf$) has been assumed as characterized by a Gaussian probability density function.

Since the offset is considered constant, this implies that $\dot{\mathbf{z}} = \dot{\hat{\mathbf{z}}}$, and $\ddot{\mathbf{z}} = \ddot{\hat{\mathbf{z}}}$ are also zero mean stationary processes.

The position in Equation (7.4), which is based on the assumption of the stationarity of the response process, greatly simplifies the analysis of the nonlinear motorcycle's response.

From this analysis the following parameters that characterize the response are obtained:

- I. The offset \mathbf{m}_z which provides information on the mean geometrical configuration of the motorcycle.
- II. The standard deviations of the relative coordinates $\sigma_{\dot{z}_i}$ which provides information on the maximum expected stroke of the front suspension.

and

- III. The standard deviation of acceleration $\sigma_{\ddot{q}}$ of the center of mass G , to provide information about the comfort of the rider.

Substituting Equation (7.4) and its time derivatives into Equation (7.3) one obtains

$$\overline{\mathbf{M}}\ddot{\mathbf{z}} + \overline{\mathbf{C}}\dot{\mathbf{z}} + \overline{\mathbf{K}}(\hat{\mathbf{z}} + \mathbf{m}_z) + \overline{\mathbf{g}}(\hat{\mathbf{z}} + \mathbf{m}_z, \dot{\hat{\mathbf{z}}}) + \mathbf{p} = -\overline{\mathbf{M}}\ddot{\mathbf{w}}; \quad (7.5)$$

Averaging both sides of Equation (7.5), yields

$$\overline{\mathbf{K}} \mathbf{m}_z + E \left[\overline{\mathbf{g}}(\hat{\mathbf{z}} + \mathbf{m}_z, \dot{\hat{\mathbf{z}}}) \right] + \mathbf{p} = \mathbf{0}; \quad (7.6)$$

From the previous equation it can be easily verified that for a linear model, the offset of the motorcycle coincides with the equilibrium static position $\mathbf{m}_z = -\overline{\mathbf{K}}^{-1} \mathbf{p}$ (i.e. $\overline{\mathbf{g}}(\hat{\mathbf{z}} + \mathbf{m}_z, \dot{\hat{\mathbf{z}}}) = \mathbf{0}$). The same result is obtained if, for the nonlinear system, only symmetric damping devices are adopted, otherwise the offset is excitation-dependent.

7.3.2 The Equivalent Linear System

Subtracting the offset equations in Equation (7.6) from Equation (7.5) one derives the system of nonlinear differential equations that governs the zero-mean response $\hat{\mathbf{z}}$. Specifically,

$$\overline{\mathbf{M}}\ddot{\hat{\mathbf{z}}} + \overline{\mathbf{C}}\dot{\hat{\mathbf{z}}} + \overline{\mathbf{K}}\hat{\mathbf{z}} + \overline{\mathbf{h}}(\hat{\mathbf{z}}, \dot{\hat{\mathbf{z}}}) = -\overline{\mathbf{M}}\ddot{\mathbf{w}}; \quad (7.7)$$

where

$$\overline{\mathbf{h}}(\hat{\mathbf{z}}, \dot{\hat{\mathbf{z}}}) = \overline{\mathbf{g}}(\hat{\mathbf{z}} + \mathbf{m}_z, \dot{\hat{\mathbf{z}}}) - E \left[\overline{\mathbf{g}}(\hat{\mathbf{z}} + \mathbf{m}_z, \dot{\hat{\mathbf{z}}}) \right]. \quad (7.8)$$

With being $\overline{\mathbf{h}}(\hat{\mathbf{z}}, \dot{\hat{\mathbf{z}}})$ is the vector that represents the actual nonlinear elements in the motorcycle model, namely the nonlinear stiffness of the springs and the energy dissipation effects of the dashpots. These effects depend only on the relative displacements and velocities between the sprung mass and each unsprung mass.

Next the nonlinear system in Equation (7.7) is replaced by the equivalent linear system

$$\overline{\mathbf{M}}\ddot{\hat{\mathbf{z}}} + (\overline{\mathbf{C}} + \overline{\mathbf{C}}_e)\dot{\hat{\mathbf{z}}} + (\overline{\mathbf{K}} + \overline{\mathbf{K}}_e)\hat{\mathbf{z}} = -\overline{\mathbf{M}}\ddot{\mathbf{w}}; \quad (7.9)$$

so that their output difference is adequately minimized according to conditions established by Equations (6.4), (6.5), and (6.6) [39, 97, 204], in which the error ε denotes the difference between the actual and the equivalent linear system.

Applying equations (6.15) and (6.16), the elements of the optimal linearizing stiffness and damping matrices $\overline{\mathbf{K}}_e$ and $\overline{\mathbf{C}}_e$ are obtained by means of the expressions

$$\overline{K}_{e,ij} = E \left[\frac{\partial}{\partial \hat{z}_j} \overline{h}_i(\hat{\mathbf{z}}, \dot{\hat{\mathbf{z}}}) \right]; \quad i, j = 1, \dots, m \quad (7.10a)$$

$$\overline{C}_{e,ij} = E \left[\frac{\partial}{\partial \dot{\hat{z}}_j} \overline{h}_i(\hat{\mathbf{z}}, \dot{\hat{\mathbf{z}}}) \right]; \quad i, j = 1, \dots, m \quad (7.10b)$$

where $\bar{h}_i(\hat{\mathbf{z}}, \dot{\hat{\mathbf{z}}})$ the i^{th} row of the nonlinear vector $\bar{\mathbf{h}}(\hat{\mathbf{z}}, \dot{\hat{\mathbf{z}}})$.

The equivalent linear system provides a good approximation of the actual nonlinear system, leading to convenient analytical solution.

To obtain the equivalent linear system, it is necessary to evaluate the quantity $E[\bar{\mathbf{g}}(\hat{\mathbf{z}} + \mathbf{m}_z, \dot{\hat{\mathbf{z}}})]$ in Equation (7.6) and the derivatives in Equation (7.10).

The vector $\bar{\mathbf{g}}(\mathbf{z}, \dot{\mathbf{z}})$ can be rearranged in a slightly different form which will be convenient for the evaluation of the equivalent linear system (ELS) discussed in the following.

A vector containing all the nonlinear functions can next be defined. There are $n = 6$ kinds of nonlinearities in the model, namely: z_i^3 , $\text{sgn}(\dot{z}_i)$, $U(\dot{z}_i)\dot{z}_i$, $U(-\dot{z}_i)\dot{z}_i$, $U(\dot{z}_i)\dot{z}_i|\dot{z}_i|^\alpha$ and $U(-\dot{z}_i)\dot{z}_i|\dot{z}_i|^\alpha$, with z_i ($i = r, f, pr, pf$) a generic Lagrangian parameter defining the motion of the system. This vector containing all the nonlinear functions must be of dimensions $[(n \cdot m) \times 1]$ and has the form

$$\begin{aligned} \tilde{\mathbf{Z}}(\mathbf{z}, \dot{\mathbf{z}}) = & (z_i^3, \dots, \text{sgn}(\dot{z}_i), \dots, U(\dot{z}_i)\dot{z}_i, \dots, U(-\dot{z}_i)\dot{z}_i, \\ & , U(\dot{z}_i)\dot{z}_i|\dot{z}_i|^\alpha, \dots, U(-\dot{z}_i)\dot{z}_i|\dot{z}_i|^\alpha, \dots)^T; \end{aligned} \quad (7.11)$$

A second vector \mathbf{B} of coefficients comprising the constant values γ and ν previously described is also defined. The dimension of vector \mathbf{B} is $[m \times (n \cdot m)]$. Then, the vector $\bar{\mathbf{g}}(\mathbf{z}, \dot{\mathbf{z}})$ can be expressed as

$$\bar{\mathbf{g}}(\mathbf{z}, \dot{\mathbf{z}}) = \mathbf{B}\tilde{\mathbf{Z}}(\mathbf{z}, \dot{\mathbf{z}}). \quad (7.12)$$

By setting $\mathbf{B} = \mathbf{0}$, Equation (7.3) leads to the equations of motion of the linear system in relative coordinates. The formulation in Equation (7.12) is particularly useful for the determination of the expressions for the equivalent matrices of the equivalent linear system.

By using the compact notation in Equation (7.12), the offset equations, and the nonlinear vector $\bar{\mathbf{h}}(\hat{\mathbf{z}}, \dot{\hat{\mathbf{z}}})$ (Equations (7.6), and (7.8)), can alternatively be expressed in the form

$$\bar{\mathbf{K}} \mathbf{m}_z + \mathbf{B} E \left[\tilde{\mathbf{Z}}(\hat{\mathbf{z}} + \mathbf{m}_z, \dot{\hat{\mathbf{z}}}) \right] + \mathbf{p} = \mathbf{0}; \quad (7.13)$$

$$\bar{\mathbf{h}}(\hat{\mathbf{z}}, \dot{\hat{\mathbf{z}}}) = \mathbf{B} \left\{ \tilde{\mathbf{Z}}(\hat{\mathbf{z}} + \mathbf{m}_z, \dot{\hat{\mathbf{z}}}) - E \left[\tilde{\mathbf{Z}}(\hat{\mathbf{z}} + \mathbf{m}_z, \dot{\hat{\mathbf{z}}}) \right] \right\}; \quad (7.14)$$

respectively, leading to the problem of determining $E \left[\tilde{\mathbf{Z}}(\hat{\mathbf{z}} + \mathbf{m}_z, \dot{\hat{\mathbf{z}}}) \right]$ instead of $E \left[\bar{\mathbf{g}}(\hat{\mathbf{z}} + \mathbf{m}_z, \dot{\hat{\mathbf{z}}}) \right]$.

Approximating the response of the equivalent linear system by a Gaussian process the equation

$$E \left[\tilde{\mathbf{Z}}(\hat{\mathbf{z}} + \mathbf{m}_z, \dot{\hat{\mathbf{z}}}) \right] = (m_i^3 + 3m_i \sigma_{\dot{z}_i}^2, \dots, 0, \dots, \sigma_{\dot{z}_i} / \sqrt{2\pi}, \dots, -\sigma_{\dot{z}_i} / \sqrt{2\pi}, \dots, 2^{\frac{1}{2}(\alpha-1)} \sigma_{\dot{z}_i}^{1+\alpha} \Gamma\left(1 + \frac{\alpha}{2}\right) / \sqrt{\pi}, \dots, -2^{\frac{1}{2}(\alpha-1)} \sigma_{\dot{z}_i}^{1+\alpha} \Gamma\left(1 + \frac{\alpha}{2}\right) / \sqrt{\pi}, \dots)^T; \quad (7.15)$$

is obtained in which the Euler Gamma function $\Gamma(\)$ has been introduced.

If only symmetric nonlinear damping devices for which the coefficient of the traction phase is equal to the coefficient of the compression phase, then because of Equation (7.15), no changes in the offset from the static equilibrium $\mathbf{m}_z = -\bar{\mathbf{K}}^{-1} \mathbf{p}$ position will be observed.

Since $E \left[\tilde{\mathbf{Z}}(\hat{\mathbf{z}} + \mathbf{m}_z, \dot{\hat{\mathbf{z}}}) \right]$ in Equation (7.13) comprises constant values as found in Equation (7.15), the derivatives in Equations (7.10), leads to

$$\bar{K}_{e,ij} = E \left[\frac{\partial}{\partial \dot{z}_j} \left(\mathbf{B} \tilde{\mathbf{Z}}(\hat{\mathbf{z}} + \mathbf{m}_z, \dot{\hat{\mathbf{z}}}) \right) \right]_i = \mathbf{B}_i E \left[\frac{\partial}{\partial \dot{z}_j} \left(\tilde{\mathbf{Z}}(\hat{\mathbf{z}} + \mathbf{m}_z, \dot{\hat{\mathbf{z}}}) \right) \right]; \quad i, j = 1, \dots, m \quad (7.16)$$

and

$$\bar{C}_{e,ij} = E \left[\frac{\partial}{\partial \dot{z}_j} \left(\mathbf{B} \tilde{\mathbf{Z}}(\hat{\mathbf{z}} + \mathbf{m}_z, \dot{\hat{\mathbf{z}}}) \right) \right]_i = \mathbf{B}_i E \left[\frac{\partial}{\partial \dot{z}_j} \left(\tilde{\mathbf{Z}}(\hat{\mathbf{z}} + \mathbf{m}_z, \dot{\hat{\mathbf{z}}}) \right) \right]; \quad (7.17)$$

where \mathbf{B}_i is the i^{th} row of the coefficient matrix \mathbf{B}

$$\mathbf{B} = \begin{pmatrix} \gamma_{r1} & \gamma_{f1} & 0 & 0 & \gamma_{r2} & \gamma_{f2} & 0 & 0 & \gamma_{r3} & \gamma_{f3} & 0 & 0 & \gamma_{r4} & \gamma_{f4} & 0 & 0 & \gamma_{r5} & \gamma_{f5} & 0 & 0 & \gamma_{r5} & \gamma_{f5} & 0 & 0 \\ -b\gamma_{r1} & a\gamma_{f1} & 0 & 0 & -b\gamma_{r2} & a\gamma_{f2} & 0 & 0 & -b\gamma_{r3} & a\gamma_{f3} & 0 & 0 & -b\gamma_{r4} & a\gamma_{f4} & 0 & 0 & -b\gamma_{r5} & a\gamma_{f5} & 0 & 0 & -b\gamma_{r5} & a\gamma_{f5} & 0 & 0 \\ -\gamma_{r1} & 0 & \nu_{r1} & 0 & -\gamma_{r2} & 0 & 0 & 0 & -\gamma_{r3} & 0 & 0 & 0 & -\gamma_{r4} & 0 & 0 & 0 & -\gamma_{r5} & 0 & 0 & 0 & -\gamma_{r5} & 0 & 0 & 0 \\ 0 & -\gamma_{f1} & 0 & \nu_{f1} & 0 & -\gamma_{f2} & 0 & 0 & 0 & -\gamma_{f3} & 0 & 0 & 0 & -\gamma_{f4} & 0 & 0 & 0 & -\gamma_{f5} & 0 & 0 & 0 & -\gamma_{f5} & 0 & 0 \end{pmatrix}, \quad (7.18)$$

In matrix form Equations (7.16) and (7.17), can be recast in the more compact form,

$$\bar{\mathbf{K}}_e = \mathbf{B} \bar{\mathbf{E}}_z \quad (7.19a)$$

$$\bar{\mathbf{C}}_e = \mathbf{B} \bar{\mathbf{E}}_{\dot{z}} \quad (7.19b)$$

where \mathbf{E}_z and $\mathbf{E}_{\dot{z}}$ are $[(n \cdot m) \times m]$ matrices having in the j^{th} column ($j = 1, \dots, m$) the averaged derivative of $\tilde{\mathbf{Z}}(\hat{\mathbf{z}} + \mathbf{m}_z, \dot{\hat{\mathbf{z}}})$ with respect to the Lagrangian coordinates $\hat{\mathbf{z}}$ and their time derivative $\dot{\hat{\mathbf{z}}}$ respectively. That is,

$$\mathbf{E}_z = \left(\frac{\partial}{\partial z_r} \left(\tilde{\mathbf{Z}}(\hat{\mathbf{z}} + \mathbf{m}_z, \dot{\hat{\mathbf{z}}}) \right) \Big|_{\dot{z}_f} \Big|_{\dot{z}_{pr}} \frac{\partial}{\partial z_{pr}} \left(\tilde{\mathbf{Z}}(\hat{\mathbf{z}} + \mathbf{m}_z, \dot{\hat{\mathbf{z}}}) \right) \Big|_{\dot{z}_{pf}} \frac{\partial}{\partial z_{pf}} \left(\tilde{\mathbf{Z}}(\hat{\mathbf{z}} + \mathbf{m}_z, \dot{\hat{\mathbf{z}}}) \right) \right) \quad (7.20)$$

and

$$\mathbf{E}_{\dot{z}} = \left(\frac{\partial}{\partial \dot{z}_r} \left(\tilde{\mathbf{Z}}(\hat{\mathbf{z}} + \mathbf{m}_z, \dot{\hat{\mathbf{z}}}) \right) \Big|_{\dot{z}_f} \Big|_{\dot{z}_{pr}} \frac{\partial}{\partial \dot{z}_{pr}} \left(\tilde{\mathbf{Z}}(\hat{\mathbf{z}} + \mathbf{m}_z, \dot{\hat{\mathbf{z}}}) \right) \Big|_{\dot{z}_{pf}} \frac{\partial}{\partial \dot{z}_{pf}} \left(\tilde{\mathbf{Z}}(\hat{\mathbf{z}} + \mathbf{m}_z, \dot{\hat{\mathbf{z}}}) \right) \right) \quad (7.21)$$

In this regard one finds:

$$E \left[\frac{\partial}{\partial \dot{z}_j} (\dot{z}_j + m_j)^3 \right] = 3 \left(m_j^2 + \sigma_{\dot{z}_j}^2 \right); \quad (7.22a)$$

$$E \left[\frac{\partial}{\partial \dot{z}_j} \text{sign}(\dot{z}_j) \right] = E \left[2\delta(\dot{z}_j) \right] = \sqrt{\frac{2}{\pi}} \frac{1}{\sigma_{\dot{z}_j}}; \quad (7.22b)$$

$$E \left[\frac{\partial}{\partial \dot{z}_j} \dot{z}_j U(\dot{z}_j) \right] = E \left[\frac{\partial}{\partial \dot{z}_j} \dot{z}_j U(-\dot{z}_j) \right] = \frac{1}{2}; \quad (7.22c)$$

and

$$E \left[\frac{\partial}{\partial \dot{z}_j} \dot{z}_j |\dot{z}_j|^\alpha U(\dot{z}_j) \right] = E \left[\frac{\partial}{\partial \dot{z}_j} \dot{z}_j |\dot{z}_j|^\alpha U(-\dot{z}_j) \right] = 2^{\frac{\alpha}{2}} \sigma_{\dot{z}_j}^\alpha \Gamma\left(\frac{3+\alpha}{2}\right) / \sqrt{\pi}; \quad (7.22d)$$

for $j = r, f, pr, pf$.

7.3.3 The Frequency-Domain Representation

The wheel-base filtering vector $\mathbf{T}(\omega, V)$ given by Equation (5.34), is introduced here to derive the correlated frequency response function of the equivalent linear system (ELS), Equation (7.9). Following the discussion provided in section 5.6.1.1 this function is found to be

$$\bar{\mathbf{H}}_f(\omega) = \left(-\omega^2 \bar{\mathbf{M}} + i\omega(\bar{\mathbf{C}} + \bar{\mathbf{C}}_e) + \bar{\mathbf{K}} + \bar{\mathbf{K}}_e \right)^{-1} \left(\omega^2 \bar{\mathbf{M}} \right) \mathbf{T}; \quad (7.23)$$

Selecting a given power spectral density function of the ground profile $S_W(\omega)$ as in Equation (3.26), the power spectral density matrix of the response in terms of Lagrangian coordinates $\hat{\mathbf{z}}$ is

$$\mathbf{S}_z(\omega) = \bar{\mathbf{H}}_f(\omega) \left(\bar{\mathbf{H}}_f(\omega) \right)^{*T} S_W(\omega). \quad (7.24)$$

The symbol $*T$ denote, the transpose-conjugate operation. Once $\mathbf{S}_z(\omega)$ is known, the covariance matrix of the response process can be determined using the equation

$$\sigma_z^2 = \int_{-\infty}^{\infty} \mathbf{S}_z(\omega) d\omega; \quad (7.25)$$

$$\sigma_{\dot{z}}^2 = \int_{-\infty}^{\infty} \omega^2 \mathbf{S}_z(\omega) d\omega \quad (7.26)$$

All of these quantities can be handled in the absolute coordinates system as well, once the linearization procedure is accomplished. In fact, after some straightforward algebraic steps and setting $\mathbf{C}_e = \bar{\mathbf{C}}_e \mathbf{A}^{-1}$ and $\mathbf{K}_e = \bar{\mathbf{K}}_e \mathbf{A}^{-1}$, the frequency response function in the new coordinate system becomes

$$\mathbf{H}_f(\omega) = \left(-\omega^2 \mathbf{M} + i\omega(\mathbf{C} + \mathbf{C}_e) + \mathbf{K} + \mathbf{K}_e \right)^{-1} \left(i\omega(\bar{\mathbf{C}} + \bar{\mathbf{C}}_e) + \bar{\mathbf{K}} + \bar{\mathbf{K}}_e \right) \mathbf{T}. \quad (7.27)$$

Thus, the spectral density matrix for the absolute coordinate vector \mathbf{q} process, is

$$\mathbf{S}_q(\omega) = \mathbf{H}_f(\omega) \left(\mathbf{H}_f(\omega) \right)^{*T} S_W(\omega). \quad (7.28)$$

By using Equation (7.28), the elements of the covariance matrix of the accelerations $\ddot{\mathbf{q}}$ are found by the equations

$$\sigma_{\ddot{\mathbf{q}}}^2 = \int_{-\infty}^{\infty} \omega^4 \mathbf{S}_q(\omega) d\omega. \quad (7.29)$$

The spectral density function of the response of the linear system (LS), can be obtained by means of Eqs. (7.24) and (7.28), by simply setting in the transfer functions in Equations (7.23) and (7.27), $\bar{\mathbf{C}}_e = \mathbf{0}$ and $\bar{\mathbf{K}}_e = \mathbf{0}$.

7.4 Implementation of the Statistical Linearization Method

The statistical linearization technique can be implemented following the scheme shown below.

Step 0:

1. In equation

$$\bar{\mathbf{M}}\ddot{\hat{\mathbf{z}}} + \bar{\mathbf{C}}\dot{\hat{\mathbf{z}}} + \bar{\mathbf{K}}\hat{\mathbf{z}} + \bar{\mathbf{h}}(\hat{\mathbf{z}}, \dot{\hat{\mathbf{z}}}) = -\bar{\mathbf{M}}\ddot{\mathbf{w}} \quad (1)$$

set the nonlinear term equal to zero, i.e. $\bar{\mathbf{h}}(\hat{\mathbf{z}}, \dot{\hat{\mathbf{z}}}) = \mathbf{0}$

2. In the equation of the equivalent system

$$\bar{\mathbf{M}}\ddot{\hat{\mathbf{z}}} + (\bar{\mathbf{C}} + \bar{\mathbf{C}}_e)\dot{\hat{\mathbf{z}}} + (\bar{\mathbf{K}} + \bar{\mathbf{K}}_e)\hat{\mathbf{z}} = -\bar{\mathbf{M}}\ddot{\mathbf{w}} \quad (2)$$

let $\bar{\mathbf{C}}_e = \mathbf{0}$, and $\bar{\mathbf{K}}_e = \mathbf{0}$ as initial guess, so that the system is completely linear ($\mathbf{B}=\mathbf{0}$).

3. Evaluate the offset of the linear system, that coincide with the static position:

$$\mathbf{m}^0 = -\mathbf{K}^{-1}\mathbf{p} \quad (3)$$

4. Work in the frequency-domain, and introduce the wheelbase filtering vector

$$\mathbf{T} = \left(0, 0, e^{-\frac{i\omega p}{V}}, 1\right)^T \quad (4)$$

and derive the filtered frequency response function in form

$$\bar{\mathbf{H}}_f^0(\omega) = \left(-\omega^2\bar{\mathbf{M}} + i\omega(\bar{\mathbf{C}} + \bar{\mathbf{C}}_e^0) + (\bar{\mathbf{K}} + \bar{\mathbf{K}}_e^0)\right)^{-1}(\omega^2\bar{\mathbf{M}})\mathbf{T} \quad (5)$$

5. Determine power spectrum of the response using the equation

$$\mathbf{S}_z^0(\omega) = \bar{\mathbf{H}}_f^0(\omega)\mathbf{S}_w(\omega)\left(\bar{\mathbf{H}}_f^0(\omega)\right)^{*T} \quad (6)$$

6. Integrate the power spectrum components in the range $[\omega_{min}, \omega_{max}]$, to determine the covariance matrix

$$\boldsymbol{\sigma}_{\hat{\mathbf{z}}}^0 = \int \mathbf{S}_{\hat{\mathbf{z}}}^0(\omega) d\omega \quad (7)$$

$$\boldsymbol{\sigma}_{\hat{\mathbf{z}}}^0 = \int \omega^2 \mathbf{S}_{\hat{\mathbf{z}}}^0(\omega) d\omega \quad (8)$$

Step i :

- i. Use $\boldsymbol{\sigma}_{\hat{\mathbf{z}}}^i$ and $\boldsymbol{\sigma}_{\hat{\mathbf{z}}}^i$ to determine \mathbf{m}^i from the equation

$$\bar{\mathbf{K}}\mathbf{m}_{\mathbf{z}} + E[\bar{\mathbf{g}}(\hat{\mathbf{z}} + \mathbf{m}_{\mathbf{z}}, \hat{\mathbf{z}})] + \mathbf{p} = \mathbf{0} \quad (9)$$

- ii. Update the values of $\bar{\mathbf{C}}_{\mathbf{e}}^i$ and $\bar{\mathbf{K}}_{\mathbf{e}}^i$ by means of the equation

$$\bar{\mathbf{Q}}_{\mathbf{e}[m \times (n \cdot m)]} = \mathbf{B}_{[m \times (n \cdot m)]} E \left[\frac{\partial}{\partial \mathbf{Y}} \tilde{\mathbf{Z}}(\hat{\mathbf{z}} + \mathbf{m}_{\mathbf{z}}, \hat{\mathbf{z}}) \right]_{[(n \cdot m) \times (n \cdot m)]}$$

$$\bar{\mathbf{Q}}_{\mathbf{e}[m \times (n \cdot m)]} = \mathbf{B}_{[m \times (n \cdot m)]} \mathbf{D}_{[(n \cdot m) \times (n \cdot m)]} \quad (10)$$

- iii. Evaluate $\bar{\mathbf{H}}_f^i(\omega)$, $\mathbf{S}_{\hat{\mathbf{z}}}^i(\omega)$, $\boldsymbol{\sigma}_{\hat{\mathbf{z}}}^i$, and $\boldsymbol{\sigma}_{\hat{\mathbf{z}}}^i$ using equations (4)-(7).

- iv. Iterate the process until the quantity

$$\sqrt{(\sigma_{z_f}^i - \sigma_{z_f}^{i-1})^2 + (\sigma_{z_r}^i - \sigma_{z_r}^{i-1})^2 + (\sigma_{z_{pf}}^i - \sigma_{z_{pf}}^{i-1})^2 + (\sigma_{z_{pr}}^i - \sigma_{z_{pr}}^{i-1})^2} \quad (11)$$

reaches a preselected value.

Chapter 8 Numerical Results

8.1 Introduction

The purpose of this chapter is to validate the effectiveness of the ELS in capturing the behavior of the nonlinear motorcycle dynamics model. For this purpose, both a linear system and a nonlinear system have been developed. All the geometric and mechanical parameters values are identical to those shown in table 5.1.

The natural vibration frequencies of the 4-DOF system described by Equation (4.12) are shown on page 97.

8.2 Case 1. Front Suspension with Nonlinear Springs and Nonlinear Dashpots

Consider for example a non-linear system (NLS) obtained by inserting in the front suspension of the linear system (LS) additional nonlinear devices leading to the vector

$$\bar{\mathbf{g}}(\mathbf{z}, \dot{\mathbf{z}}) = \begin{pmatrix} 0 \\ \gamma_{f1} z_f^3 + \gamma_{f3} \dot{z}_f U(\dot{z}_f) + \gamma_{f4} \dot{z}_f U(-\dot{z}_f) + \gamma_{f5} \dot{z}_f |\dot{z}_f|^\alpha U(\dot{z}_f) + \gamma_{f6} \dot{z}_f |\dot{z}_f|^\alpha U(-\dot{z}_f) \\ 0 \\ 0 \end{pmatrix}, \quad (8.31)$$

The nonlinear terms, are $F_{elastic}(z_f)$ and viscous constitutive law $F_{viscous}(\dot{z}_f)$ of the front suspension are defined as follows

$$F_{elastic}(z_f) = k_f z_f + \gamma_{f1} z_f^3 = k_f z_f (1 + \varepsilon_1 z_f^2); \quad (8.32)$$

$$\begin{aligned} F_{viscous}(\dot{z}_f) &= \\ &= c_f \dot{z}_f + \gamma_{f3} \dot{z}_f U(\dot{z}_f) + \gamma_{f4} \dot{z}_f U(-\dot{z}_f) + \gamma_{f5} \dot{z}_f |\dot{z}_f|^\alpha U(\dot{z}_f) + \gamma_{f6} \dot{z}_f |\dot{z}_f|^\alpha U(-\dot{z}_f) \\ &= c_f \dot{z}_f \left(1 + U(\dot{z}_f) (\varepsilon_3 + \varepsilon_5 |\dot{z}_f|^\alpha) + U(-\dot{z}_f) (\varepsilon_4 + \varepsilon_6 |\dot{z}_f|^\alpha) \right); \end{aligned} \quad (8.33)$$

They are shown in Figure 8.1 and Figure 8.2, for a particular set of mechanical parameters and they are compared to the linear counterpart of the linear system. The range of the response of the LS is indicated to show the difference between the linear and the nonlinear systems.

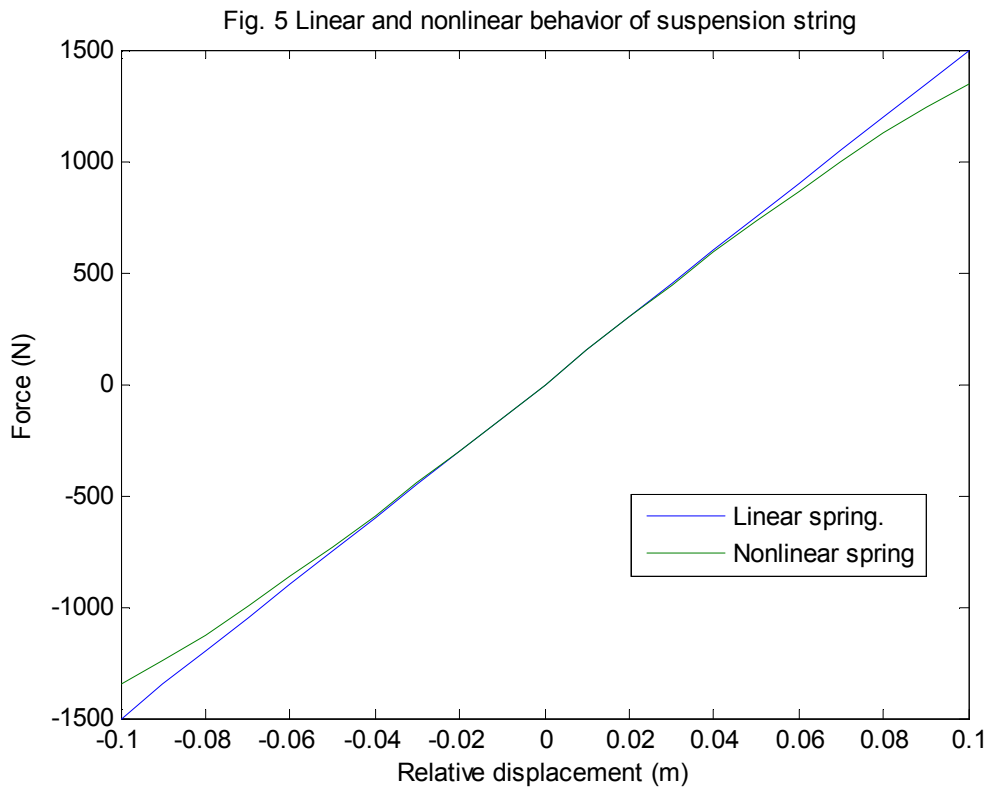


Figure 8.1 Comparison of the linear and nonlinear behavior of a common motorcycle suspension. Elastic force.

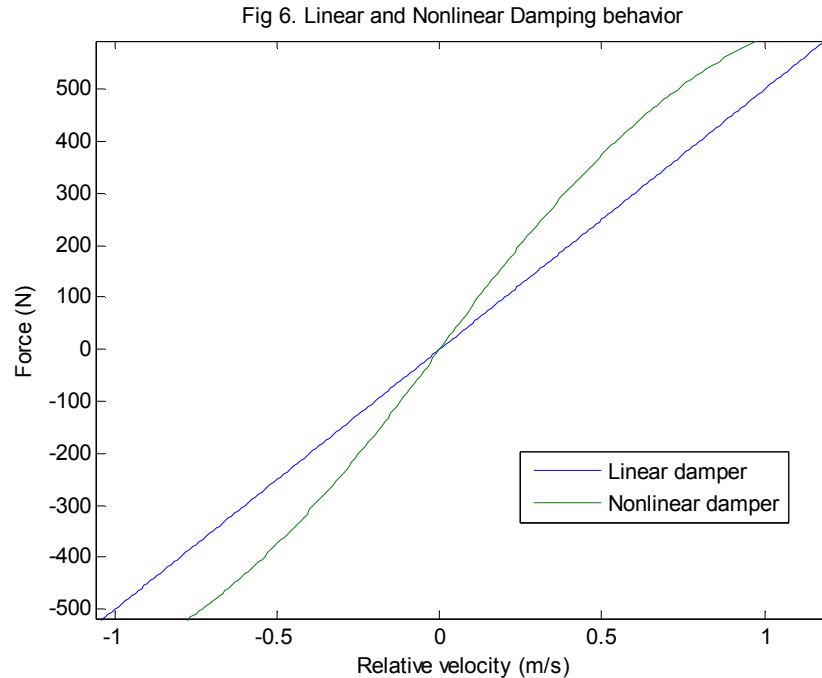


Figure 8.2 Comparison of the linear and nonlinear behavior of a common motorcycle suspension. Viscous force.

8.2.1 Monte Carlo Simulation

As it was earlier mentioned, to validate the results obtained by the statistical linearization method, a Monte Carlo simulation in the time-domain is performed. This procedure is done for both the linear system and the nonlinear system. An ensemble of $n = 5000$ realizations of the response process of $\ddot{q}(t)$ and $z_f(t)$ is generated.

The response of the systems has been sampled adopting a cut-off frequency ω_b exceeding the value eight times the highest fundamental frequency ($\omega_b = 800 \text{ rad/s}$) of the linear system.

The power spectrum of the road roughness excitation and its fitting by the AR filter are presented in Figure 8.3 and Figure 8.6. In the same figures a third fitting is shown corresponding to the power spectrum generated by using the function PWELCH available in Matlab.

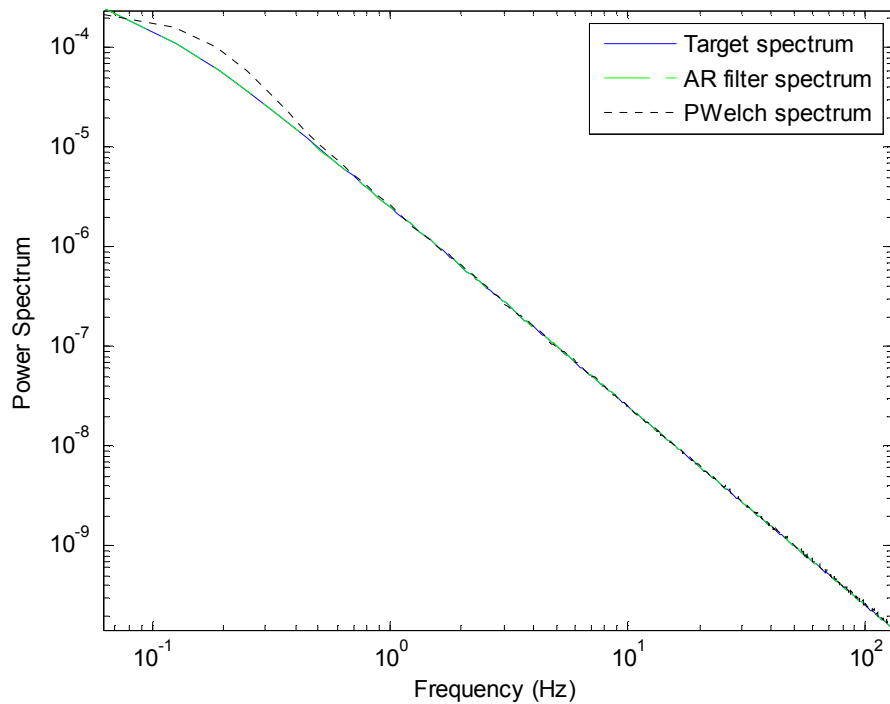


Figure 8.3 displacement PSD fitting by AR filter and function PWELCH.

Note there is a small discrepancy between the target power spectrum of the displacements and the PWELCH spectrum. This small discrepancy is magnified by the log-log format given to the graph. However, besides being small, the discrepancy occurs in the range of frequencies between zero and 0.5 Hz, which is far from the 2 Hz value that corresponds to the minimum frequency relevant in the dynamic behavior of motorcycles. Thus, the discrepancy has almost negligible effect on the fidelity of the signal.

Figure 8.4 shows a sample time history out of the many generated with the AR filter. An autocorrelation test for that signal is shown in Figure 8.5. From this test it can be seen that the autocorrelation decays quite rapidly with time.

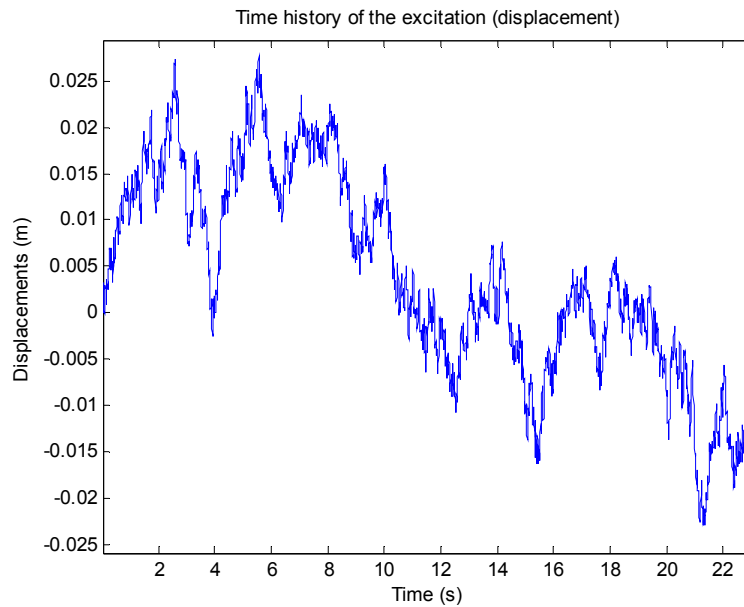


Figure 8.4 Sample time history obtained from the displacement PSD fitting by AR filter.

The same test is also performed on the velocity signals, and similar results are obtained. With the autocorrelation test and the use of the PWELCH function, it is verified that the AR filter implemented in Matlab works correctly, and that the reliability of the signals obtained is high.

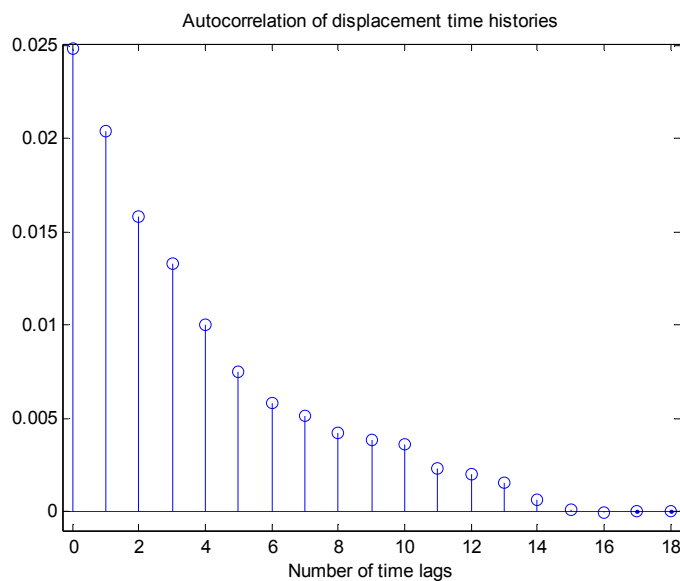


Figure 8.5 Autocorrelation of AR filter time histories (displacement).

A sample time history from the velocity PSD is shown in Figure 8.7, and its corresponding source PSD is shown in Figure 8.6.

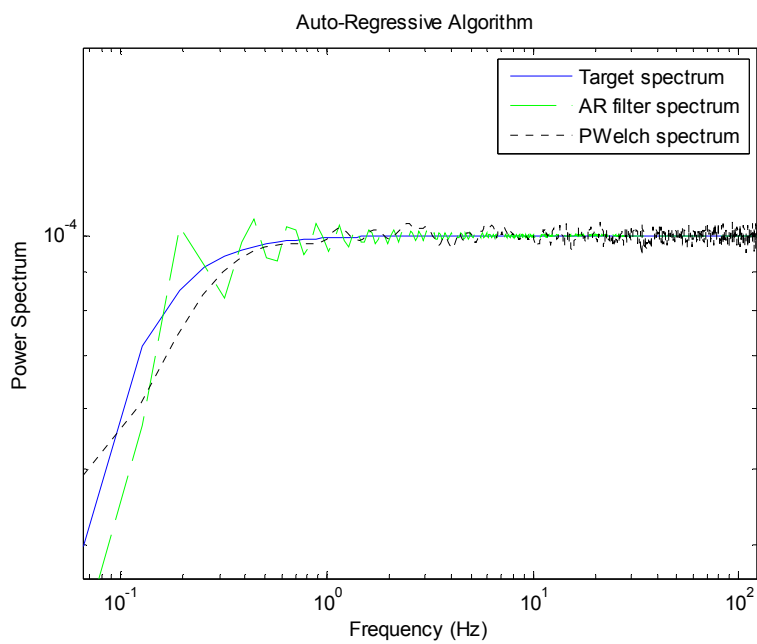


Figure 8.6 Velocity PSD fitting by AR filter and function PWELCH.

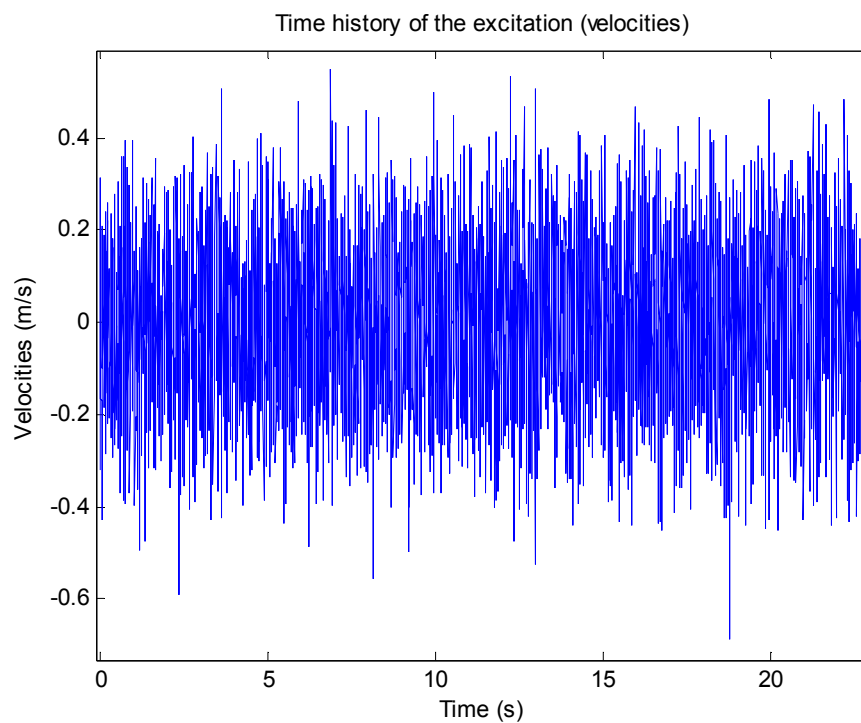


Figure 8.7 Sample time history obtained from the velocity PSD fitting by AR filter.

Once the input or excitation signals have been generated, the next step includes generating the ensemble of the response. This step is accomplished by using a fourth order Runge-Kutta scheme for which it is necessary to rewrite the system of ODE's in state-space form. Figure 8.8 gives a sample of an ensemble of response time histories, in this case for the absolute coordinate q .

By defining $x_j(t_i)$ as the j^{th} realization of the generic random variable extracted at the instant $t_i = (i-1)T$, the first and second order statistics are evaluated from an amount of n samples of the response of $\ddot{q}(t)$ and $z_f(t)$. These computations require the use of Equations (4.1) and (4.2). The result of applying Equation (4.1) to the ensemble of Figure 8.8 is shown in Figure 8.9.

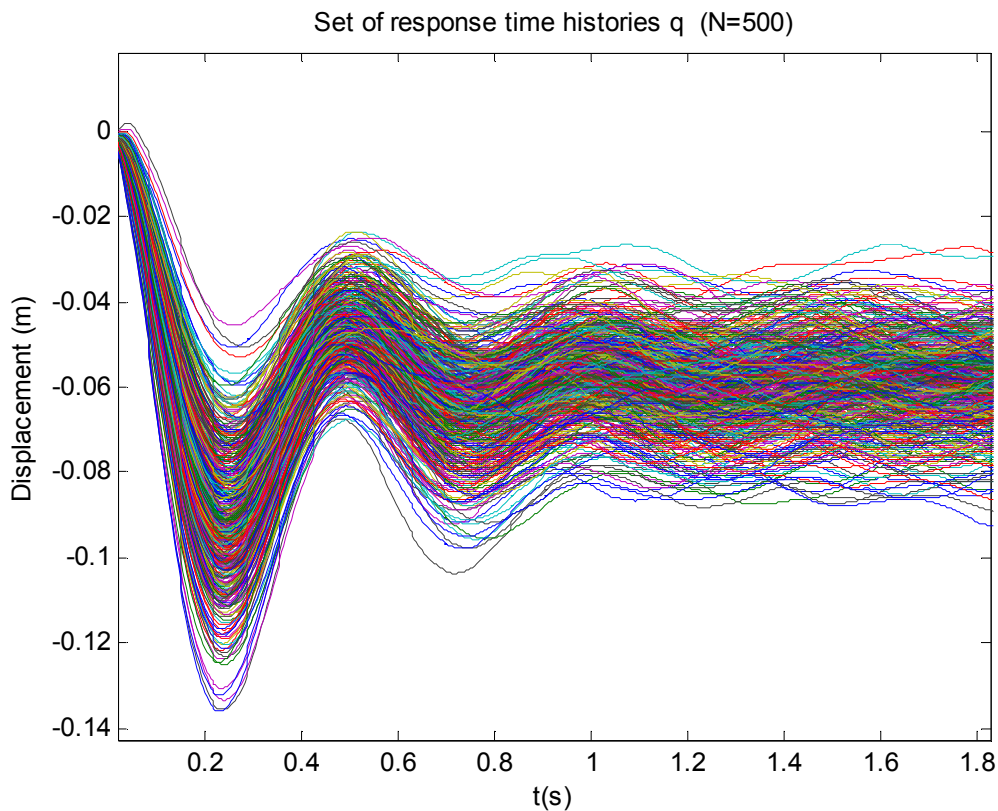


Figure 8.8 Ensemble of response time histories.

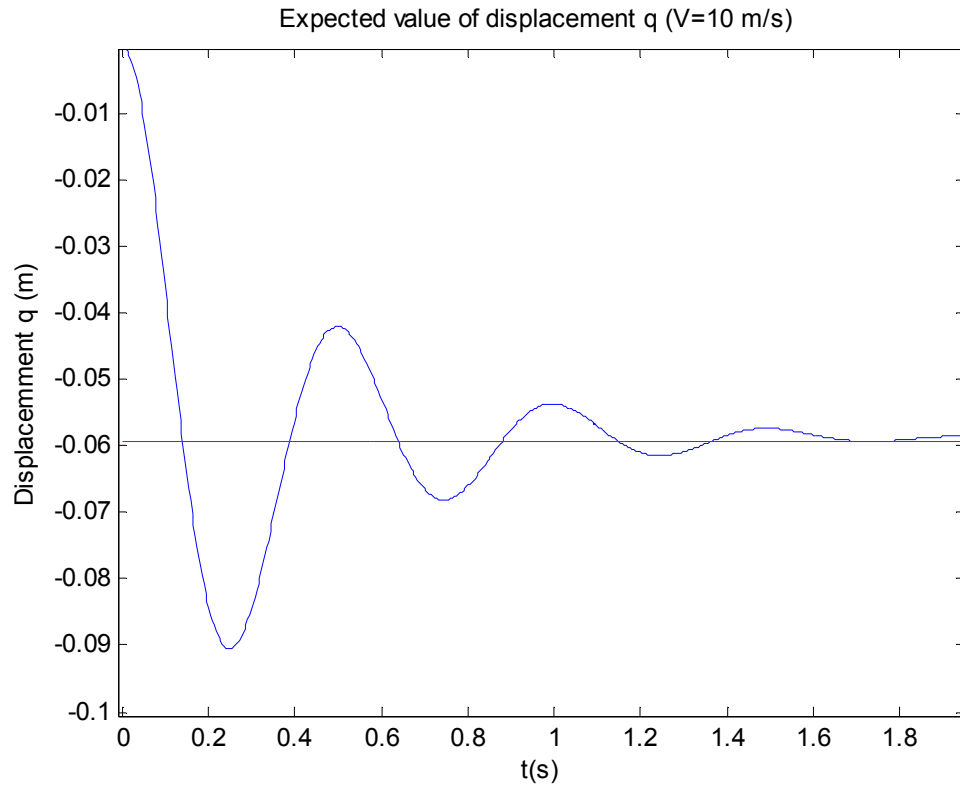


Figure 8.9 Averaged response time history for $q(t)$.

Figure 8.10 and Figure 8.11 show the results obtained for the averaged responses and their corresponding variances of both, the linear system's and the nonlinear system's $z_f(t)$ relative coordinate. The associated values for the stationary solution of each system are included as well.

From the evolution of the previously mentioned statistics one can readily gauge how both the linear system and the nonlinear system exhibit practically a stationary response after only 2 seconds of non-stationary behavior.

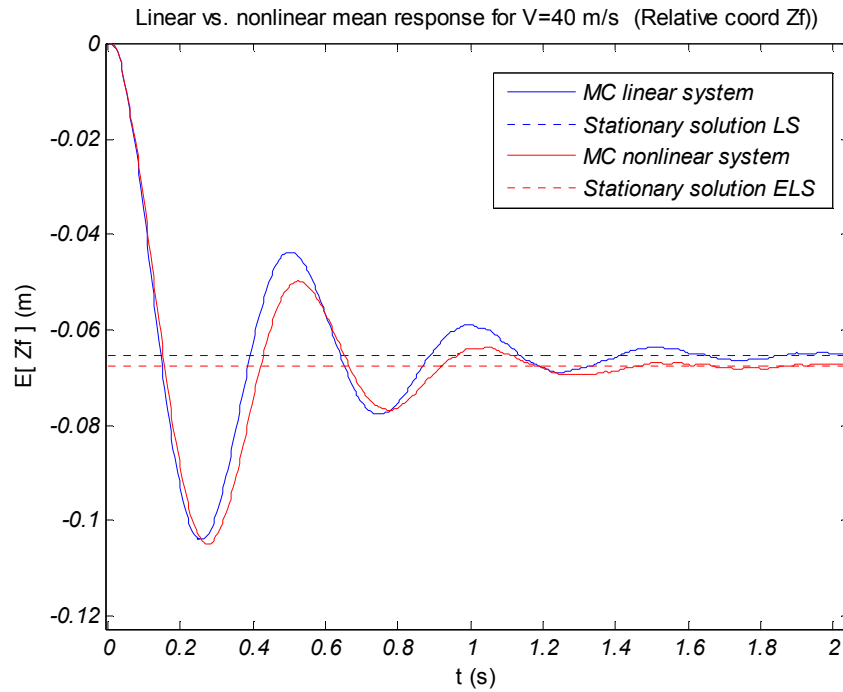


Figure 8.10 Averaged response time histories for $z_f(t)$

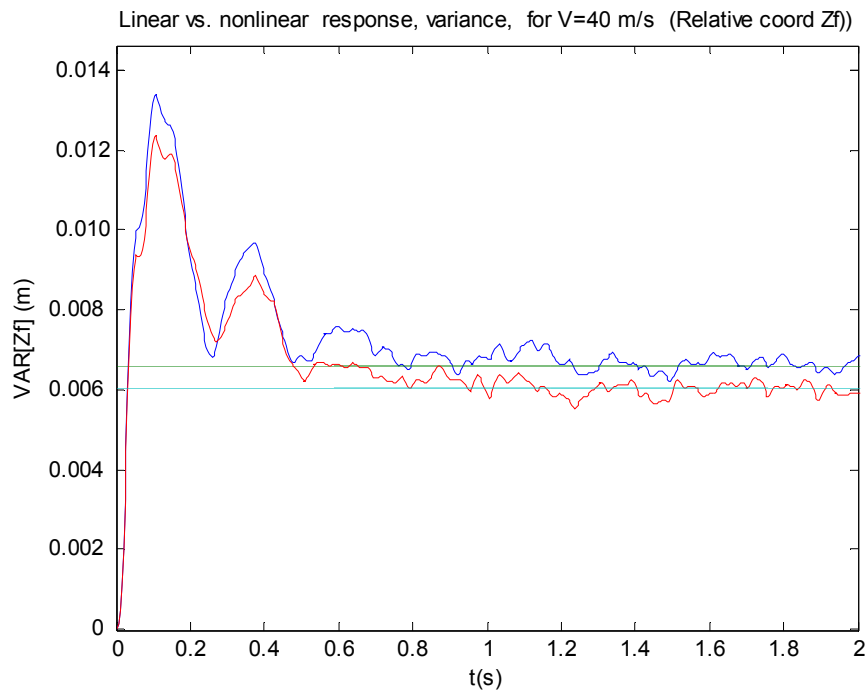


Figure 8.11 Variance of response time history for $z_f(t)$

In a similar manner, the response histories for the acceleration $q''(t)$ in absolute coordinates and its corresponding variance are shown in Figures 8.12 and 8.13.

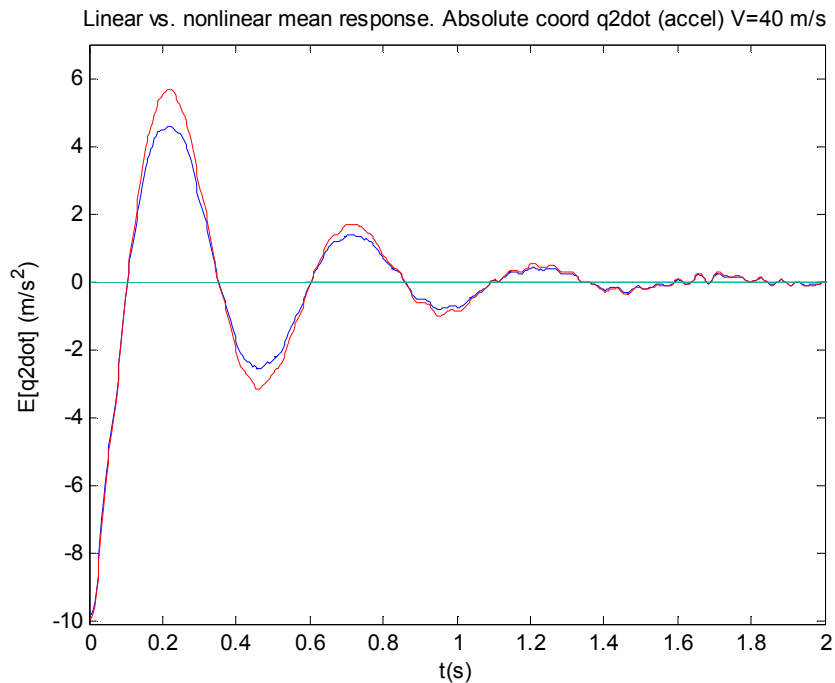


Figure 8.12 Averaged response time history for $q''(t)$.

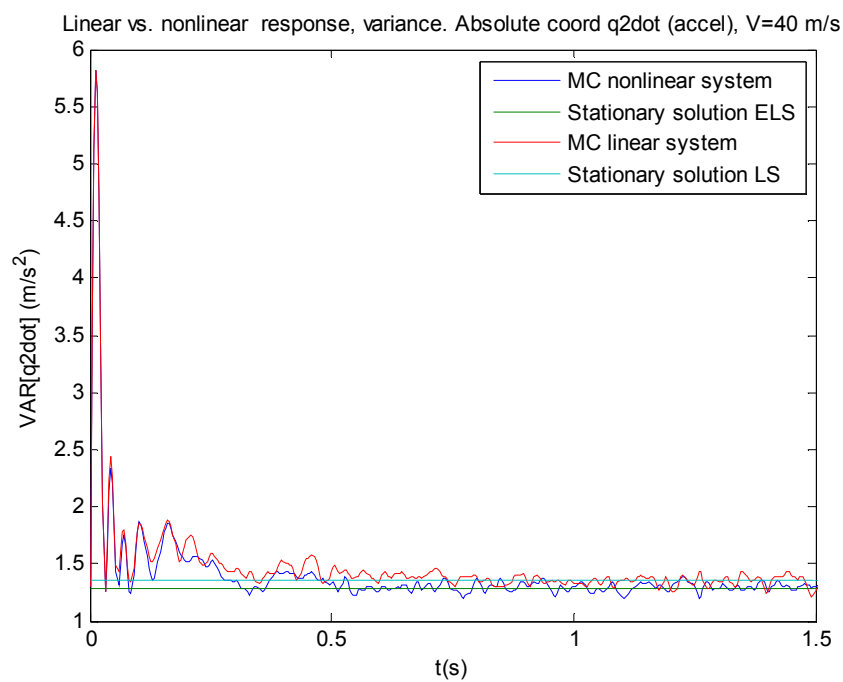


Figure 8.13 Variance of response time history for $q''(t)$.

The standard deviations $\sigma_{\ddot{q}}(t)$ of the center of mass acceleration referred to the NLS approaches, as predicted by the stationary solution of the ELS, to a smaller value than the one associated to the LS, providing therefore an improved comfort for the rider.

The standard deviations $\sigma_{z_f}(t)$ of the stroke of the front suspension referred to the NLS approaches, as predicted by the stationary solution of the ELS, to a smaller value than the one associated to the LS, leading therefore to designing less cumbersome devices.

The mean of the stroke process $E[z_f(t)]$ approaches quite rapidly the values of the static equilibrium position $\mathbf{m}_z = -\overline{\mathbf{K}}^{-1} \mathbf{p}$ for the LS and the values of the offset given by the solution of Eq. (7.6) in the case of the NLS.

8.2.1.1 Normality Test

Once the first and the second order statistics have been evaluated, one can examine the normality assumption of the response of the NLS, treating statistically, for example, the stroke of the front suspension through Monte Carlo simulation.

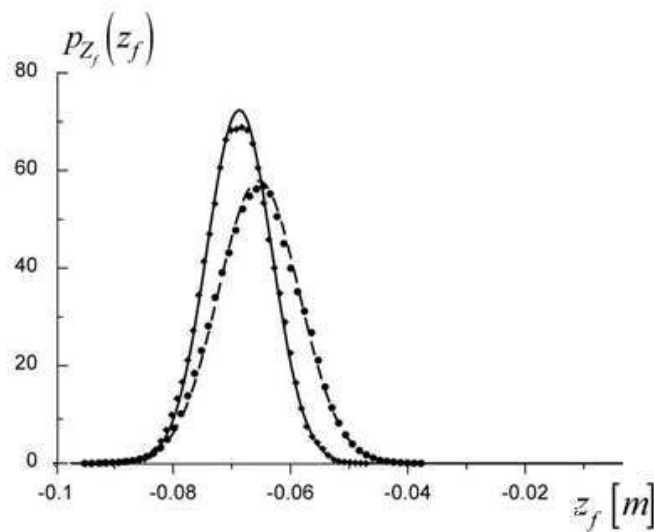


Figure 8.14 Normality test.

This has been done in Figure 8.14 for the extracted random variable $z_f(t = 5s)$, showing a discrepancy between the theoretical and the actual distribution, which is attributed to the non-Gaussian nature of the nonlinear response.

The same considerations can be obtained alternatively working in the frequency-domain assuming the stationarity of the response. In this regard the analytical two-sided PSD function $S_{\ddot{q}}(\omega)$ of the center of mass acceleration is reported for both the LS and the ELS; it is compared with the PSD functions evaluated from the Monte Carlo simulation ($n = 500$ samples, $60s$ sample) of the LS and NLS respectively, showing a good agreement for the chosen set of parameters.

In closure, by varying the speed of the vehicle V and maintaining the other characteristics of the PSD function of the road roughness reported in Equation (3.6), the curves in Figures (8.15) and (8.16) are produced.

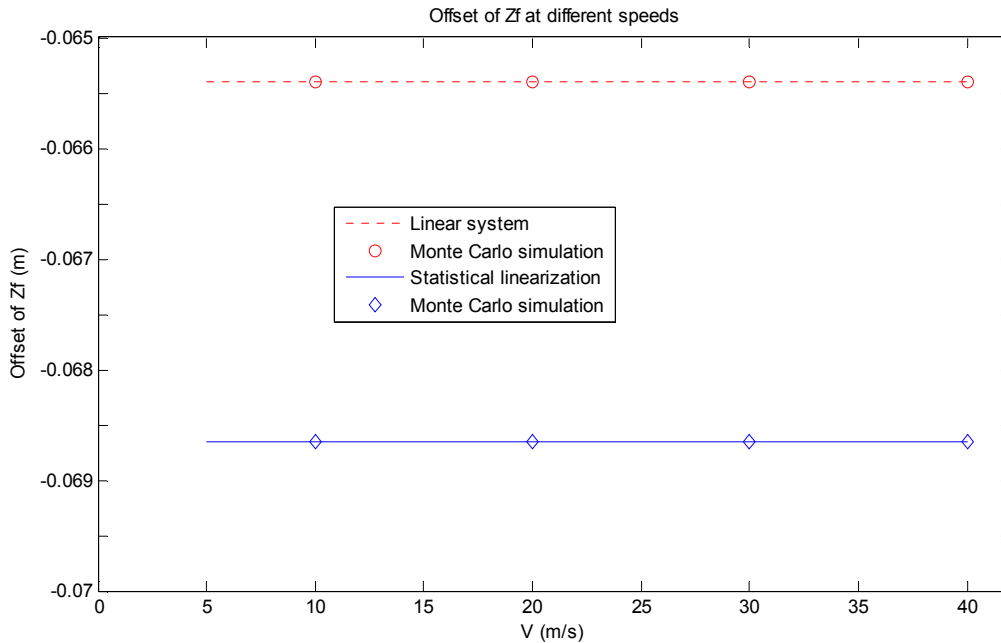


Figure 8.15 Offset of motorcycle Z_f at different speeds.

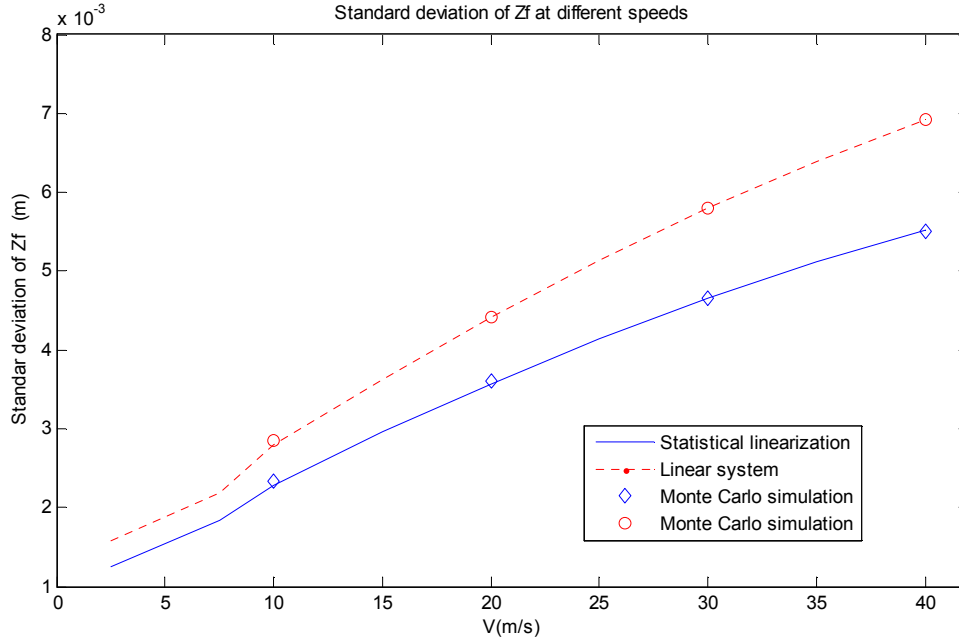


Figure 8.16 Standard deviation of Z_f at different speeds.

8.3 Case 2. Front Suspension with Linear Springs and Nonlinear Dashpots

A different behavior may be observed considering a nonlinear system with a front suspension modeled by the equation

$$F_{elastic}(z_f) = k_f z_f; \quad (8.34)$$

$$F_{viscous}(\dot{z}_f) = c_f \dot{z}_f + \gamma_{f2} \text{sign}(\dot{z}_f) + \gamma_{f3} \dot{z}_f U(\dot{z}_f) = c_f \dot{z}_f (1 + \varepsilon_3 U(\dot{z}_f)) + \frac{M g}{20} \varepsilon_2; \quad (8.35)$$

In this case a linear elastic spring and a nonlinear asymmetric viscous dashpot with friction is included. The value of the offset deviation of z_f versus various speeds is shown in Figure 8.17.

Also in this case the equivalent linear system provides a good approximation of the actual nonlinear system, but increasing the speed V , a greater variation than the one observed in Figure 8.15 can be seen.

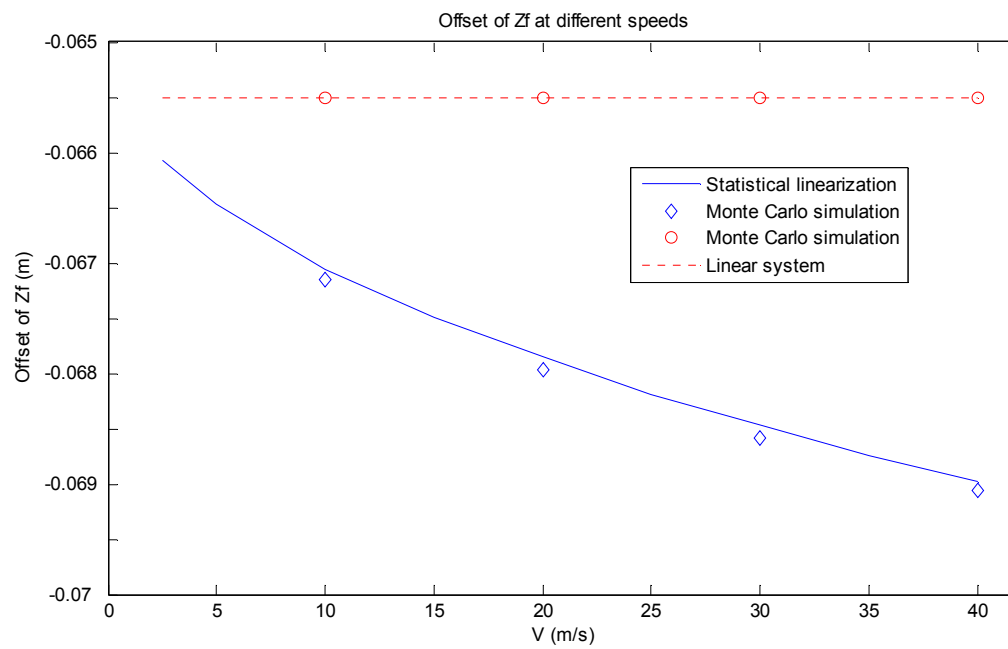


Figure 8.17 Offset of motorcycle at different speeds Z_f .

Chapter 9

Concluding Remarks

9.1 Conclusions

In this thesis the significance of the nonlinear behavior in the dynamic response of motorcycles has been discussed. Motorcycles are complex dynamical systems that can be subjected to strong road excitations. Such excitations have a random nature and can drive the suspension system to experience extreme excursions, which in turn induce nonlinear behavior. This behavior requires the adoption of nonlinear springs and dashpots models in the design of the suspension that could limit its excursions.

Specifically, a 4-DOF motorcycle model that includes a variety of nonlinear components has been employed to secure a realistic representation of the characteristics of modern motorcycles. The simplifying criteria considered to derive the model have been explained, along with the derivation of the model. First, a linear 4-DOF model has been derived and used to delineate the general steps of solution in the dynamic analysis. This model has served as to derive an enhanced 4-DOF nonlinear model. This model includes several nonlinear elements, each of them described mathematically. Additional issues regarding the nonlinear behavior of the model have been discussed.

The representation of a random environment, namely the road roughness, via an AR filter has also been proposed. It has been found to be a quite reliable way of generating excitation time histories that are obtained from an specific road power spectrum. Specifically, it has been shown that the AR filter is capable of synthesizing time histories with statistical metrics which are compatible with the prescribed power spectrum. Various criteria of assessing the quality of the signals have been applied. Further, the time histories

generated by the AR filter have been used to perform accurate Monte Carlo simulations. The Monte Carlo method has been used to validate the results obtained by the statistical linearization method. In this context, the frequency domain solution of a linear multi-degree-of-freedom (M-DOF) system has been used to calibrate the Monte Carlo algorithm implemented and to determine the minimum number of time histories needed to derive reliable numerical results.

An important contribution of this study is the establishment of the method of statistical linearization as an efficient tool for analyzing M-DOF motorcycle models with strong nonlinearities, such as a motorcycle with nonlinear suspension components. In this sense, the general methodology of implementation of the statistical linearization method, intended for MDOF systems has been delineated. Indeed, the frequency domain solution of a nonlinear MDOF system based on the statistical linearization has been discussed in detail. Further, specific comments regarding the motorcycle dynamics have been included in the application of the method, and a detailed computational scheme of analysis has been established.

The importance of the wheelbase filtering effect on the dynamic behavior of the motorcycle has been noted and taken into account when deriving the computational steps of the statistical linearization method. This effect has also been considered when implementing the Monte Carlo method, and an algorithm has been developed to determine an integration time step which is compatible with the traversing velocity of the motorcycle.

Numerical examples have demonstrated the validity of the statistical linearization methodology developed for the stochastic dynamic analysis of the nonlinear motorcycle model.

9.2 Future Work

Additional work on line with this thesis could pertain to enhanced roughness modeling by including potholes encountered in roads. In the case of in-plane motion the assumption of a driver firmly attached to the motorcycle's body may be eliminated with the inclusion of a driver model. Further, the effect of hysteresis in the suspension elements of the motorcycle models can be the focus of further meritorious studies.

References

- [1] Limebeer, D.J.N. and Sharp, R.S., *Bicycles, Motorcycles and Models Single-track vehicle modeling and control*, IEEE Control Systems Magazine, Oct 2006.
- [2] Sharp, R.S., *The stability and control of motorcycles*, *Jour. Mech. Eng. Sci.*, vol. 13, no. 5, pp. 316–329, 1971.
- [3] Sharp, R.S., *The influence of frame flexibility on the lateral stability of motorcycles*, *Jour. Mech. Eng. Sci.*, vol. 15, no. 2, pp. 117–120, 1974.
- [4] Jennings, G., *A study of motorcycle suspension damping characteristics*. SAE 740628, 1974.
- [5] Black, S.H., Taylor, D.L., *Simulation of Off-Road Motorcycle Ride Dynamics*, SAE paper 790261, 1979.
- [6] De Molina, C., *Application of a finite element code in the analysis of motorcycle road behaviour*. Computers and Structures Vol. 31. No. 5, pp. 189–794, 1989.
- [7] Goncalves, J.P.C., Ambrosio, J.A.C., 2003, *Optimization of vehicle suspension systems for improved comfort of road vehicles using flexible multibody dynamics*. *Nonlinear Dynamics*, Vol. 34 (Dordrecht: Kluwer Academic Publishers), pp. 113–131.
- [8] Tuluie, R., Stewart, G., *Motorcycles suspension development Using Ride Comfort with a Laboratory Test System*, SAE 1999 164-171 1999-01-3276 9938031.
- [9] Koyano M., Kimishima, T., Nakayama, K., *Quantification of static seating comfort of motorcycle seats*, *JSAE Review* 24, pp. 471-475, 2003.
- [10] Klein, F., Sommerfeld, A. *The Theory of Gyroscope*, Vol. IV, Technical Applications. Berlin and Leipzig, 1910.
- [11] Whipple F. J. W. *The Stability of the Motion of a Bicycle*, *Quart, Journal of Pure and Applied Mathematics*, 30, 1899.
- [12] Döringh E., Braunschweig, *Stability of Single Track Vehicles*, *Forschung Ing. Wes.* 21, no. 2, 50-62, 1955.
- [13] Collins, R.N., *A Mathematical Analysis of the Stability of Two Wheeled Vehicles*, Ph.D. thesis, University of Wisconsin, 1963.

- [14] Singh, D., *Advanced Concepts of the Stability of Two-Wheeled Vehicles. Application of Mathematical Analysis to Actual Vehicles*. Ph.D. thesis, University of Wisconsin, 1964.
- [15] Roe, G. E., *Theory of castor oscillations*, Journal of Mechanical Engineering Science, Vol. 15, no. 5, pp. 379-381, 1973.
- [16] Roe, G. E. and Thorpe, T. E., *Experimental investigation of the parameters affecting the castor stability of road wheels*, Journal of Mechanical Engineering Science, Vol. 15, no. 5, pp. 365-369, 1973.
- [17] Roe, G. E. and Thorpe, T. E., *A Solution of the Low-Speed Wheel Flutter Instability in Motorcycles*, Journal of Mechanical Engineering Science, Vol. 18, no. 2, pp. 57-65, 1976.
- [18] Sharp, R.S., *The stability of motorcycles in acceleration and deceleration*, *Inst. Mech. Eng. Conference Proceedings on "Braking of Road Vehicles"*. London: MEP, 1976, pp. 45-50.
- [19] Limebeer, D.J.N., Sharp, R.S., and Evangelou, S., *The stability of motorcycles under acceleration and braking*, J. Mech. Eng. Sci., vol. 215, no. 9, pp. 1095-1109, 2001.
- [20] Bartlett, M.S., *Periodogram analysis and continuous spectra*, *Biometrika*, 1950, 31:1-16.
- [21] Kane, T.R., *The Effect of Frame Flexibility on High Speed Weave of Motorcycles*, SAE Paper 780306, 1978.
- [22] Verma, M.K., Scott, R.A. and Segel, L., *Effect of frame compliance on the lateral dynamics of motorcycles*, *Vehicle Syst. Dyn.* 9 (1980).
- [23] Cossalter, V., Doria, A. and Mitolo, L., *Inertial and Modal Properties of Racing Motorcycles*, SAE Paper 2002-01-3347, 2002.
- [24] Sharp, R.S. and Alstead, C.J., *The influence of structural flexibilities on the straight-running stability of motorcycles*, *Vehicle System Dynamics*, 9 (1980).
- [25] Pacejka, H. B. and R. S. Sharp, *Shear force development by pneumatic tyres in steady state conditions: A review of modeling aspects*, *Vehicle System Dynamics*, vol. 20, no. 3-4, pp. 121-176, 1991.
- [26] Nigam, N.C. and S. Narayanan, *Applications of Random Vibrations*, Springer-Verlag, 1994.

- [27] Spierings, P.T.J., *The effects of lateral front fork flexibility on the vibrational modes of straight-running single-track vehicles*, Vehicle System Dynamics, vol. 10, no. 1, pp. 21–35, 1981.
- [28] Sharp, R.S., Evangelou, S. and Limebeer, D.J.N., *Advances in the modeling of motorcycle dynamics*, Multibody System Dynamics, vol. 12, no. 3, pp. 251–283, 2004.
- [29] Cossalter, V. and Lot, R., *A motorcycle multi-body model for real time simulations based on the natural coordinates approach*, Vehicle System Dynamics, vol. 37, no. 6, pp. 423–447, 2002.
- [30] Limebeer, D.J.N., Sharp, R.S., and Evangelou, S., *Motorcycle steering oscillations due to road profiling*, Transactions of the ASME, Journal of Applied Mechanics, vol. 69, no. 6, pp. 724–739, 2002.
- [31] Sharp, R.S., and Limebeer, D.J.N., *A motorcycle model for stability and control analysis*, Multibody System Dynamics, vol. 6, no. 2, pp. 123–142, 2001.
- [32] Yokomori, M., Oya, T., Katayama, A., *Rider control behavior to maintain stable upright position at low speed*, JSAE Review 21 (2000) 61-65.
- [33] Cossalter, V., Lot, R., and Maggio, F., *The modal Analysis of a Motorcycle in Straight Running and on a Curve*, Meccanica 39 (2004) 1-16.
- [34] Cossalter, V., Doria, A., Lot, R., *Development and Validation of a Motorcycle Riding Simulator*, FISITA 2004, F2004F134.
- [35] Qichang He, Xiumin Fan, Dengzhe Ma, *Full Bicycle Dynamic Model for Interactive Bicycle Simulator*, Journal of Computing and Information Science in Engineering, December 2005, Vol. 5.
- [36] Cossalter, V., Doria, A., Garbin, S. and Lot, R., *Frequency-Domain Method for Evaluating the Ride Comfort of a Motorcycle*. Vehicle System Dynamics, Vol. 44, pp.339-355, 2006.
- [37] Nehaoua, L., Hima, S., Arioui, H., Seguy, N., *A New Motorcycle Simulator Platform: Mechatronics Design*, Dynamics Modeling and Control. Proceedings of the 17th World Congress, The International Federation of Automatic Control, Seoul, Korea, July 6-11, 2008.
- [38] Kane, T.R., *Fundamental Kinematical Relationships for Single-Track Vehicles*. Int. J. mech. Sci., Vol. 17, pp. 499-504, 1975.
- [39] Roberts, J.B. and Spanos, P.D., *Random Vibration and Statistical Linearization*. Dover, 2003.

- [40] Crandall, S.H. and Mark, W.D., *Random Vibration in Mechanical Systems*. Academic Press, 1963.
- [41] Newland, D.E., *An Introduction to Random Vibrations and Spectral Analysis*. Longman, 1975.
- [42] Robson, J.D., *An Introduction to Random Vibration*. Edinburgh University Press, 1964.
- [43] Cossalter, V., *Motorcycle Dynamics*. Race Dynamics, 2002.
- [44] Gkaras, V., *A Monte Carlo Study of Vibration Isolation Systems Using Linear and Nonlinear Multiple Tuned Mass Damper Oscillators*. M.Sc. Thesis, Rice University, 2005.
- [45] Inman, D.J., *Engineering Vibration*. Prentice Hall, 1994.
- [46] Newland, D.E., *Mechanical Vibration Analysis and Computation*. Longman, 1989.
- [47] Meirovitch, L., *Introduction to Dynamics and Control*, John Wiley and Sons, 1985.
- [48] Craig, R.R., *Structural Dynamics, An Introduction to Computer Methods*, John Wiley and Sons, 1981.
- [49] Close, C.M., Frederick, D.K., *Modeling and Analysis of Dynamical Systems*, Second ed., John Wiley and Sons, 1995.
- [50] Roberts, M.J., *Signals and Systems: Analysis Using Transform Methods and Matlab*, McGraw-Hill, 2004.
- [51] Palm, W.J., *System Dynamics*, McGraw-Hill, 2005.
- [52] Thomson, W.T., Dahleh, M.D., *Theory of Vibration with Applications*, Prentice Hall, 5th ed., 1998.
- [53] Meirovitch, L., *Elements of Vibration Analysis*, McGraw-Hill, 2nd ed, 1986.
- [54] Clough, R.W., Penzien, J. *Dynamics of Structures*, McGraw-Hill, 2nd ed, 1982.
- [55] Lutes, L.D., Sarkani, S., *Random Vibrations: Analysis of Structural and Mechanical Systems*, Elsevier Inc, 2004.
- [56] Stark, H., Woods, J.W., *Probability and Random Processes with Applications to Signal Processing*. 3rd ed., Prentice Hall, 2002.

- [57] Papoulis, A., Pillai, S.U., *Probability, Random Variables and Stochastic Processes*. 4th Ed., McGraw-Hill, 2002.
- [58] Dorsey, J. *Continuous and discrete control systems: modeling, identification, design, and implementation*, McGraw-Hill, 2002.
- [59] Aplevich, J.D., *The essentials of linear state-space systems*, John Wiley and Sons, Inc., 1999.
- [60] Inman, D. J., *Vibration with control*, John Wiley and Sons, Ltd., 2006.
- [61] Preumont, A., *Random Vibration and Spectral Analysis*, Kluwer Academic Publishers, 1994.
- [62] Garcia de Jalon, J.C., Bayo, E., *Kinematic and Dynamic Simulation of Multibody Systems*, Springer-Verlag, New York, 1994.
- [63] Shinozuka, M. and Deodatis, G., *Simulation of Stochastic Processes by Spectral Representation*. Applied Mechanics Reviews, Vol 44 (4), 191-203, 1991.
- [64] Spanos, P.D. and Hansen, J.E., *Linear Prediction Theory for Digital Simulation of Sea Waves*. Journal Energy Resources Technology, V. 103, 243-249, 1981.
- [65] Spanos, P.D., *ARMA Algorithms for Ocean Wave Modeling*, Transactions of the ASME, V. 105, 300-309, 1983.
- [66] Spanos, P.D., *Spectral Representation of High-Frequency Space Shuttle Data*, Journal of Aerospace Engineering, Vol. 7, No. 3, 315-327, 1992.
- [67] Dodds, C.J. and Robson, J.D., *The description of Road Surface Roughness*, Journal of Sound and Vibration (1973) 31(2), 175-183.
- [68] Davis, B.R. and Thompson, A.G., *Power Spectral Density of Road Profiles*, Vehicle System Dynamics (2001), Vol. 35, No. 6, pp. 409-415.
- [69] Hamming, R. W. *Digital Filters*, Prentice-Hall, 1983.
- [70] Hunt, H.E.M., *Modeling of Road Vehicles for Calculation of Traffic-Induced Ground Vibration as a Random Process*, Journal of Sound and Vibration (1991) 144(1), 41-51.
- [71] Kavanagh, R.J., Ramanathan R., *Computer Simulation of Road Surface Profiles for a Four-Wheeled Vehicle*, Proceedings of the 1982 Winter Simulation Conference. Highland, Chao, Madrigal, Editors, IEEE, 1982.

- [72] Kropác, O. Múcka, P., *Be Careful When Using the International Roughness Index as an indicator of road unevenness*, Journal of Sound and Vibration 287 (2005) 989–1003.
- [73] Sun, L., *Optimum design of “road-friendly” vehicle suspension systems subjected to rough pavement surfaces*, Applied Mathematical Modelling 26 (2002) 635–652.
- [74] Öijer, F. and Edlund, S., *Complete Vehicle Durability Assessments Using Discrete Sets of Random Roads and Transient Obstacles Based on Q-distributions*, Vehicle System Dynamics Supplement 37 (2002), pp. 67-74.
- [75] Schiehlen, W., *White noise excitation of road vehicle structures*, Sadhana Vol. 31, Part 4, August 2006, pp. 487–503.
- [76] Schiehlen, W., *Probabilistic analysis of vehicle vibrations*, Probabilistic Engineering Mechanics, 1986, Vol. 1, No. 2, 99-104.
- [77] Sprinc, J. Kropac, O., Sprinc M., *Characterization of Longitudinal Road Unevenness in the Light of the International PIARC -EVEN Experiment 1998*, Vehicle System Dynamics, 2002, Vol. 37, No. 4, pp. 263-281.
- [78] Narayanan, S. and Senthil, S., *Stochastic Optimal Active Control of a 2-DOF Quarter Car Model with Non-Linear Passive Suspension Elements*, Journal of Sound and Vibration (1998) 211(3), 495-506.
- [79] Xu, D. M., Mohamed, A. M. O., Yong, R. N., Caporuscio F., *Development of a Criterion for Road Surface Roughness Based on Power Spectral Density Function*, Journal of Terramechanics, Vol. 29, No. 4/5, pp. 477-486, 1992.
- [80] Dinca, F. and Sireteanu, T., *Random Vibrations in the Dynamics of Motorvehicles*, Rev. Roum. Sci. Techn.-Mec. Appl., Tome 14, No. 4, pp. 869-894, Bucarest, 1969.
- [81] Hayes, M. H., *Statistical Digital Signal Processing and Modeling*, John Wiley & Sons, Inc., 1996.
- [82] Recktenwald, G., *Numerical Methods with MATLAB: implementations and applications*, Prentice-Hall, 2000.
- [83] Yonglin, Z. and Jiafan, Z., *Numerical simulation of stochastic road process using white noise filtration*, Mechanical Systems and Signal Processing 20 (2006) 363–372.
- [84] Proakis, J.G. and Manolakis, D.G., *Digital Signal Processing*, 4th ed., Pearson Prentice Hall, 2007.

- [85] Blackman, R.B. and Tukey, J.W., *The Measurement of Power Spectra*, Dover Publications Inc., 1958.
- [86] Bogsjö, K. and Forsén, A., *Fatigue relevant road surface statistics*, Vehicle System Dynamics Supplement 41 (2004), p. 734-743.
- [87] Bendat, J.S. and Piersol, A.G., *Random Data: Analysis and Measurement Procedures*, 2nd ed., Wiley-Interscience, 1986.
- [88] Turkay, S. and Akcay, H., *A study of random vibration characteristics of the quarter-car model*, Journal of Sound and Vibration 282 (2005) 111–124.
- [89] Akcay, H. and Turkay, S., *Frequency domain subspace-based identification of discrete-time power spectra from nonuniformly spaced measurements*, Automatica 40 (2004) 1333–1347.
- [90] Hammersley, J.M., and Handscomb, D.C., *Monte Carlo Methods*, Methuen, London, 1975.
- [91] Sobol, I. M., *A primer for the Monte Carlo method*, CRC Press, 1994.
- [92] Manolakis, D.G., Ingle, V.K., Kogon, S.M. *Statistical and Adaptive Signal Processing*, McGraw-Hill, 2000.
- [93] Gillespie, T.D., *Fundamentals of Vehicle Dynamics*, SAE, Warrendale, 1992.
- [94] Krylov N., Bogoliubov N., *Introduction to nonlinear mechanics*, New York: Princenton University Press, 1943.
- [95] Caughey T.K., *Equivalent linearization techniques*, J. Acoustical Soc. Am. 1963, 35:1706–1711.
- [96] Iwan W.D., *A generalization of the concept of equivalent linearization*, International Journal of Nonlinear Mechanics, 1973, 8:279–87.
- [97] Atalik T.S., Utku S., *Stochastic linearization of multi-degree of freedom non-linear systems*, Earthquake Engineering Structural Dynamics 1976, 4:411–20.
- [98] Faravelli, L., Casciati F., Singh M.P., *Stochastic equivalent linearization algorithms and their applicability to hysteretic systems*, Meccanica 1988;23:107–12.
- [99] Spanos, P.D., Iwan, W.D., *On the existence and uniqueness of solutions generated by equivalent linearization*, Int. J. Non-Linear Mech. 1978, 13:71–8.

- [100] Spelta, C., Savaresi, S., Fabbri, L., *Experimental analysis of a motorcycle semi-active rear suspension*, Control Engineering Practice 18 (2010) 1239–1250.
- [101] Bouc, R., *Forced vibration of mechanical systems with hysteresis (Abstract)*, In: Proceedings of the Fourth Conference on Nonlinear Oscillation, Prague, 1967.
- [102] Wen, Y.K., *Approximate method for non-linear random vibration*, Journal of Engineering Mechanics 1975; 101: 389–401.
- [103] Baber, T.T., Wen Y.K., *Random vibration of hysteretic, degrading systems*, Journal of Engineering, Mechanics Div., ASCE 1981, 107: 1069–87.
- [104] Casciatti F, Faravelli L. *Methods of non-linear stochastic dynamics for the assessment of structural fragility*, Nuclear Engineering Des., 1985; 90: 341–56.
- [105] Foliente G.C., Singh M.P., Noori M.N., *Equivalent linearization of generally pinching hysteretic, degrading systems*, Earthquake Engineering Structural Dynamics 1996; 25: 611–29.
- [106] Cunha, A.M.F., *The role of the stochastic equivalent linearization method in the analysis of the non-linear seismic response of building structures*, Earthquake Engineering Structural Dynamics, 1994; 23: 837–57.
- [107] Sues, R.H., Wen Y.K., Ang, A.H.S., *Stochastic evaluation of seismic structural performance*, Journal of Structural Engineering, 1985; 111: 1204–18.
- [108] Sues, R.H., Mau, S.T., Wen, Y.K., *System identification of degrading hysteretic restoring forces*, Journal of Engineering Mech., 1988; 114: 833–46.
- [109] Wen, Y.K., Eliopoulos, D., *Method for nonstationary random vibration of inelastic structures*, Probabilistic Engineering Mechanics 1994; 9: 115–23.
- [110] Pires, J.E.A., Wen, Y.K., Ang, A.H.S., *Stochastic analysis of liquefaction under earthquake loading*, Civil Engineering Studies, Report SRS No. 504, University of Illinois at Urbana-Champaign, 1983.
- [111] Casciatti, F., Faravelli, L., *Stochastic equivalent linearization for 3-D frames*, Journal of Engineering Mechanics, ASCE 1989; 114: 1760–71.
- [112] Lin, B.C., Tadjbakhsh, I.G., Papageorgiu, A.S., Ahmadi, G., *Response of base-isolated building to random excitations described by the Clough–Penzien spectral model*. Earthquake Engng. Struct. Dynamics 1989, 18: 49–62.
- [113] Yang, J.N., Li, Z., Vongchavalitkul, S., *Stochastic hybrid control of hysteretic structures*, Probabilistic Engineering Mechanics, 1994, 9: 125–33.

- [114] Li, Z., Katsukura, H., *Markovian hysteretic characteristics*, Journal of Engineering Mechanics, ASCE 1990, 116, 1798–811.
- [115] Kobori, T., Minai, R., Suzuki, Y., *Stochastic response of hysteretic structures*, Bulletin of the Disaster Prevention Research Institute. Kyoto University 1977, 26: 57–70.
- [116] Kimura, K., Yasumuro, H., Sakata, M., *Non-gaussian equivalent linearization for nonstationary random vibration of hysteretic system*, Probabilistic Engineering Mechanics, 1994, 9: 15–22.
- [117] Iwan, W.D., Paparizos, L.G., *The stochastic response of strongly yielding systems*, Probabilistic Engineering Mechanics, 1988, 3: 75–82.
- [118] Pradlwarter, H.J., Schueller, G.I., *The method of statistical equivalent linearization*, In: Schueller, G.I., editor, Structural Dynamics—Recent Advances. Berlin: Springer-Verlag, 1991.
- [119] Nataf, A., *Determination des distributions dont les marges sont données*, Comptes rendues de l’Académie des Sciences, 1962, 225: 42–3.
- [120] Park, Y.J., *Equivalent linearization for seismic responses. I: Formulation and error analysis*, Journal of Engineering Mechanics, ASCE 1992, 118: 2207–26.
- [121] Yell, C.H., *Modeling of nonstationary earthquake ground motion and biaxial and torsional response of inelastic structures*, Ph.D. thesis, University of Illinois, 1989.
- [122] Hurtado, J.E., Barbat, A.H., *Improved stochastic linearization method using mixed distributions*, Struct. Safety 1996, 18: 49–62.
- [123] Pradko, F., Lee, R., Kaluza, V., *Theory of Human Vibration Response*, U.S. Army Tank-Automotive Center, Warren, Michigan, 1965.
- [124] Shinozuka, M., Sato, Y., *Simulation of nonstationary random processes*, Journal of Engineering Mechanics Div., 1967, 93: 11–40.
- [125] Yang, J.N., Liu, S.C., *Distribution of maximum and statistical response spectra*, J. Engng. Mech. Div. 1981, 107: 1089–102.
- [126] Caughey, T.K., *Response of Van der Pol’s Oscillator to Random Excitation*, Journal of Applied Mechanics, 1959: 345-348.
- [127] Caughey, T.K., *Random Excitation of a System with Bilinear Hysteresis*, Journal of Applied Mechanics, 1960: 27: 649-652.

- [128] Kropáč, O. Múčka, P., *Effect of obstacles on roads with different waviness values on the vehicle response*. Vehicle System Dynamics Vol. 46, No. 3, March 2008, 155–178
- [129] Caughey, T.K., *Nonlinear Theory of Random Vibrations*, Advanced Applied Mechanics, 1971, 11: 209-253.
- [130] Caughey, T.K., *On the Response of Nonlinear Oscillators to Stochastic Excitation*, Probabilistic Engineering Mechanics, 1986, 1: 2-4.
- [131] Shinozuka, M. and Jan, C.M., *Digital Simulation of Random Processes and its Applications*, Journal of Sound and Vibration (1972) 25 (1), 111-128.
- [132] Nigam, N.C., *Introduction to Random Vibrations*, Cambridge, 1983, MA, M.I.T. Press.
- [133] Lutes, L.D., *Equivalent Linearization for Random Vibration*, Journal of Engineering Mechanics, 1970, 96: 227-242.
- [134] Lutes, L.D. and Sarkani, *Stochastic Analysis of Structural and Mechanical Vibrations*, Prentice-Hall, 1997.
- [135] Iwan, W.D. and Lutes, L.D., *Response of the Bilinear Hysteretic System to Stationary Random Excitation*, Journal of the Acoustical Society of America, 1968, 43: 545-552
- [136] Bendat, J., S., *Nonlinear Systems Techniques and Applications*, Wiley-Interscience, 1998.
- [137] Lin, Y.K. and Cai, G.C., *Probabilistic Structural Dynamics; Advanced Theory and Applications*, New York, McGraw-Hill, 1995.
- [138] Nayfeh, A.H. and Mook, D.T., *Nonlinear Oscillations*, New York, John Wiley, 1979.
- [139] Novak, S. and Frehlich, R.G., *Transition to Chaos in the Duffing Oscillator*, The American Physical Society Physical Review, 1982, A 26(6): 3660-3663.
- [140] Guckenheimer, J. and P. Holmes, *Nonlinear Oscillations, Dynamical Systems and Bifurcations of Vector Fields*. Springer-Verlag, New York, 1983.
- [141] Smyth, A. W. and Masri, S., *Nonstationary Response of Nonlinear Systems Using Equivalent Linearization with a Compact Analytical Form of the Excitation Process*, Probabilistic Engineering Mechanics, 2002, 17: 97-108.
- [142] Nayfeh, A.H., Balachandran, B., *Applied Nonlinear Dynamics: Analytical, Computational and Experimental Methods*, Wiley, 1995.

- [143] Bender, C.M. and Orzag, S.A., *Advanced Mathematical Methods for Scientists and Engineers*, McGraw-Hill, 1978.
- [144] Shinozuka, M., *Monte Carlo Solution of Structural Dynamics*, Computers and Structures, 2:855-874, 1972.
- [145] Spanos, P.D. and M.D. Mignolet, *ARMA Monte Carlo Simulation in Probabilistic Structural Analysis*, The Shock and Vibration Digest, vol. 21, pp.3-14, 1989.
- [146] Karnopp, D., Margolis, D., Rosenberg R., *Systems dynamics: A unified approach*, John Wiley, 1990.
- [147] Bos, A.M., *A Bond Graph Approach to the Modelling of a Motorcycle*. Vehicle System Dynamics, Jan 1987, Vol. 16 Issue sup1, p289-314, 26p.
- [148] Klosner, J., M., et.al., *Response of non-linear systems with parameter uncertainties*, Int. J. Non-Linear Mechanics, Vol 27, No. 4, pp. 547-563, 1992.
- [149] Soong, T.T., *Random Differential Equations in Science and Engineering*, Academic, New York, 1973.
- [150] Lin, Y.K., *Probabilistic Theory of Structural Dynamics*, McGraw-Hill, New York, 1967.
- [151] Kraichan, R.H., *The Closure Problems of Turbulence Theory*, Symposium of Applied Mathematics, 1962, 13: 199-225.
- [152] Iyengar, R.N. and P.K. Dash, *Study of Random Vibration of Nonlinear Systems by Gaussian Closure Technique*, J. of Applied Mechanics, 1978, 45: 393-399.
- [153] Iwan, W.D., *On Defining Equivalent Systems for certain Ordinary Nonlinear Differential Equations*, Int. Journal of Nonlinear Mechanics, 1969, 4: 325-334.
- [154] Cuong, H.T., et al., *The Generation of Digital Random Time Histories*, Ocean Engineering, Vol. 9, No 6, pp.581-588, 1982.
- [155] Elishakoff, I., Colajanni, P., *Stochastic Linearization Critically Re-examined*, Chaos, Solitons & Fractals, Vol. 8, No. 12, pp. 1957-1972, 1997.
- [156] Li, J., Chen, B., *Probability density evolution method for dynamic response analysis of structures with uncertain parameters*, Computational Mechanics 34 (2004) 400-409.
- [157] Chen, B., Li, J., *Dynamic response and reliability analysis of non-linear stochastic structures*, Probabilistic Engineering Mechanics 20 (2005) 33-44.

- [158] Li, J., Chen, B., *The probability density evolution method for dynamic response analysis of non-linear stochastic structures*, Int. J. Numer. Meth. Engng 2006; 65: 882-903.
- [159] Liu, Z., J., Li, J., *Probabilistic response and reliability evaluation of nonlinear structures under earthquake*, The 14th World Conference on Earthquake Engineering, October 12-17, 2008, Beijing, China.
- [160] Xu, J., Chen, J., Li, J., *Probability density evolution analysis of engineering structures via cubature points*, Comput Mech (2012) 50: 135-156.
- [161] Li, J., et.al, *Advances of the probability density evolution method for nonlinear stochastic systems*, Probabilistic Engineering Mechanics 28 (2012) 132-142.
- [162] *The Pneumatic Tire*, U.S. Department of Transportation, National Highway traffic Safety Administration, 2006.
- [163] Happian-Smith, Julian, *An Introduction to Modern Vehicle Design*, Butterworth-Heinemann, 2002.
- [164] Bekker, M.G., *Introduction to Terrain-Vehicle Systems*, The University of Michigan Press, 1969.
- [165] Cossalter, V., Doria, A., *The relation between contact patch geometry and the mechanical properties of motorcycle tyres*, Vehicle System Dynamics, Vol. 43, Supplement, 2005, 156-167.
- [166] Gavin McGee, C., et al., *A Frequency Domain Technique for Characterizing Nonlinearities in a Tire-Vehicle Suspension System*, Journal of Vibration and Acoustics, ASME, Feb. 2005, Vol. 127, pp. 61-76.
- [167] Fujioka, T., Goda, K., *Tire cornering properties at large camber angles: mechanism of the moment around the vertical axis*, JSAE Review 16 (1995) 257-261.
- [168] Giannitrapani, F., Virzi Mariotti, G., *Dynamic Analysis of Motorcycle Behaviour on the Road with Steering Plate Structural Optimisation*, Beograd 2005 EAEC European Automotive Congress, 2005.
- [169] Lot, R., *A Motorcycle Tire Model for Dynamic Simulations: Theoretical and Experimental Aspects*, Meccanica 39: 207–220, 2004.
- [170] Lot, R., Cossalter, V., Massaro, M., *The Significance of Frame Compliance and Rider Mobility on the Motorcycle Stability*, Multibody Dynamics 2005, ECOMAS Thematic Conference, J.M. Goicolea, J. Cuadrado, J.C. García Orden (eds.), Madrid, Spain, 21-24 June 2005.

- [171] Tezuka, Y., Ishii, H., Kiyota, S., *Application of the magic formula tire model to motorcycle maneuverability analysis*, JSAE Review 22 (2001) 305–310.
- [172] Versteden, W.D., *Improving a tyre model for motorcycle simulations*, Master's thesis, 2005, Eindhoven University of Technology.
- [173] Choi, B., S., Choi Y., T., Park, D., W., *A Sliding Mode Control of a Full-Car Electrorheological Suspension System Via Hardware in-the-Loop Simulation*, Journal of Dynamic Systems Measurement and Control, Vol. 122, March 2000.
- [174] Duysinx, P., et al., *Optimization of mechatronic systems: application to a modern car equipped with a semi-active suspension*, 6th World Congresses of Structural and Multidisciplinary Optimization Rio de Janeiro, 30 May - 03 June 2005, Brazil.
- [175] Welch, P.W., *The use of fast Fourier transform for the estimation of power spectra: A method based on time averaging over short, modified periodograms*, IEEE Trans. Audio Electroacoustics, 1967, 15(2):70-76.
- [176] Marzbanrad, J., et al., *Stochastic optimal preview control of a vehicle suspension*, Journal of Sound and Vibration 275 (2004) 973–990.
- [177] Tamboli, J.A., Joshi, S.G., *Optimum Design of a Passive Suspension System of a Vehicle Subjected to Actual Random Road Excitations*, Journal of Sound and Vibration (1999) **219**(2), 193-205.
- [178] Uys, P.E., Els, P.S., Thoresson, M., *Suspension settings for optimal ride comfort of off-road vehicles travelling on roads with different roughness and speeds*, Journal of Terramechanics 44 (2007) 163–175.
- [179] Mavroudakos, B. Eberhard, P., *Analysis of Alternative Front Suspension Systems for Motorcycles*, Vehicle System Dynamics Vol 00, No. 00, August 2005, 1-10.
- [180] Cossalter, V., et al., *On the non-linear behaviour of motorcycle shock absorbers*, Proc. IMechE Vol. 224 Part D: J. Automobile Engineering, July 2009
- [181] Beghi, A., et al., *Grey-box modeling of a motorcycle shock absorber for virtual prototyping applications*, Simulation Modeling Practice and Theory 15 (2007) 894–907.
- [182] Poussot-Vassal, C., *Commande Robuste LPV Multivariable de Châssis Automobile*, These Docteur, Grenoble Institut Polytechnique, 2008.

- [183] Richards, C.M. and Summers, T.W., *Transient Response Simulation of an Off-Road Motorcycle with Conventional and Multicell Tire Inflation Mechanisms*, Tire Science and Technology, TSTCA, Vol. 35, No. 1, January – March 2007, pp. 2-22.
- [184] Cui, Y., Kurfess, T R., Messman, M., *Testing and Modeling of Nonlinear Properties of Shock Absorbers for Vehicle Dynamics Studies*, WCECS 2010, October 20-22, San Francisco, USA.
- [185] Tootkaboni, M., Graham-Brady, L., *Stochastic direct integration schemes for dynamic systems subjected to random excitations*, Probabilistic Engineering Mechanics 25 (2010) 163–171.
- [186] Cossalter, V., Doria, A., *Identificazione delle caratteristiche meccaniche dei pneumatici motociclistici*, AIMETA '03, XVI Congresso AIMETA di Meccanica Teorica e Applicata.
- [187] Cossalter, V., et al., *Dynamic Properties of Motorcycle and Scooter Tires: Measurement and Comparison*, Vehicle System Dynamics 2003, Vol. 39, No.5, pp. 329-352.
- [188] Koo, J., Goncalves, F.D., and Ahmadian M., *A comprehensive analysis of the response time of MR dampers*, Smart Mater. Struct. 15 (2006) 351–358.
- [189] Basso, R., Fabbri, L., Zagatti, E., *A Method to Analyse the Dynamic Behavior of a Motorcycle Front Suspension Equipped with Sequential Dampers*, Vehicle System Dynamics, 29 (1998), pp. 213-230.
- [190] Evangelou, S., *Control of motorcycles by variable geometry rear suspension*, 2010 IEEE Multi-Conference on Systems and Control Yokohama, Japan, September 8-10, 2010.
- [191] Seong, M.S., Choi, S.B., Han, Y.M., *Damping force control of a vehicle MR damper using a Preisach hysteretic compensator*, Smart Mater. Struct. 18 (2009) 074008 (13pp).
- [192] Akcay, H. and Turkay, S., *Influence of tire damping on mixed H_2/H_∞ synthesis of half-car active suspensions*, Journal of Sound and Vibration 322 (2009)15–28.
- [193] Gravatt, J.W., *Magneto-Rheological Dampers for Super-sport Motorcycle Applications*, Master's Thesis, Virginia Polytechnic Institute and State University, 2003.
- [194] Wakeham, K.J., Rideout, D.G., *Model complexity requirements in design of half car active suspension controllers*, Proc. ASME Dynamic Systems and Controls Conference, Arlington, VA Oct. 31-Nov.2, 2011.

- [195] Cossalter, V., Doria, A., *Model simulation. The Latest dynamic developments for motorcycle tires*, Tire Technology International, September 2001.
- [196] Audenino, A. L., Belingardi, G., *Modelling the dynamic behaviour of a motorcycle damper*, Proc. IMechE, Part D: J. Automobile Engineering, 1995, pp. 249–262.
- [197] Arnold, M., et al., *Numerical methods in vehicle system dynamics: state of the art and current developments*, Vehicle System Dynamics, Vol. 49, No. 7, July 2011, 1159–1207.
- [198] Pacejka, H.B., *Tire and Vehicle Dynamics*, SAE 2002.
- [199] Borgman, L.E., *Ocean wave simulation for engineering design*, Journal of Waterways and Harbors Division, Proceedings of the American Society of Civil Engineers WW4, 1969, 556-583.
- [200] Sayers, M.W., Karamihas, S.M., *The Little Book of Profiling*, The Regent of the University of Michigan, 1998.
- [201] Kozin, et al., *Statistical Studies of Stable Ground Roughness*, U.S. Army Land Locomotion Lab. Rep. No. 8391 (LL 95), ATAC, Warren, Michigan, 1963.
- [202] Spanos, P.D., *Formulation of stochastic linearization for symmetric or asymmetric M.D.O.F. nonlinear systems*, Journal of Applied Mechanics, 1980, 47: 209-211.
- [203] Spanos, P.D., Monte Carlo simulations of responses of non-symmetric dynamic system to random excitations. Computers & Structures, 1981, 13:371-376.
- [204] Spanos, P.D., *Stochastic linearization in structural dynamics*, Applied Mechanics Reviews, 1981, 34(1): 1-8.
- [205] Cossalter, V., Lot, R., Rota, S., *Objective and subjective evaluation of an advanced motorcycle riding simulator*, Eur. Transp. Res. Rev. (2010) 2:223–233.
- [206] Saccon, A., Hauser, J., *An efficient Newton method for general motorcycle kinematics*, Vehicle System Dynamics: International Journal of Vehicle Mechanics and Mobility, Volume 47, Issue 2, 2009.
- [207] Digital image. *Harley Davidson XL1200R Roadster Front Right Side View. Motorcycle Cruiser*, Source Interlink Media, n.d. Web. 29 Jan. 2013. <http://www.motorcyclecruiser.com/newsandupdates/2004_harley_davidson_lineup/photo_01.html> .

- [208] Digital image. *2009 Suzuki GSX-R1000*. *Total Motorcycle*, n.d., Web. 06 Dec.2012. <<http://www.totalmotorcycle.com/modelhistorytimelines/Suzuki-GSXR1000-2009-2011-Page5.htm>>.
- [209] Digital image. *2006 Yamaha YZ250*. *Total Motorcycle*, n.d., Web. 06 Dec.2012. <<http://www.totalmotorcycle.com/photos/2006models/2006models-Yamaha-YZ250.htm>>.
- [210] Digital image. Motorcycle Technology. Bike Tires Dunlop video, n.d. Web. 06 Aug. 2012. < www.dunlop.eu/dunlop_euen/mc/videos/index.jsp >